YAZAN-ZAID

Pre-Processed And Combined EEG Data For Epileptic Seizure Classification Using Deep Learning

MASTER THESIS

2022


**NEAR EAST UNIVERSITY**

**INSTITUTE OF GRADUATE STUDIES**

**DEPARTMENT OF COMPUTER ENGINEERING**


# PRE-PROCESSED AND COMBINED EEG DATA FOR EPILEPTIC SEIZURE CLASSIFICATION USING DEEP LEARNING

**M.Sc. THESIS**


**Yazan ZAID**


**Nicosia**

**January, 2022**

**NEAR EAST UNIVERSITY**

**INSTITUTE OF GRADUATE STUDIES**

**DEPARTMENT OF COMPUTER ENGINEERING**

**……………………………………………. ………………..**

# Pre-Processed And Combined EEG Data For Epileptic Seizure Classification Using Deep Learning

**M.Sc. THESIS**

**Yazan ZAID**

**Supervisors**

**Assoc Prof Dr Melike ŞAH DİREKOĞLU**

**Assist Prof Dr Cem DİREKOĞLU**

**Nicosia**

**January, 2022**

# APPROVAL

We certify that we have read the thesis submitted by Yazan Zaid titled **"Pre-Processed And Combined EEG Data For Epileptic Seizure Classification Using Deep Learning**" and that in our combined opinion it is fully adequate, in scope and in quality, as a thesis for the degree of Master of Educational Sciences.

| Examining Committee | Name-Surname | Signature |
|---|---|---|

Head of the Committee: Prof Dr Rahib Abiyev

Committee Member:

Assoc Prof Dr Kamil Dimililer

Supervisors:

Assoc Prof Dr Melike Şah Direkoğlu

Assist Prof Dr Cem Direkoğlu

Approved by the Head of the Department

…../…../20…

………………………..

Title, Name-Surname

Head of Department

Approved by the Institute of Graduate Studies

…../…../20…

Prof. Dr. Kemal Hüsnü Can Başer

Head of the Institute

## DECLARATION

I hereby declare that all information, documents, analysis and results in this thesis have been collected and presented according to the academic rules and ethical guidelines of Institute of Graduate Studies, Near East University. I also declare that as required by these rules and conduct, I have fully cited and referenced information and data that are not original to this study.

Yazan Zaid

16/01/2022

Day/Month/Year

## ACKNOWLEDGEMENTS

To my parents, family, friends, supervisors and everyone helped make this work possible. Special thanks to Assoc Prof Dr Melike Şah Direkoğlu and Assist Prof Dr Cem Direkoğlu for their efforts and supporting me. Many thanks to my little brother Mohammad, yazan atatrah and fares abubaker for their great help.

**Yazan Zaid**

## ABSTRACT

**Pre-Processed And Combined EEG Data For Epileptic Seizure Classification Using Deep Learning**

**Zaid, Yazan**
**M.Sc., Department of Computer Engineering**
**January, 2022, 111 Pages**

Epilepsy is a neurological disease that affects nearly 60 million people around the world. It manifests as a loss of consciousness for different periods of time due to a sudden rush in the electrical fields of the brain. Electroencephalography (EEG) is the measurement of the brain's electrical potentials which can be used to detect epileptic seizures' sudden electrical rushes. Experts struggle to diagnose seizure activities by visual inspection since it requires long periods of examination and years of experience. With the assistance of machine learning based technologies, the diagnosis of seizure activities became more accurate and fast. However, many machine learning algorithms still depend on hand crafted features that is input to classifiers for training and testing. On the other hand, deep learning methods eliminate the feature engineering process and replace it with feature learning and classification. Deep learning methods provide a robust performance for medical aid systems. The most of the research in the field of epileptic seizure detection focus on testing different deep learning architectures on datasets, but none of them experiments modified EEG input signals. In this thesis, we study and experiment modified, pre-processed and combined EEG signals as an input to deep neural networks for epilepsy seizure classification. A variety of preprocessing and combinations of EEG signals have been proposed and evaluated on three different deep learning architectures. We study 2-class and 3-class epileptic seizure classification problems on UCI-Bonn dataset. In particular, a Deep Neural Network (DNN) and two different 1D-Convolutional Neural Networks (CNN) are implemented with the proposed input EEG signals. We tested the following input EEG signals with the deep learning methods mentioned above: The original EEG data of UCI-Bonn dataset, standardized EEG signal, squared signal combined with the original EEG, differentiated signal combined with the original EEG, and the Fast Fourier Transform (FFT) signal combined with the original EEG signal. Various metrics are employed to evaluate the performance of the models. The best results are achieved with the input signal created with the combination of FFT and original EEG signal. Among the three different deep learning architectures, 1D-CNNs perform better than DNN. Extensive evaluations and comparisons are conducted and presented.

***Keywords:*** deep neural networks, preprocessing, EEG combinations, epileptic seizure, classification.

# TABLE OF CONTENTS

## LIST OF TABLES

## LIST OF FIGURES

## ABBREVIATIONS

AI: Artificial Intelligence

EEG: Electroencephalograph

ML: Machine Learning

DL: Deep Learning

TL: Transfer Learning

NN: Neural Network

CNN: Convolutional Neural Network

1D-CNN: One-dimensional Convolutional Neural Network

2D-CNN: two-dimensional Convolutional Neural Network

DNN: Deep Neural Network

DCNN: Deep Convolutional Neural Network

Resnet: Residual Network

VGG: Visual Geometry Group

ANN: Artificial Neural Network

RNN: Recurrent Neural Network

GA: Genetic Algorithm

SVM: Support Vector Machine

KNN: K-Nearest Neighbor

MRI: Magnetic Resonance Imaging

GAP: Global Average Pooling

GBUs: Graphic Processing Units

TPU: Tensor Processing Unit

CPU: Central Processing Unit

Colab: Colaboratory

V(2): Version two

GHz: Giga hertz

DBN: Deep Belief Network

LSTM: Long Short-Term Memory

Bi-LSTM: Long Short-Term Memory

PCA: Principal Component Analysis

ReLU: Rectified Linear Unit

LDA: Linear Discriminant Analysis

AE: Auto-Encoder

QLDA: Quadratic Linear Discriminant Analysis

MOEA: Multi-Objective Evolutionary Algorithm

SDCAE: Supervised Deep Convolutional Autoencoder

GRU: Gated Recurrent Unit

FPR: False Positive Rate

TPR: True Positive Rate

FFT: Fast Fourier Transform

INN: Improved Neural Network

SEA: Stacking Ensemble based Approach

WT: Wavelet Transform

PSR: Phase-Space Reconstruction

ED: Euclidean Distance

GBM: Gradient Boosting Machine

GSO: Grid search Optimizer

RF: Random Forest

rmsProp: Root Mean Square Propagation

K-fold-CV: K-fold Cross Validation

CEEMDAN: Complete Ensemble Empirical Mode Decomposition with Adaptive Noise

P-1D-CNN: Pyramidal one dimensional Convolutional Neural Network

LVQ: Learning Vector Quantization

FBSE: Fourier-Bessel Series Expansion

WMRPE: Weighted Multi-scale Renyi Permutation Entropy

MPC-GA: Multi parent crossover-Genetic Algorithm

OWFB: Orthogonal Wavelet Filter Banks

TQWT: Tunable Quality factor Wavelet Transform

EWT: Empirical Wavelet Transform

EMD: Empirical Mode Decomposition

WPD: Wavelet Packet Decomposition

RQA: Recurrence Quantification Analysis

GP: Genetic Programming

RBF: Radial Basis Function

DWT: Discrete Wavelet Transform

HOS: Higher Order Spectra

GMM: Gaussian Mixture Model

RBFNN: Radial Basis Function Neural Network

LMBPNN: Levenberg-Marquardt Backpropagation Neural Network

SNN: Spiking Neural Network

RProb: Resilient backpropagation

HT: Hilbert Transform

# CHAPTER I

## Introduction

This chapter presents the research problem. The aim of the study is explained that describes the proposed work. Then, we discuss the significance of the study to explain the novelty and why our work is important. The limitations of the study are also discussed, then the problem statement, the methodology and an overview of the thesis are given.

### Introduction

There are several serious diseases that afflict humans, and medical spe-cialties seek to diagnose and attempt to treat them. However, the seriousness of diagnosing of these diseases requires the intervention of other disciplines such as artificial intelligence to find ways, programs and devices that help diagnose and treat diseases. One of these challenging diseases for diagnosis is epilepsy. Epilepsy is a disease prevalent in humans regardless of their age and gender. Epilepsy is classified as a neurological disorder in the brain, usually in the form of sudden seizures for the patient and this disease is not contagious (Ghassemi et al., 2019)(Shoeibi, Khodatars, et al., 2021). There are different types of these seizures, affecting a large number of people, estimated at 60 million people around the world (Shoeibi, Ghassemi, Alizadehsani, et al., 2021). To diagnose epileptic seizures, several methods have been used over time, one of which is evaluated based on the Electroencephalography (EEG). Electroencephalography is defined as “the non-invasive measurement of the brain’s electric fields” (Biasiucci et al., 2019, p1), however, there is an invasive method for EEG that can give better performance (Ball et al., 2009). The current flow in and around neurons generates voltage potential that can be recorded by electrodes placed on the scalp (Biasiucci et al., 2019). The EEG method is distinguished from the rest of the tests in that it is clearer in rhythms, in addition to being economical in general (Subasi et al., 2019)(Acharya, Oh, Hagiwara, Tan, Adeli, & Subha, 2018). Diagnosis of these seizures began by reading the EEG by doctors, manually using the eye, but this is not accurate as it requires great experience and a long time (Boonyakitanont et al., 2020). With the era of ML and DL, new methods started to prove their reliability, high performance and rapidness. The ML learning approaches depend on the feature extraction phase followed by a classification phase. Feature extractions remain human-dependent since they must be engineered by experts either manually or by algorithms that select some characterized features which yielded non-optimal performance or accuracies despite being better than the bare-eye detection.

DL introduced the solution of feature engineering deficiency. The features are rather learned by the model not engineered, this method proved higher performance and much more accurate classifications, in general. The superiority and novelty of the DL approach motivated us to evaluate our method by DL architectures(Shoeibi, Khodatars, et al., 2021). We proposed the preprocessed and combined EEG data as an input to DL architectures. We concentrated on the data inputs as there was no other research, as far as we know, that did it similar to our way. Basically, we proposed three operations to modify datasets then combine them with the original EEG dataset of UCI-Bonn. The evaluations were done with many variations of inputs and models and they were tested with a reproduced state-of-art model of (Abiyev et al., 2020) to assess the validity and efficiency of our method. We observed strong indications of improvements on the evaluated architectures.

### Aim of the Study

The aim of this work is to evaluate the preprocessed and combined EEG signals as an input to deep learning models, which can assist to aid clinical experts with seizure diagnosis, especially in tough cases. In particular, this work reaches these diagnoses aid situations through the classifications of 2-class and 3-class brain activities related to epileptic seizure categories in EEG recordings based on the UCI-Bonn dataset. Identifying brain activity is a challenging task that takes time and experience, our purpose is to classify epileptic brain activity with high confidence to reduce the load on clinical experts, leaving them with the most complex diagnoses and rare types of seizures. We used deep CNN and deep NN architectures with different EEG signal cases, namely, raw (original EEG) and preprocessed and combined to learn the chaotic features of EEG and classify some types of epileptic brain activity. The suggested methods were evaluated and compared against some known methods of classification and with some high-performance proposed architectures as in (Abiyev et al., 2020) model which guaranteed accuracy with relative simplicity. It was observed that preprocessing and combinations of EEG data can give enhancement effects, especially in simple models.

### Significance of the study

Because of deep learning, major improvements have been achieved in the medical sector and neuroscience over the last decade. Epileptic seizure detection and classification aid systems can give a leap in the early diagnoses of seizures and real-time observation of the disease which helped increase reaction speed and prevent severe harm. Seizure detection was time-consuming before the introduction of these techniques and highly dependent on clinical expert opinions that can be subjective and error-prone. Computer-aided technology is therefore much needed to overcome such constraints because the health sector needs accurate, fast and reliable methods to diagnose complicated issues such as epilepsy. Thus, we provide a method for the detection and classification of different types of brain activities using deep learning architectures based on various signal shapes appears after combinations and preprocessing in our study with the aid of EEG data.

### Limitations of the Study

There are some limitations that need to be considered while dealing with epileptic seizure classification.

The first limitation is datasets, finding a dataset with enough samples, labels and open access is quite problematic which can be reasonable since the data is actually collected from real patients who do not prefer to share their medical records, however, this will be on the expense of the development of the field due to its vast reliance on human patients. One of the most famous datasets in this field is the Bonn dataset which comprises 500 samples of different categories of EEG signals, it was an open-access one until its shutdown by the original team. Many other datasets were also shut down over the years and replaced by closed access datasets such as the European Epilepsy Database EPILEPSIAE.

Also, another dataset related limitation is mapping the various labels of a dataset to another dataset, especially in the Bonn dataset with its various labeling systems such as the UCI version of labeling or others.

Another limitation is the multiclass classification, the brain activity is non-stationary, dynamic and non-linear which makes it rich with signals, data and hard to detect phenomena. In epilepsy, as far as we know, it is still impossible to implement a system that covers all types of seizures and their sub-types or rare variations. Even the prediction of a seizure from a healthy or preictal case recording is still problematic and uncertain whether by deep learning or human experts.

At last, real-time detection and diagnosis are crucially needed for patients to assess their environment carefully and find a safe way on preictal phases or seizure episodes to pass the seizure or report it to others in case of urgent need of help. Although there are some suggestions for real-time systems now, they are far from enough and further from perfection.

**Problem Statement**

Epilepsy is a hard-to-diagnose disease in the medical field, due to the harsh nature of EEG recordings of brain activity, its seizure classification is difficult, in general, and the more difficult thing is its preictal state.

The classification of epileptic seizures can be divided into two categories, the binary 2-class classification of seizure and non-seizure classes and the multiclass 3-class classification of seizure, preictal and normal classes although there are other types of multiclass classifications the normal, preictal and seizure 3-class category is almost the most confusing and many research studies are directed towards it.

Automatic seizure detection and classification into different kinds of brain activity is a hard issue that gained a lot of attention. In this thesis, we use deep learning models with preprocessed and combined EEG data signals to tackle the epileptic seizure classification problem from a unique view.

### Methodology

The purpose of this thesis is to evaluate the effects of the preprocessed and combined EEG signals of epileptic nature by applying deep learning. Here, we review the various distinctive models such as deep CNN and deep NN with the modified EEG signals using the UCI-Bonn epilepsy dataset. The proposed strategy involves the following stages, preprocessing and combination operations which were applied on the EEG dataset before feeding them to the deep learning algorithms. The evaluated operations are standardization and combination. combinations include combining a preprocessed dataset with a specific operation, namely, the squared dataset, the discretely differentiated dataset and the absolute fast Fourier transformed dataset with the original dataset. standardization, which is normalizing the datasets to have zero mean and one standard deviation, including standardizing the original EEG data and the combined EEG data. Also, the raw original dataset was tested along with the standardized versions of the original EEG dataset and other combinations.

Finally, using the deep learning architectures, the classification of various input cases was done by repeating each test five times with recording the averages of the five tests and in different train/test splitting ratios, namely, 50/50, 60/40, 70/30 and 80/20. One of the evaluated architectures was (Abiyev et al., 2020) 1D-CNN model to widen our testings on state-of-art methods that are effective yet, simple and reproducible.

### Overview of the Study

The thesis includes the following chapters to achieve the epileptic seizure classification systematic study.

The first chapter includes an introduction to the topic of the thesis with a summary describing the purposes, significances, limitations, problem statement and methodology.

The second chapter presents a literature review on the field with comparative studies that were evaluated against our methods. In this chapter, some of the most used architectures of deep learning for seizure detection and classification will be presented. we will give a review of the related work focusing on high-achieving methods and try to compare them to show the advancement of the field.

The third chapter discusses the EEG data in general and presents some samples of EEG signals for different brain activity.

The fourth chapter discusses the details of deep deep learning architectures in a comprehensive view.

The fifth chapter specifies the exact ways of operations and preprocessings.

The sixth chapter explains the runtime environment in which the coding, training and evaluations took place. The dataset is also viewed in detail along with the metrics and scores, architectures and signal samples.

The seventh chapter represents the experimental result analysis of the models and input cases, with discussions and comparisons.

The eighth chapter highlights the conclusions and suggests some future works.

# CHAPTER II

## Literature Review

This chapter presents the theory and related works in the field of epileptic seizure detection. The research problem is explained. Traditional methods, ML methods and DL based methods are reviewed. The plentifulness of the research is justified due to the difficulty of the problem at hand which is discussed in detail.

### Theoretical Framework

The need for automized recognition of epileptic seizures was seen by researchers and (Gotman et al., 1979) suggested the first efficient method “the spike and sharp wave recognition” which had good accuracy and provided a shred of evidence on one of the most reliable features of a seizure which is a spike in the EEG recording that has a huge amplitude and lasts for almost 70 milliseconds. An EEG recording is chaotic by its nature and defining robust features of any abnormal behavior could be challenging with the need for well-trained experts and feature engineers. With the advancement of technologies, new methods appeared with machine learning algorithms then deep learning architectures. Both methods mainly rely on two key components for automized seizure detection and classification which are feature extraction or learning phase followed by a classification phase.

At this point, there is a wide variety of ML algorithms and DL architectures with many ways of training and evaluation methods based on different metrics. Some of the conventional ML algorithms for feature extractions include PCA and LDA while SVMs, logistic regression, K-nearest neighbors and decision tree algorithms are used for the classification. DL architectures include NN, CNN and RNN which are used for the feature learning and classification processes with high accuracies and an intensive focus is directed on them by researchers to test their capabilities on divergent types of problems. In the field of epileptic seizure recognition, many ML algorithms and DL architectures have been tested over the years.

The team of (Nandy et al., 2019) has tested their approach on the CHB-MIT database.

They used MOEA as a feature selection algorithm after the EEG averaging extraction algorithm to choose the optimal features then they tested three classifiers. LDA, QLDA and SVM as classifiers, the accuracies were 76.41%, 80.79% and 97.05% respectively.

The problem with the machine learning approach was with the feature extraction and selection phase since they were handcrafted either with human experts or algorithms and that was a crucial limitation for this approach which compromised reliability and optimal classification accuracy.

In the deep learning approach, the features are not extracted or selected, they are learned by the model which eliminated the previous limitations. Many research teams tested deep learning architectures as artificial neural networks ANNs and their variations and convolutional neural networks CNNs and their variations, the most successful architecture, arguably, in the field is 2D-CNN since it was tested many times and gave the highest accuracies. Also, many pre-trained architectures are used in the field as AlexNet, VGGNET and DenseNet (Shoeibi, Khodatars, et al., 2021).

As a general view on the theoretical frameworks that were used for epileptic seizure detection, a divergent set of DL methods will be presented. In (Hossain et al., 2019), a CNN with AE, a semi-supervised method, model was used to learn the general structure of a seizure from Boston Children's Hospital epilepsy dataset then it was evaluated for cross-patient EEG data and it gave an average accuracy of 99.46%. In another study, the team in (A. Abdelhameed & Bayoumi, 2021) suggested a novel method of supervised deep convolutional autoencoder (SDCAE), they evaluated some variations of it giving an average accuracy of 98.79% for the best one. For the same purpose, (A. M. Abdelhameed et al., 2018) based on the Bonn dataset, evaluated Bidirectional Long Short-Term Memory (Bi-LSTM) which is a variation of recurrent neural networks (RNNs) on two classes, normal and ictal (seizure) states, and three classes, normal, inter-ictal and ictal states. The average accuracies were 100% and 99.33% respectively. Other research teams focused on recurrent neural networks and their variations other than LSTM like Gated Recurrent Unit (GRU), for example, (Talathi, 2017) evaluated the previous method which resulted in an overall accuracy close to 100%. While most of the previously mentioned methods were supervised or semi-supervised models, the team in (Zhou et al., 2018) used an unsupervised deep belief network (DBN) which gave an accuracy of 96.87% and promising use for unsupervised methods.

The overall view on the field suggests that automatically extracted features and classifications out-perform the human-engineered ones and with the technological advances, seizure detection can be less costly, more accurate, easier and reliable.

**Related Work**

Next, the papers which were shown in the comparison tables will be presented as the related work.

First, the binary classifications on the Bonn dataset were presented by (Nagabushanam et al., 2020), they proposed a NN, two-layers LSTM and four-layers improved neural network and their results on Adam optimizer, binary cross-entropy loss function, Relu activation within the layers and sigmoid activation for the output layer are recorded. they got accuracies of 61.43%, 71.38% and 78.92%, precisions of 62.72%, 71.66% and 72.98%, sensitivities of 61.65%, 73.38% and 93.70% and F1-scores of 62.18%, 72.51% and 82.05% for the NN, LSTM and the improved NN respectively.

For the same purpose, the team in (S.-H. Lee et al., 2014) proposed a combined method that uses wavelet transform, phase-space reconstruction and Euclidean distance built on a NN with fuzzy membership functions and reported a 96.33%, 100% and 98.17% for sensitivity, specificity and accuracy respectively.

In another study, (Wang et al., 2019) did many tests and evaluated with Symlets wavelets, statistical mean energy std and PCA, GBM, RF, SVM techniques on 10-fold-cross validation, the evaluation on the Bonn dataset that regarded a seizure and non-seizure (all other labels) scenario gave an accuracy of 98.4% as an SVM –GSO binary classifier.

Türk and Özerdem (2019) used CNN with scalogram technique, they applied Continuous Wavelet Transform to EEG records to get the 2D frequency-time scalograms then the images were given as an input into two convolutional layers then to a 1000-neurons dense layer. the team reported many binary classification cases depending on the input dataset, the closest results for the comparisons with our scenario (ABCD-E equivalent) were the ones with the E (seizure) subset as one of them. the accuracy, sensitivity, specificity and f- Score were, for A-E input 99.50%, 99.00%, 100% and 99.50%, for B-E input 99.50%, 100%, 100% and 99.50%, for C-E input 98.50%, 98.01%, 98.98% and 98.50% and for D-E input 98.50, 98.01%, 98.98% and 98.50% all respectively.

In some older studies, (Polat & Güneş, 2007) used a hybrid classifier based on fast Fourier transform (FFT) and decision tree and they recorded an accuracy, specificity and sensitivity of 98.72%, 99.31% and 99.40% for 10-fold-cv and 98.68%, 98.50% and 98.87% for 5-fold-cv, they evaluated their classifier on the Bonn dataset.

Authors in (Abiyev et al., 2020) used a deep CNN architecture with four double convolutional layers, three max-pooling layers one after each double convolutional layer, global average pooling layer after the last convolutional layer for the feature learning and four dense layers for the classification with rmsprop optimizer, Relu activation within the network and softmax activation for the output layer and 10-fold-cv which gave testing loss, sensitivity, specificity and accuracy of 0.013878, 96.67%, 98.33% and 96.67% respectively and the model was reproduced and tested for our input cases.

Also, the stacking ensemble-based deep neural network model (SEA-DNN) gave a high performance that qualifies it to be a decision support system for clinical diagnosis according to (Akyol, 2020) which reported an accuracy, sensitivity and specificity of 97.17%, 93.11% and 98.18% respectively.

The paper (Hassan et al., 2020) proposed the complete ensemble empirical mode decomposition with adaptive noise (CEEMDAN) which was employed on many cases of the Bonn dataset, the one of interest is the A-D-E case which gave an accuracy, sensitivity and specificity of 98.67%, 98.67% and 98.72% respectively.

In (Thara et al., 2019), four different feature scaling techniques were evaluated using a deep neural network of four dense layers, Relu activation within the layers and sigmoid output activation for the binary classification. The StandardScaler with mean square error loss scenario achieved an accuracy of 97.21%, Sensitivity of 98.17% and Specificity of 94.93%.

In another binary classification method, (Ullah et al., 2018) suggested pyramidal 1D-CNN (P-1D-CNN) which was evaluated on the Bonn dataset with 10-fold-cv. In the BD-E case, it reached an accuracy of 99.6%.

For the same problem of binary classification, (Vipani et al., 2017) proposed a scheme of Hilbert transform with learning vector quantization based classifier, its average accuracy found to be 89.31%.

Another binary classification method used by (Gupta & Pachori, 2019) included noise addition to the EEG recordings of the Bonn dataset and evaluating different classifiers, the one of interest is the ABCD vs E case with FBSE based rhythms of EEG signals, WMRPE and regression classifier with 10-fold-cv which yielded an accuracy of 98.6% on the noiseless input.

A genetic algorithm approach was implemented and evaluated on the UCI version of the Bonn dataset for binary classification of seizure vs non-seizure classes and achieved an accuracy of 98.01%, a sensitivity of 94.99% and specificity of 98.65% based on 10-fold-cv by (Al-Sharhan & Bimba, 2019).

In another case of interest on multiclass classification with the Bonn dataset, subsets B, D and E were used for healthy, preictal and seizure classes respectively. Using a 13-layered CNN proposed by (Acharya, Oh, Hagiwara, Tan, & Adeli, 2018), an accuracy of 88.7%, a specificity of 90% and a sensitivity of 95% were reported.

The orthogonal wavelet filter banks method was suggested for epileptic seizure detection by (M. Sharma et al., 2017) which was evaluated on the Bonn dataset for seizure vs seizure-free classes, corresponding to CD vs E subsets, and seizure vs non-seizure classes as ABCD vs E. the first evaluation reached an accuracy of 99%, a sensitivity of 98% and a specificity of 99%. while the second evaluation reported 99.2%, 98% and 99.75% for accuracy, sensitivity and specificity respectively.

The authors in (Bhattacharyya et al., 2017) developed a system with tunable-Q wavelet transform to decompose EEG signals to sub-bands, then use K-NN to select the optimal features from the sub-bands, then feed the features to SVM classifier which obtained an accuracy of 98.6% for three-class classification on the Bonn dataset subsets equivalent to AB-CD-E case.

Reference (Bhattacharyya & Pachori, 2017) evaluated a random forest classifier fed by multivariate extension of EWT as a feature extraction method which used CHB-MIT dataset EEG inputs that have a seizure and non-seizure labels (binary) and obtained an accuracy, specificity and sensitivity of 99.41%, 97.91% and 99.57% respectively.

In (Martis et al., 2012), researchers suggested deploying their method on large scale clinical validation, which consists of empirical mode decomposition features fed to C4.5 random forest classifier tested on the three classes in the Bonn dataset, namely, normal, inter-ictal and ictal activity. their method yielded 95.33% average accuracy, 98% average sensitivity and 97% average specificity.

In (Acharya et al., 2012), the authors decomposed the EEG signals of the three categories in the Bonn dataset namely, ictal, inter-ictal and healthy, by wavelet packet decomposition (WPD) then used a Sugeno fuzzy classifier to get 99%, 96%, 95% and 96.7% for specificity, inter-ictal sensitivity, ictal sensitivity and accuracy respectively.

Recurrence quantification analysis (RQA) parameters were used to quantify the importance of the features of the EEG signals categories of normal, inter-ictal and ictal from the Bonn dataset then feed the features to the SVM classifier which reached 95.6% accuracy, sensitivity and specificity of 98.9% and 97.8%, respectively according to (Acharya, Sree, Chattopadhyay, et al., 2011).

In another multiclass study, the equivalents of the A-D-E subsets of the Bonn dataset were evaluated by (Guo et al., 2011) with genetic programming (GP) feature extraction approach and K-NN classifier which obtained an accuracy of 93.5%.

The authors in (Acharya, Sree, & Suri, 2011) tested the SVM classifier based on radial basis function (RBF) kernel with WPD as an extension on the discrete wavelet transform (DWT) for feature extraction using 3-fold-cv which gave an accuracy of 96.3%, sensitivity of 100 and specificity of 97.9%, note that the authors considered the ictal and inter-ictal cases as one class of positive test (C, D and E) and the other healthy categories as a negative test (A and B), from the Bonn dataset.

In (Faust et al., 2010), the authors used one subset from the healthy class (A or B), one subset from the preictal class (C or D) and the seizure subset (E) of the Bonn dataset to evaluate many models, the best was the SVM classifier which reached an accuracy of 93.3%, a sensitivity of 98.3% and a specificity of 96.7% and it outperformed the evaluated ANN 4-layered architecture.

The research in (Chua et al., 2011) did another multiclass evaluation on the ictal, preictal and normal classes of the Bonn dataset with higher-order spectra (HOS) features and GMM classifier which achieved 93.11% average accuracy, 89.67% preictal sensitivity and 94.83% preictal specificity.

The research team in (Ghosh-Dastidar et al., 2008) presented the PCA-enhanced cosine radial basis function neural network classifier which achieved the highest accuracy on the binary classification of a subset of the inter-ictal(C or D) and a subset of the normal categories (A or B), as the most difficult ones to be distinguished by clinical experts, of the Bonn dataset reaching 99.3%. In (Ghosh-Dastidar et al., 2007), using the mixed-band feature space with the LMBPNN method on one of the normal, one of the preictal and the ictal classes of the Bonn dataset, the authors achieved 96.7% accuracy as the best method in the study. For the same purpose and with the same dataset settings, (Ghosh-Dastidar & Adeli, 2007) developed and evaluated another model, SNN with RProb learning algorithm, an accuracy of 92.5% was achieved.

Finally, (Shoeibi et al., 2022) presented many works and useful summaries are shown in (Shoeibi et al., 2022, fig.9).

# CHAPTER III

## EEG and Epileptic Seizures

This chapter presents the EEG data, epilepsy, seizures with some discussions on the collection methods of EEG data and sample figures of different brain activities.

### *EEG and Epileptic Seizures*

Electroencephalography is the measurement of electrical brain activities that represents the various states of modality.

An EEG can be acquired in two main ways, generally, an invasive method or a non-invasive method. The non-invasive method is the one used in the Bonn dataset recordings and it is the easier way but at the expense of performance. Usually, a matrix of electrodes is put on the scalp surface area to collect the EEG signals which make it a safe method. Invasive method, on the contrary, the electrodes are put inside the scalp within the brain which needs surgery and makes it risky although it can give better performance compared to the non-invasive methods.

EEG signals can be captured with devices as the brain-computer interfaces that vary depending on the application in sampling rates, filtering or other factors. Some open source hardware for EEG recordings are available as openBCI, then further processing can be done with any software designated for EEG analysis, a free software example is EEGLAB that works with MatLAB or other tools. The devices usually have the electrodes arranged in a specific placement as the 10/20 standard. Each electrode is oftenly called an EEG channel, in the Bonn dataset there are 500 channels representing the whole dataset (McGill, 2021) (Jebelli et al., 2018). Next in figure 1 the 10/20 electrode placement is shown and figure 2 presents a brain-computer interface device as a cap of EEG recording electrodes.

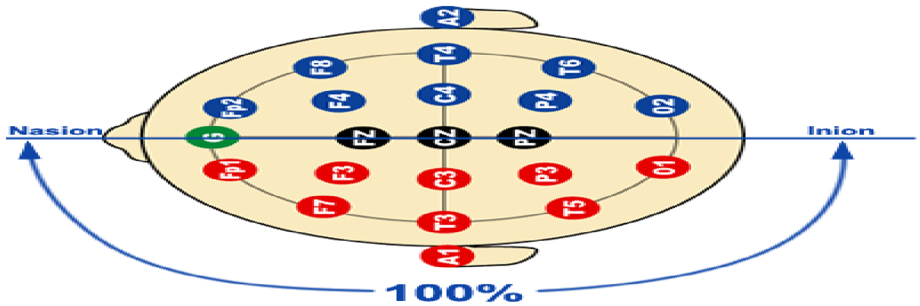


Figure 1
*McGill (2021, 10/20 System of electrode placement)*

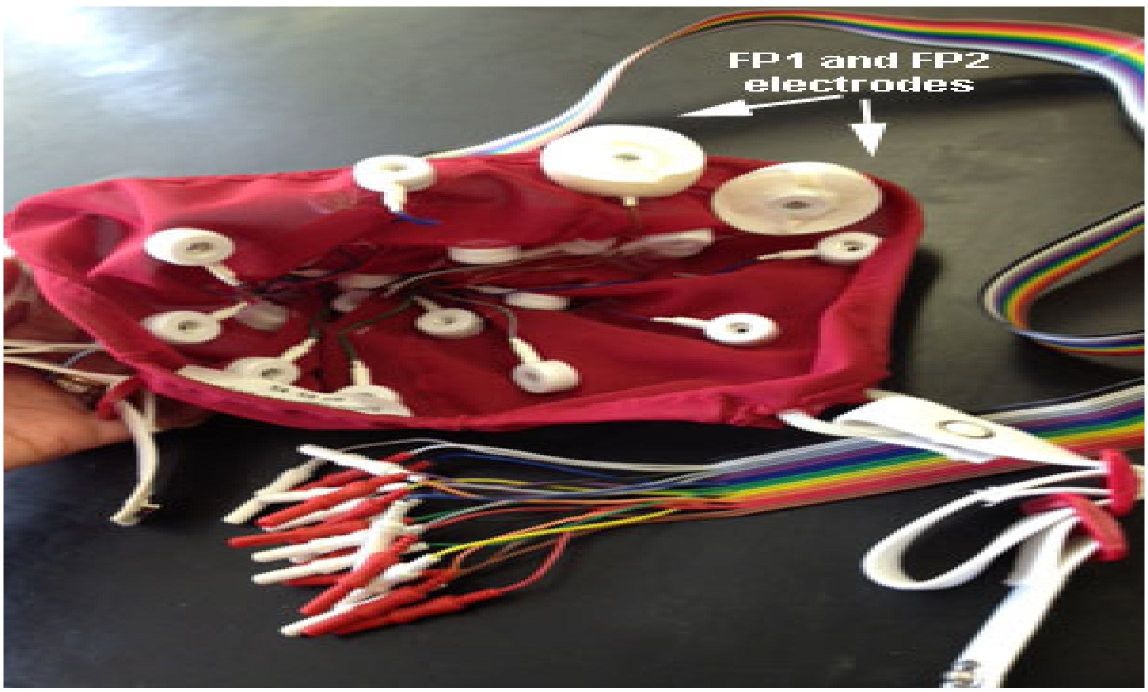


Figure 2
*McGill (2021, EEG electrodes)*

The neuronal signals are extracted from the raw EEG signal after removing the noise, muscle and eye movements and other unwanted artifacts which generates the final EEG that can be used for further analysis with DL, ML or any other operations (Waldert, 2016).

Some applications and fields that rely upon EEG data include sleep studies, cognitive performance measurements, emotional state measurements, cognitive behavioral therapy, stroke rehabilitation, neuroscience, brainwave gaming and many others. It can be noticed that EEG data can be used in a wide range of applications from health care to entertainment (Emotiv, 2021).

Epilepsy is a neurological disorder that presents itself as periods of consciousness loss due to a sudden rush of electrical signals in the brain. The sudden electrical rushes are called seizures and they can vary in their effects from undetectable brief periods to vicious shaking and loss of awareness.

Epileptic seizures are mostly recognized by abnormal electrical brain activity and EEG is the measurement of that, so EEG is considered one of the best ways to detect and classify the seizures or the abnormalities of the brain activity, in general (WHO, 2022).

The old method of epileptic seizure detection was manual detection by eye which was done by clinical experts who look to screens presenting EEG recording and decide if there is a seizure or not. That method is exhausting, takes long time and is subjective depending on the expert opinion.

Modern methods are mainly characterized by automatic detection of seizures and classification. ML methods still rely on the human factor to construct the features that need to be fed to the classifiers which was a liability. DL methods are the most common now since they eliminate the human factor almost entirely, a feature learning process takes the place of feature engineering in ML.

The previously discussed reasons encouraged us to pursue the thesis work based on DL methods and propose the preprocessing and combinations of EEG data since it is never tested in the way we did it.

Another related class of brain activity is the preictal category which is usually the phase in between seizures (inter-ictal) or directly before a seizure as an indicator of its forthcoming. EEG recordings have many ways of presentation like time domain, frequency domain or others. The Bonn dataset is a time series in time domain presentation. Also, EEG signals have different ranges of values, but on average it is between 0.05 to 0.1 millivolts for the normal activity while seizure activity ranges between -0.5 to 1.0 millivolts. The toughness of the problem manifests as the abnormal ranges of EEG signals do not necessarily mean a seizure is happening, there might be other factors to cause it (Das et al., 2020). Figure 3 shows an EEG sample with time and frequency rhythms.

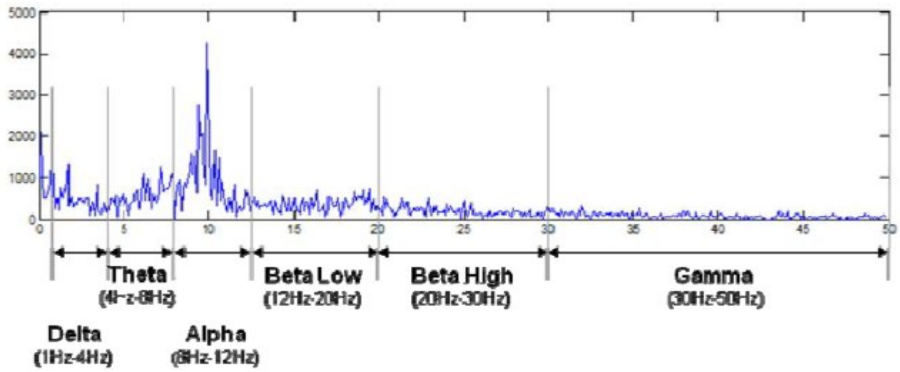


Figure 3
*Roman-Gonzalez (2010, Fig 2.) EEG Rhythms In Time And Frequency Domain.*

Another way to look into the different brain activities is frequencies as it was noticed in figure 3. The commonly studied average range of a normal EEG recording is between 0.5 to 30 hertz, divided into five bands known as delta from 0.5 to 4 hertz, theta from 4 to 7 hertz, alpha from 8 to 12 hertz, sigma from 12 to 16 hertz and beta from 13 to 30 hertz (Nayak & Anilkumar, 2021). Higher frequencies might still be considered normal. After entering the range of 80 to 100 hertz, preictal activity indications have been reported and seizure activity is associated with frequencies higher than 100 hertz (Stamoulis et al., 2012).

### *EEG Data Samples*

Some samples of EEG signals will be presented. A seizure form, a healthy/normal form and a preictal brain activity are also presented in 4, all the samples of it are from the UCI-Bonn dataset. In figure 5, all the samples are from another dataset presented by (Swami et al., 2016) shown to give clearer visualizations of the EEG data. Note that the x-axis data are time series points and y-axis data are amplitudes in microvolts, in the UCI-Bonn dataset each 178 points of time series represent 1 second and in the dataset of (Swami et al., 2016) each 1024 points represent 5.12 seconds.

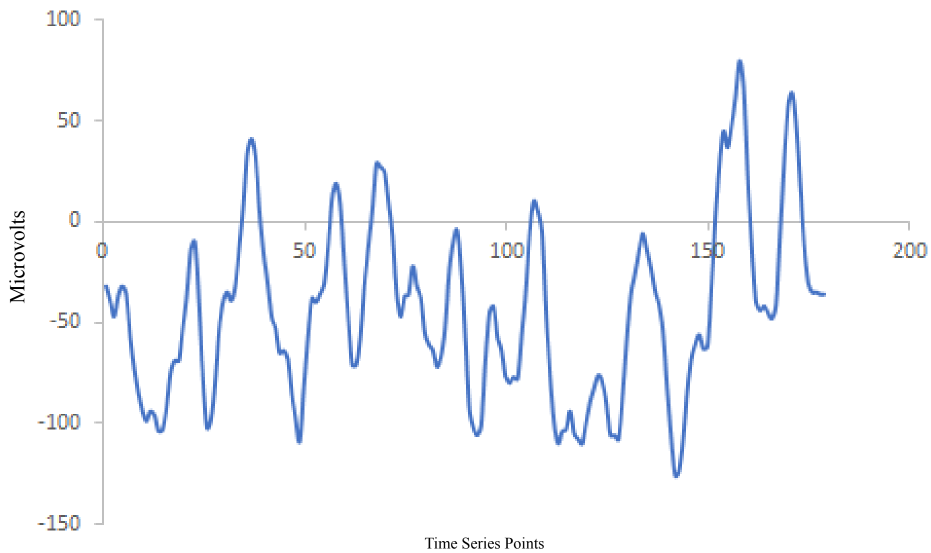


(a) Normal Activity

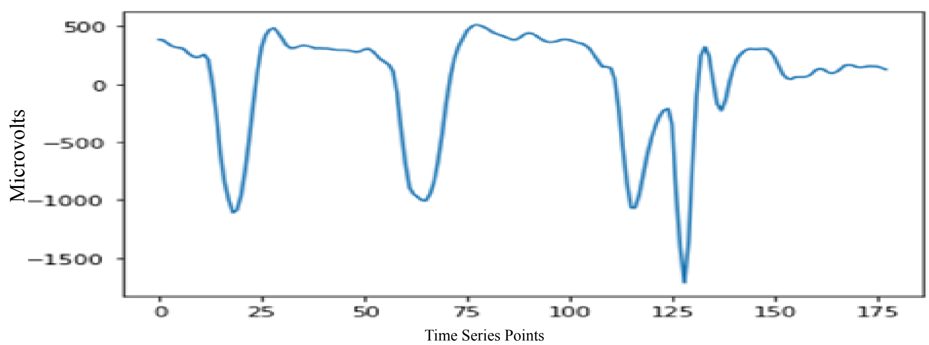


(b) Seizure Activity

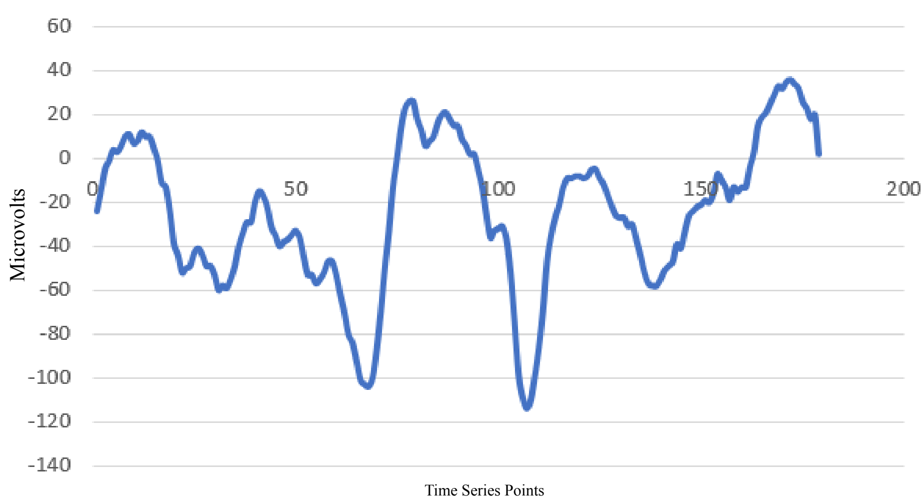


(c) Preictal Activity

Figure 4
EEG Signals Of Various Brain Activity

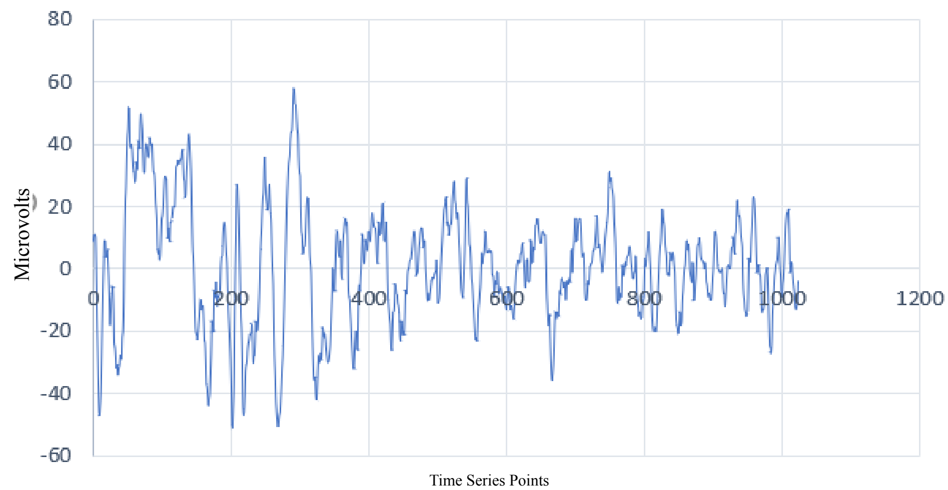

(a) Normal Activity

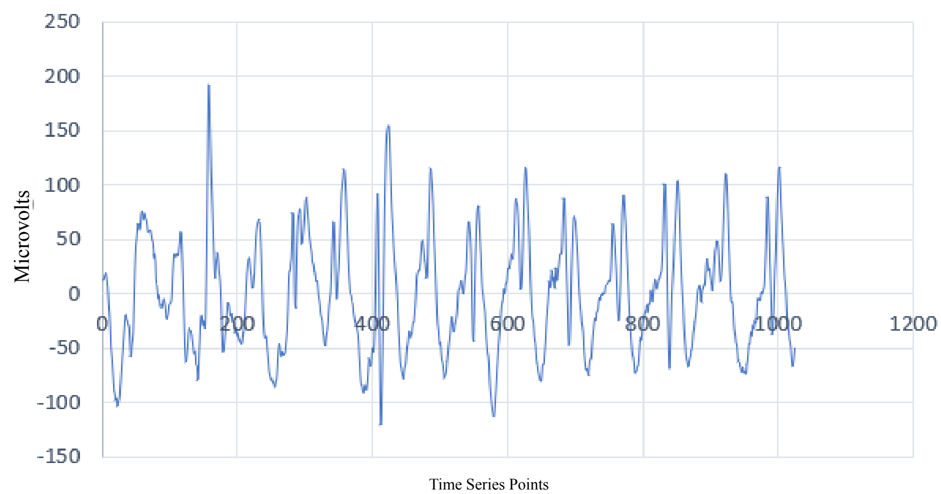

(b) Seizure Activity

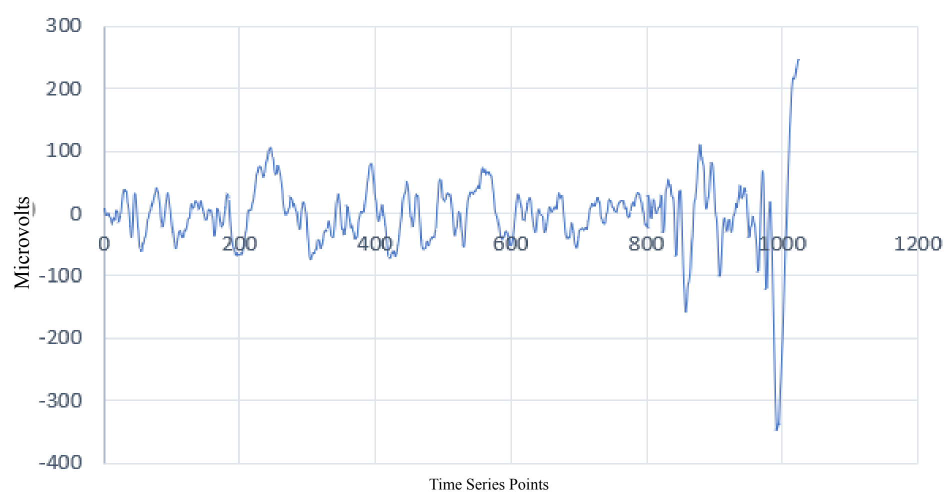

(c) Preictal Activity

Figure 5
EEG Signals Of Various Brain Activity, Additional Samples

# CHAPTER IV

# Deep Learning

This chapter discusses the concepts of deep learning and presents the different parts that were used in the thesis. The first section goes through the various neural network types and their related components. In the second section, the activation functions applied in the thesis are discussed, then in the third section the loss functions, then the optimizers in the fourth section and lastly the various metrics and scores used in the thesis.

## Deep Neural Networks

Neural networks were built to mimic the organic neural networks of humans mainly. They consist of units called neurons arranged in layers. Usually, any network that has more than three layers between the input and output is considered deep. The next section will go through the different types of layers and present their functionality.

### *Learning Types Of Deep Learning*

ML is a subset of artificial intelligence (AI), it is basically a system that can learn from an input dataset and get smarter over time, in terms of accuracy and prediction for instance, based on an algorithm and it usually learns from small datasets. While DL, which can be seen as a subset of ML, relies on big datasets for its learning process, it is conceptually equivalent to ML, but its algorithms are different. The learning process is usually called training and it could take a long time depending on the dataset size, data type and algorithms. it is mainly done on specific types of hardware different from regular processors, there are many cloud services dedicated to training DL or ML algorithms since its needed hardware and processing power are difficult to acquire, costly and might be unnecessary or useless for other tasks.

Starting with Learning, it has three main types in both ML and DL which are supervised learning, unsupervised learning and reinforcement learning. In supervised learning the algorithm is given a target or outcome variable that must be predicted from labeled input datasets by generating a mapping function and the training will be kept going until a certain accuracy level is reached. Unsupervised learning on the other hand does not have a given target for prediction and it deals with unlabeled datasets, it is widely used for image segmentation and clustering as it has the capability to uncover hidden patterns and groupings, from the human perspective, on its own. Reinforcement learning is the training of a model or algorithm for consequence decision-making processes by setting rewards and penalties on its decisions and the model has to come up with a way, sequential decisions, that maximizes the reward.

***Neural Networks***

They are the core of DL algorithms that were built to simulate the natural/organic neural networks as layers of connected neurons. NN consist of multiple serial algorithms that takes input datasets, analyze them to find underlying relationships and give the output. The basic functionality of the neuron is multiplying its input with weight then adding a bias value. The weights are assigned randomly at first then the model keeps changing them to obtain the best results. The layers that do the processing are the hidden layers or dense layers which are between the input and output layers. The consequently connected dense layers with the input and output layers can be then considered as a classifier or a neural network. Next, in figure 6 a general diagram represents the NN.

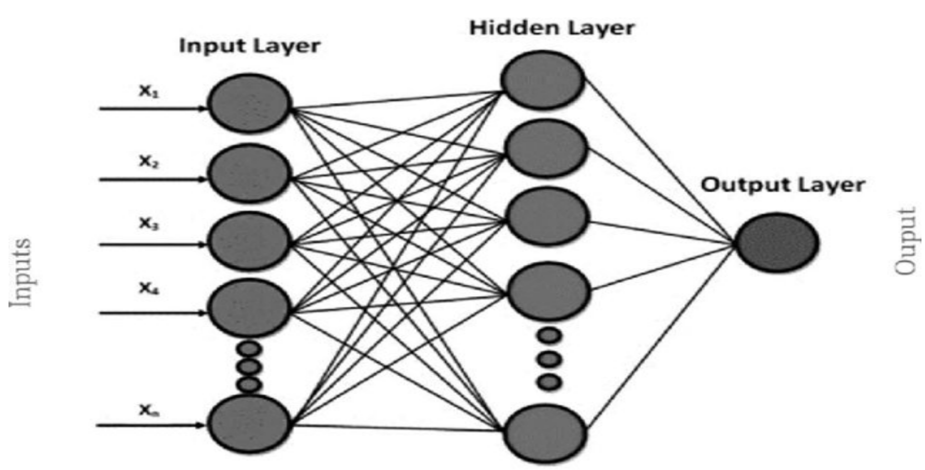


Figure 6
*Karadurmuş et al. (2019, fig.2), NN Diagram.*

### *One Dimensional Convolutional Neural Networks*

Convolutional neural networks usually have convolutional layers before the dense layers that do the classification. CNN is another class of networks that was built mainly to analyze pixel data, so it is the most used architecture of DL in image segmentation and processing. It takes relatively less pre-processing compared to traditional methods of image analysis and with unsupervised learning it could be independent of any expert intervenes which makes it a simple yet powerful method especially for image segmentation and feature extraction which then are fed to the dense layers for classifications. Although CNNs were built for images (2D) they are also used with one dimensional (1D) data as EEG signals. In python TensorFlow, the 1D-CNN takes an input matrix of three dimensions (x, y, z), for signal input, the z dimension can be added as one to keep the data the same. Convolutional layers can be seen as filters enforced on the input data to extract features by doing element-wise product and sum up the results in a feature map. Next, in figure 7 a general diagram represents the 1D-CNN.

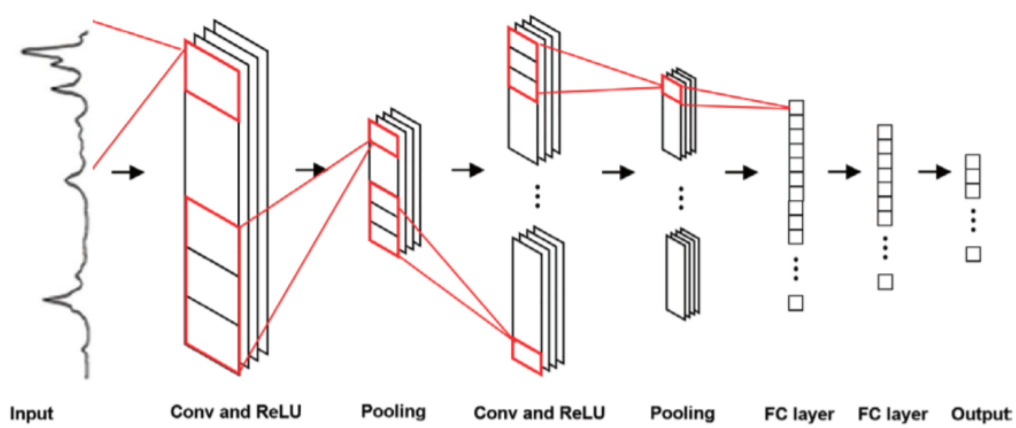


Figure 7
*Mozaffari and Tay (2020, fig.1), 1D-CNN Diagram.*

The next figure represents the convolutional operation that takes place in the convolutional layers.

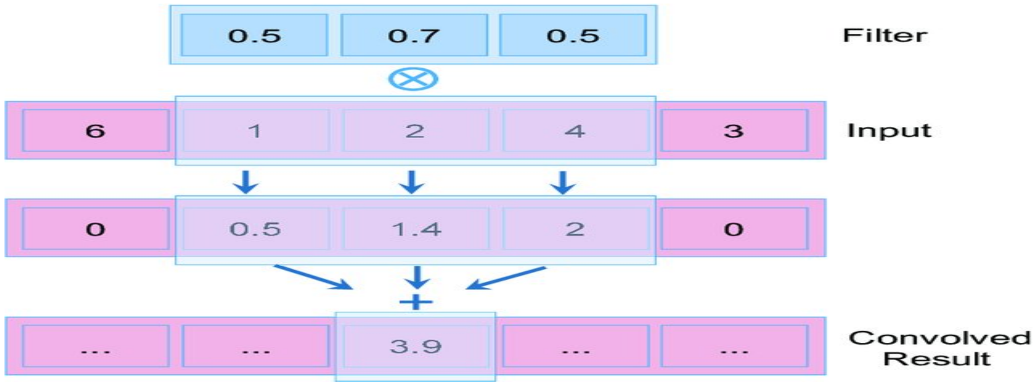


Figure 8
*Mujeeb et al. (2019, fig 3.), Convolutional Operation In Convolutional Layers.*

## Layer Types

### *Fully Connected and Dropout Layers*

The layers of any neural network can be either fully connected or partially connected. The partially connected ones must have randomly assigned units of zero value to prevent them from passing their output. A dropout layer does the previous operation. They are applied during the training phase of the model. The primary benefit of dropout layers is to help models avoid overfitting. The position of the dropout layer, among other layers, might be crucial in some networks, however, in our thesis the position was irrelevant as it was tested in many positions and nothing changed.

### *Maxpooling Layers*

Maxpooling layers are usually used within the convolutional layers to reduce vector sizes. This is done because of the selection operation which chooses the maximum values of the feature map within a region matching the layer size which was 2*2 in (Abiyev et al., 2020) model. The output of the maxpooling layer contains the most outstanding features of the feature map input. Next, in figure 9 the maxpooling operation is shown.

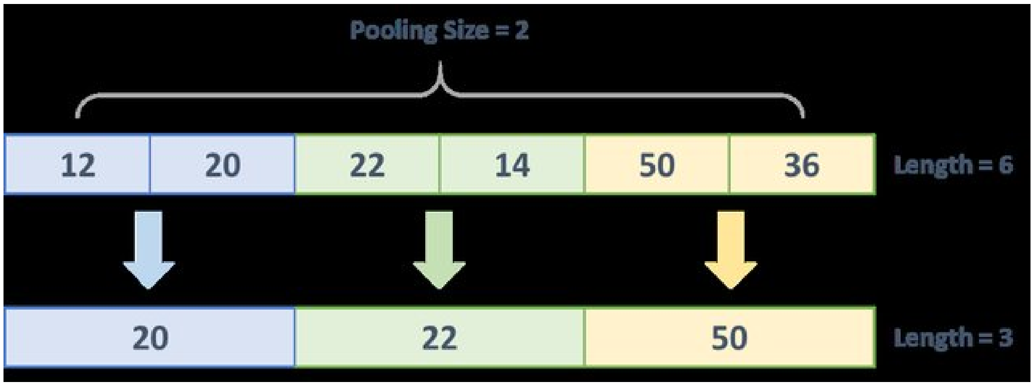


Figure 9
*Ragab et al. (2020, Fig 3.), Maxpooling.*

***Global Average Pooling Layers***

Unlike maxpooling, the average pooling chooses the average of the region of the layer in the feature map. The global operation means that the average pooling is done by reducing the feature map to a single value. So, the output of the global average pooling layer has one dimension less than the input. Next, in figure 10 the global average pooling operation is shown.

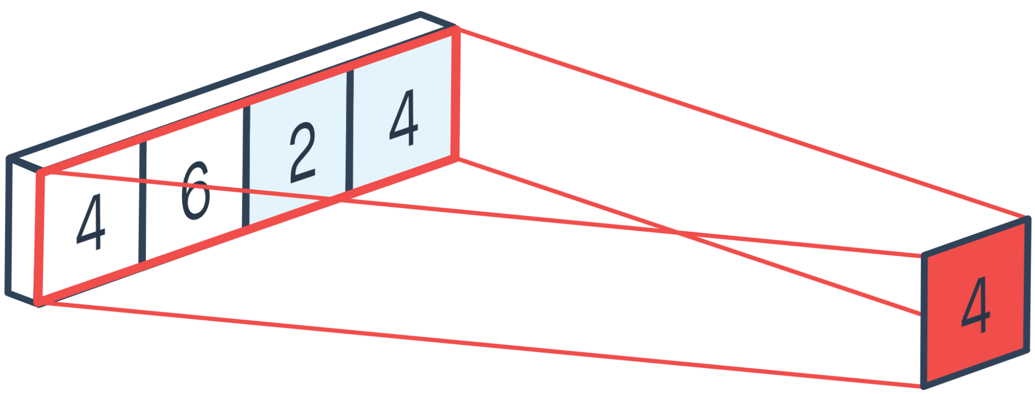


Figure 10
*Peltarion (2022), Global Average Pooling 1D.*

**Activation Functions**

The neurons that build the neural networks generally have one simple operation which is to multiply the input values with weights and add a random value of bias and because of that, it can have an infinitely vast variety of values without any decision-making system, so here activation functions come to help in making the decision based on a specific function. There are many activation functions within neural networks, the ones used in the thesis will be explained.

***Relu***

Relu activation function is a basic one used within the hidden layers usually, it prevents any negative values from passing to other neurons and layers. because of its simplicity, it shows excellent performance and reduction training time compared to some other activations as the hyperbolic tangent or sigmoid activation function, also Relu function rectification helps resolve the vanishing gradient issue. The mathematical form of the rectified linear unit Relu is shown in equation 1, in (O. Sharma, 2019) more details might be seen. Also, figure 11 shows the Relu function.

$$Relu(x) = max(0, x) \tag{1}$$

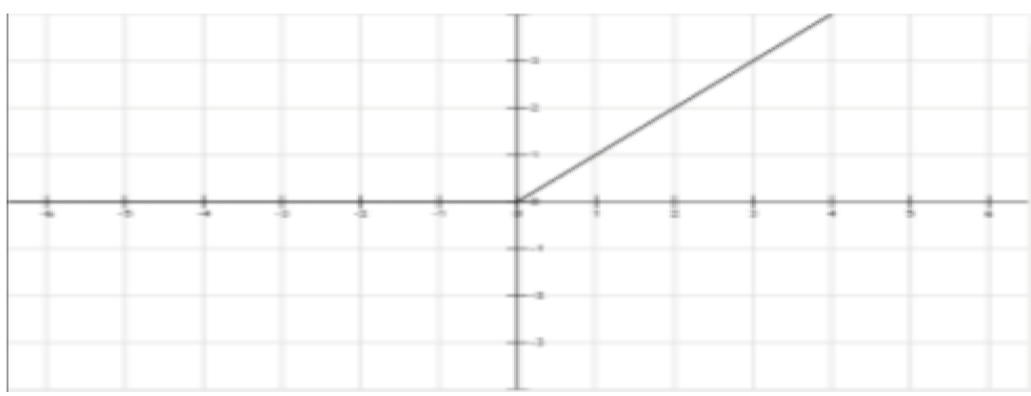

Figure 11
*O. Sharma (2019, fig 1.), Relu Function.*

***LeakyRelu***

LeakyRelu is an activation function based on Relu, however, instead of a zero slope coefficient on the negative domain, it has a small value. In python Keras documentation, the negative domain slope coefficient by default is 0.3, since EEG data have negative values that are permitted to pass by LeakyRelu it was preferred in two models.

The mathematical form for LeakyRelu is in equation 2, (O. Sharma, 2019) explained this activation function deeply among other ones. A visual representation of the LeakyRelu function is shown in 12.

$$LeakyRelu(x) = \begin{matrix} x, & if\ x >= 0 \\ \alpha * x, & otherwise \end{matrix} \tag{2}$$

where $\alpha$, is the negative slope coefficient.

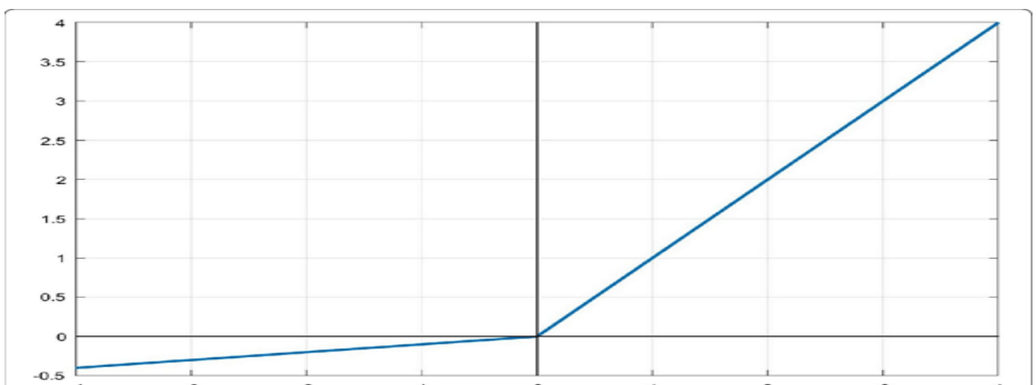


Figure 12
*vidyasheela (2022), LeakyRelu Function.*

***Sigmoid***

Sigmoid activation is usually used in the output layer to give a probability between zero and one for the output values, it was merely used for the binary classification which is the popular use of this type of activation. The mathematical form can be found in 3, also (O. Sharma, 2019) presented it. A visual representation of the sigmoid function is shown in 13

$$Y = \frac{1}{1 + e^{-x}} \tag{3}$$

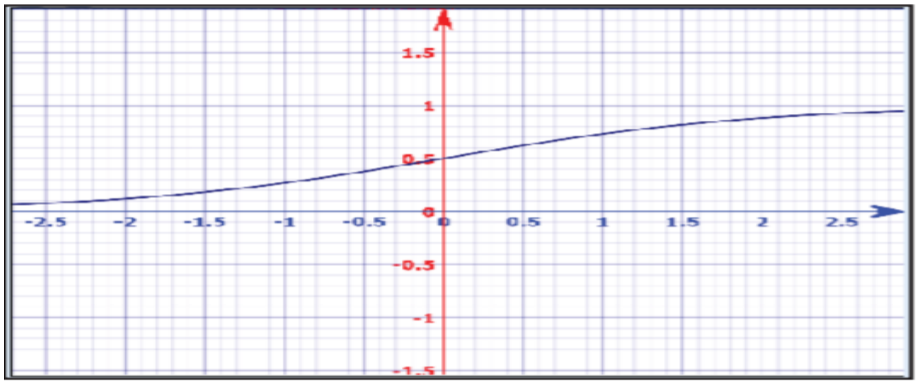


Figure 13
*O. Sharma (2019, fig 2.), Sigmoid Function.*

### *Softmax*

Softmax activation, On the other hand, is more popular for multiclass classification problems and claims more effective results, its output is a set of probabilities, presenting each class, that sum up to one. The highest probability value can be considered as the output prediction label. In figure 14, the softmax function is presented as a graph and in (Chen et al., 2017) more information can be found.

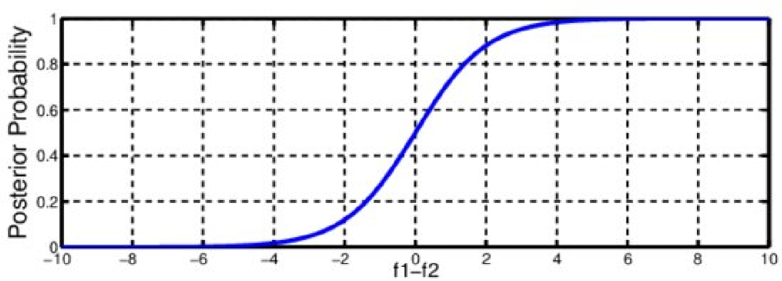


Figure 14
*Chen et al. (2017), Softmax Activation.*

## Loss Functions

Loss function or cost function can be considered as a method of quantifying the goodness of the model and its performance, this is done by computing the difference between the current output and the true expected one. They mainly have two types, a regression type that deals with continuous values of predictions and a classification type that deals with binary and multiclass situations.

binary crossentropy loss function was the one used for all the binary models. It gives a probability between zero and one as a classification result, then it calculates the average difference between the output probabilities and the ground truth labels.

sparse categorical crossentropy was the loss function for the multiclass problem in all models. It has a similar function to the binary crossentropy, but it deals with three classes, in our case, labeled as 0, 1 and 2. Since the classes in our problem are mutually exclusive, sparse categorical crossentropy was the preferred function. Another alternative is the categorical crossentropy loss function which is usually preferred for multilabel tasks when outputs can have many labels, however, it requires one-hot encoding (T.-H. Lee, 2008). Note that the loss functions names are put as they were named in Keras.

**Optimizers**

Optimizers or learning algorithms are crucial hyperparameters. They update the model parameters in the backpropagation process to reduce the loss function values and increase the efficiency, choosing a bad optimizer may lead to longer training times or over-fitting due to the difficulty of model updates.

The only applied optimizer was the root mean square propagation (rmsprop), which is a gradient-dependent technique that helped give a high-performance training with relatively medium training times. It is one of the most used optimizers in DL field (Postalcıoğlu, 2020).

# CHAPTER V

## Proposed Pre-Processed and Combined EEG Signals Using Deep Neural Networks

This chapter presents the novel proposed method of EEG preprocessing and combinations. It will discuss the various operations of interest with their outputs that are fed to deep neural networks for training and evaluation.

### Preprocessing and EEG Signal Combinations

The preprocessing that was used in this work is divided into standardization and combination. The standardization is also called Z-score normalization which makes the data of zero mean and one standard deviation. The combination process is done by a few steps, namely, doing the operation of interest on the original dataset, concatenating the output dataset of the previous step with the original dataset on its last column which gives double-sized signals of $178 * 2$ then standardizing the resultant dataset. The operations that were tested are squaring the signals, differentiating the dataset (discrete differentiation) and the absolute fast Fourier transform operation (FFT). Note that we took in consideration the three dataset combination , we tested original-square-FFT combination but the results were swinging between the only original and the FFT combination with the original most of the time, but more intensive evaluations should be done by other teams. Therefore, we focused on combination of 2 types of signals. Equation 4 shows the mathematical form of the standardization, equation 5 shows squaring operation, equation 6 shows differentiation operation and equation 7 presents the FFT operation formula.

$$standard_{value} = \frac{value - \mu}{\sigma} \tag{4}$$

where value is the non-standard data, $\mu$ is the average and $\sigma$ is the standard deviation. note that standardization operation is done on the data column by column.

$$squared = value * value \tag{5}$$

note that this operation was done on the whole dataset directly so value represents a dataset.

$$differentiated = \frac{x_2 - x_1 \;\; x_3 - x_2 \;\; ... \;\; x_m - x_{m-1}}{h} \tag{6}$$

where $h$ represents the step size that was assumed to be one to prevent scaling the values. This operation is done row by row, so each $x$ in the equation is a row, the operation output will have one row less ($rows - 1$, the first one) than the input.

$$absolute\ FFT = \mid FFT(x) \mid \tag{7}$$

where $x$ represents the original dataset, this operation and the differentiation in equation 6 were done by MATLAB, the FFT operation is by default done on the columns (assumes the signals as columns) which corrupted the waveforms so the dataset input was transposed the re-transposed after the output, the accurate FFT waveforms were achieved by this. The absolute value was used to get rid of the negative complex parts of the FFT output. Note that the FFT is an algorithm implemented on the discrete Fourier transform in equation 8 to give faster results.

$$X_k = \sum_{n=0}^{N-1} x_n e^{-2\pi ikn/N} \tag{8}$$

The resultant waveforms after the operations are presented for the same signal in the middle of figure 4 as examples (seizure activity). in figure 15 the standard original signal, in figure 16 the squared signal, in figure 17 the differentiated signal and in figure 18 the FFT waveform.

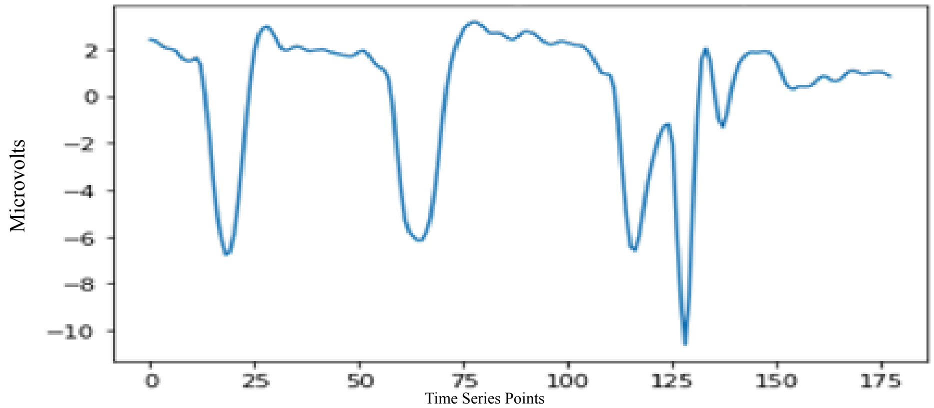


Figure 15
*Standardized Wave Form.*

It can be noticed that range values are different now.

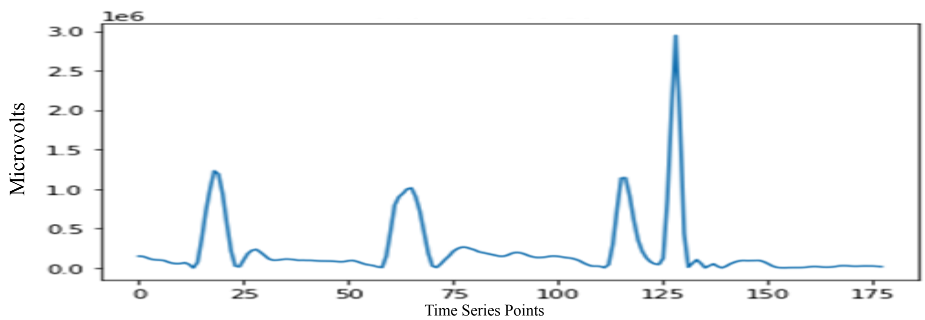


Figure 16
*Squared Wave Form.*

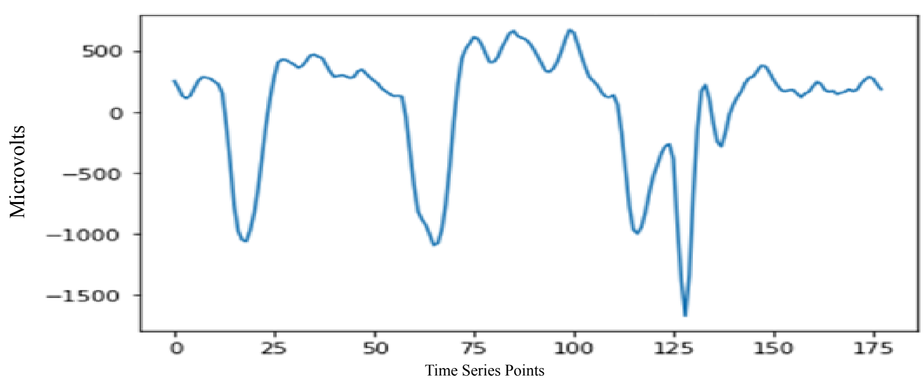


Figure 17
*Differentiated Wave Form.*

It can be seen that this waveform is slightly similar to the original wave but with sharper spikes.

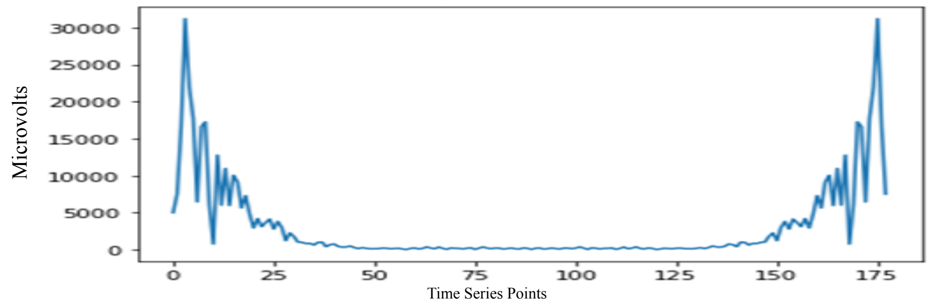


Figure 18
*Absolute FFT Wave Form.*

The combinations then are the exact figure 15 with the other operations outputs in a different range of values because of the standardization phase that is done at last. those combinations might be referred to as squared combined with original, differentiated combined with original and FFT combined with original along with the only original referring to the raw input as in the middle of figure 4 and standard original as in figure 15. Figure 19 visually represents the combined standardized inputs, which are referred as modified inputs in the next section as architecture inputs, for seizure activity, figure 20 presents the combined EEG signals for normal activity and figure 21 for preictal activity samples.

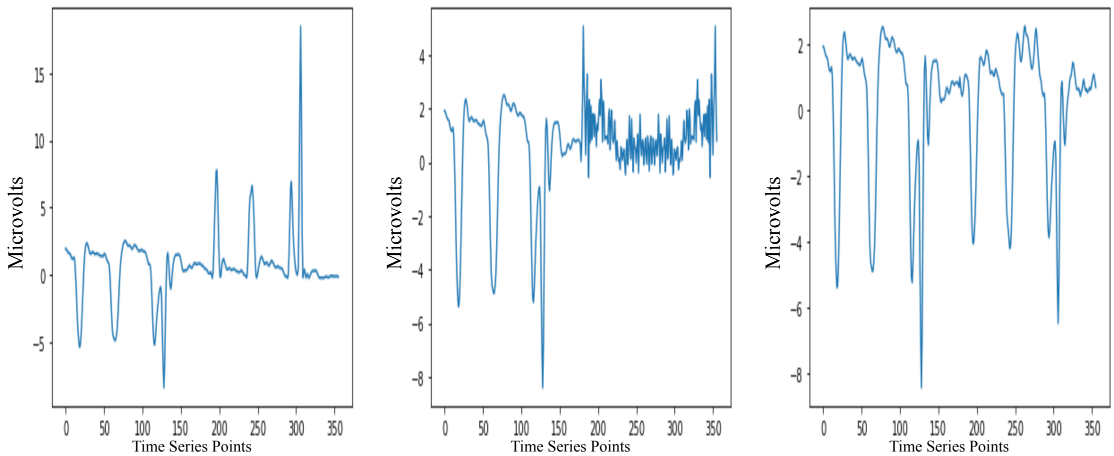


(a) The Squared signal combined with the original EEG

(b) The FFT signal combined with the original EEG

(c) The differentiated signal combined with the original EEG

Figure 19
Combined And Standardized EEG Signals Of Seizure Activity

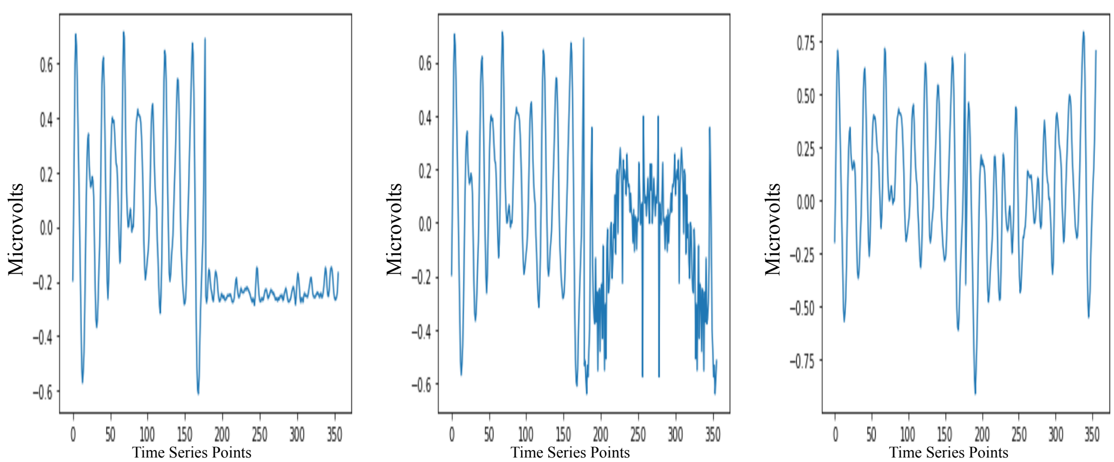


(a) The Squared signal combined with the original EEG

(b) The FFT signal combined with the original EEG

(c) The differentiated signal combined with the original EEG

Figure 20
Combined And Standardized EEG Signals Of Normal Activity

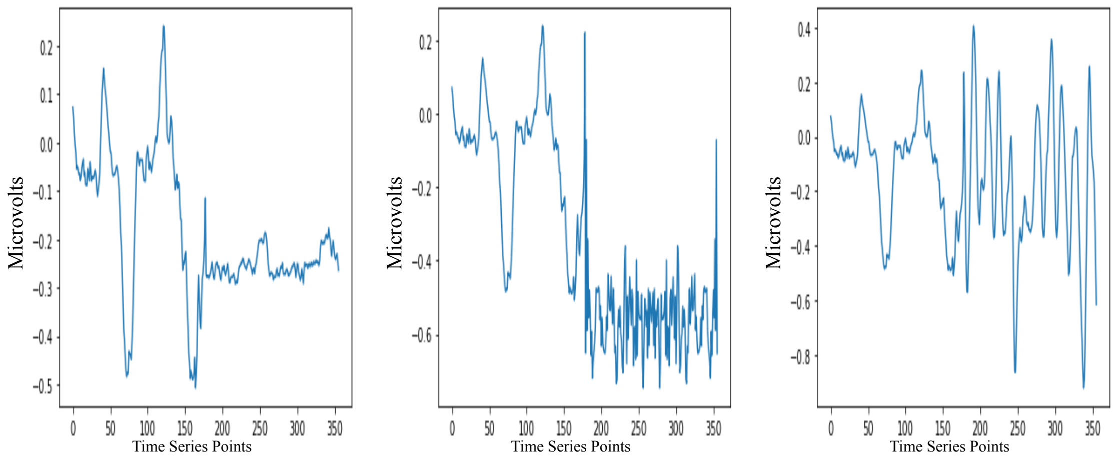


(a) The Squared signal combined with the original EEG

(b) The FFT signal combined with the original EEG

(c) The differentiated signal combined with the original EEG

Figure 21
Combined And Standardized EEG Signals Of Preictal Activity

### Deep Learning Architectures

There are three different architectures evaluated with the same input data, splitting ratios and number of repetitions which will be detailed in the next subsection. One deep neural network and two 1D-CNNs were tested, while the DNN and one of the CNNs were implemented by us for the sake of evaluations the other CNN was a reproduction of the model proposed by (Abiyev et al., 2020) which was chosen for its deepness (complexity), recent testing and validation with high performance and was published in a reputable journal with its specific details that allowed reproduction. Since the only original and the standard original cases have different sizes of the signals (178) than the combinations which had a 356 (178*2), the input layer sizes differ with them and some other values of the vectors within the architectures, especially in the 1D-CNN models, also, the binary classification models have some differences from the multiclass ones. So, the architectures will be shown to comprise the various cases as a model summary. In figure 22, the DNN model is presented for the only original and standard original cases (non-combined) and modified input (combined) cases, but the detailed view is in table 1. Note that the modified inputs are like the ones represented in figure 19 (combined) and all the input data were the 1D values of the signals not images.

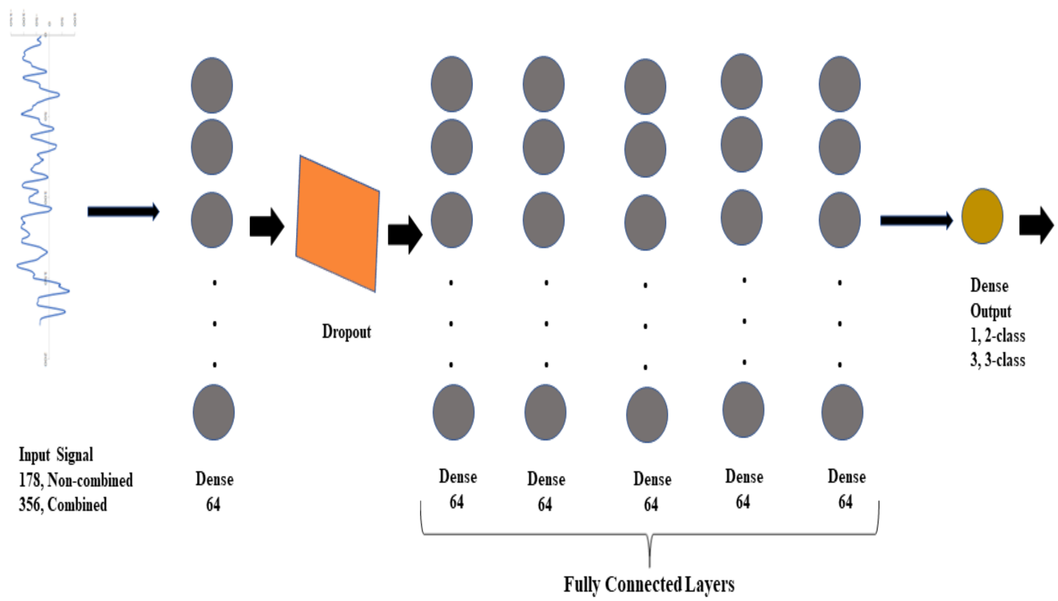


Figure 22
DNN Model

Table 1.
*DNN Model Architectures Summary, Non-combined (NC) And Combined CB Inputs*

| Layer Type | Output Shape | Number Of Parameters |
|---|---|---|
| Dense 1 (input) | 64 | NC, 11456<br>CB, 22848 |
| Dropout (0.5) | 64 | 0 |
| Dense 2 | 64 | 4160 |

continue on the next page

Table 1. (continued).

| | | |
|---|---|---|
| Dense 3 | 64 | 4160 |
| Dense 4 | 64 | 4160 |
| Dense 5 | 64 | 4160 |
| Dense 6 | 64 | 4160 |
| Dense 7 (output) | 1, (2-class)<br>3, (3-class) | 65, (2-class)<br>195, (3-class) |

The proposed 1D-CNN model for the original and standard EEG inputs (non-combined) is next in figure 23 with the modified (combined) inputs model visualization, while in table 2 the details of the model are presented. Note that there was no feature extraction process in the DNN model because there were no convolutional layers, unlike the 1D-CNN models.

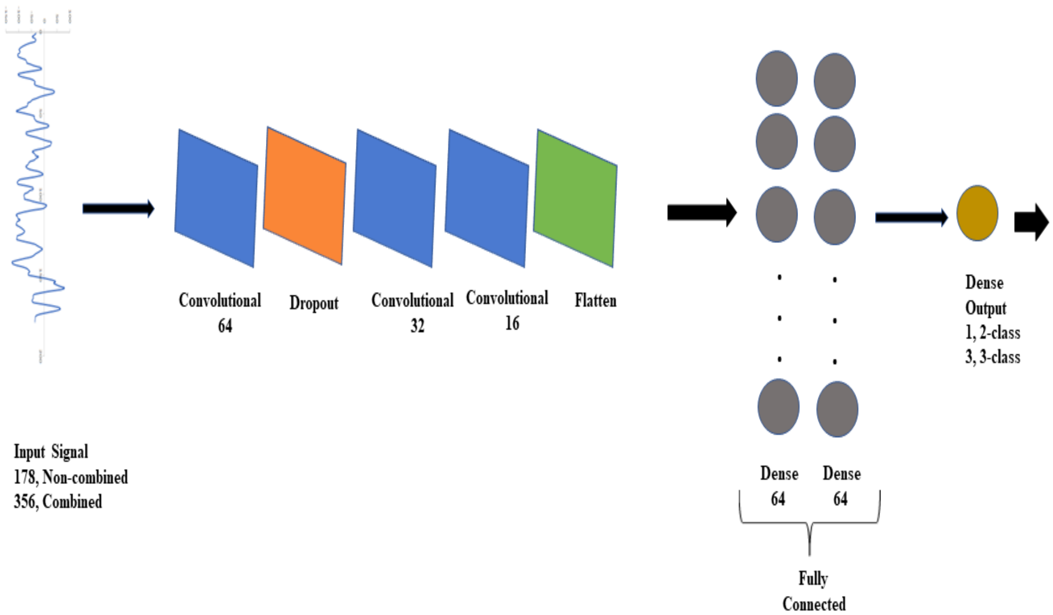


Figure 23
1D-CNN Model

Table 2.
*1D-CNN Model Architectures Summary, Non-combined (NC) And Combined CB Inputs*

| Layer Type | Output Shape | Number Of Parameters |
|---|---|---|
| Conv1D 1 (input) | NC, (172, 64)<br>CB, (350, 64) | 512 |
| Dropout (0.5) | NC, (172, 64)<br>CB, (350, 64) | 0 |

continue on the next page

Table 2. (continued).

| | | |
|---|---|---|
| Conv1D 2 | NC, (172, 32)<br>CB, (348, 32) | 6176 |
| Conv1D 3 | NC, (169, 16)<br>CB, (347, 16) | 1040 |
| Flatten | NC, 2704<br>CB, 5552 | 0 |
| Dense 1 | 64 | NC, 173120<br>CB, 355392 |
| Dense 2 | 64 | 4160 |
| Dense 3 (output) | 1, (2-class)<br>3, (3-class) | 65, (2-class)<br>195, (3-class) |

The evaluated 1D-CNN model of (Abiyev et al., 2020) for the original and preprocessed and combined EEG inputs is next in figure 24. The modified waveforms inputs and original ones shape details in the model are shown in table 3, note that these details are different than the original model since it was tested with our inputs.

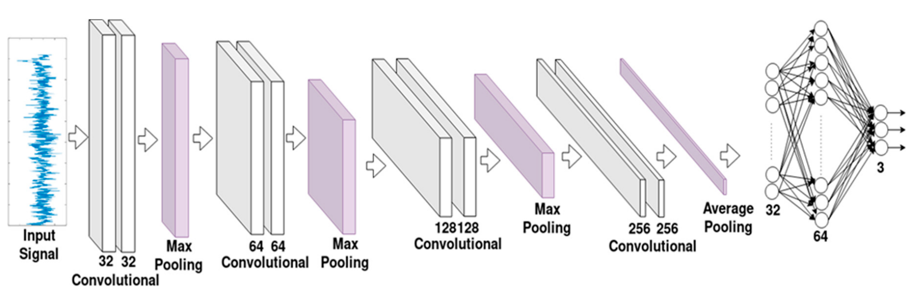


Figure 24
Abiyev et al. (2020, Fig. 1) 1D CNN Model

Table 3.

*Abiyev et al. (2020) 1D-CNN Reproduced Model Architectures Summary, Non-combined (NC) And Combined CB Inputs*

| Layer Type | Output Shape | Number Of Parameters |
|---|---|---|
| Conv1D 1 (input) | NC, (172, 32)<br>CB, (350, 32) | 256 |
| Conv1D 2 | NC, (170, 32)<br>CB, (348, 32) | 3104 |
| Maxpooling1D 1 | NC, (85, 32)<br>CB, (174, 32) | 0 |
| Conv1D 3 | NC, (84, 64)<br>CB, (173, 64) | 4160 |
| Conv1D 4 | NC, (83, 64)<br>CB, (172, 64) | 8256 |
| Maxpooling1D 2 | NC, (41, 64)<br>CB, (86, 64) | 0 |
| Conv1D 5 | NC, (40, 128)<br>CB, (85, 128) | 16512 |
| Conv1D 6 | NC, (39, 128)<br>CB, (84, 128) | 32896 |
| Maxpooling1D 3 | NC, (19, 128)<br>CB, (42, 128) | 0 |

continue on the next page

Table 3. (continued).

| | | |
|---|---|---|
| Conv1D 7 | NC, (18, 256)<br>CB, (41, 256) | 65792 |
| Conv1D 8 | NC, (17, 256)<br>CB, (40, 256) | 131328 |
| Global Average Pooling 1D | 256 | 0 |
| Dropout (0.5) | 256 | 0 |
| Dense 1 | 32 | 8224 |
| Dense 2 | 64 | 2112 |
| Dense 3 (output) | 1, (2-class)<br>3, (3-class) | 65, (2-class)<br>195, (3-class) |

Note that the multiclass classification models have the same structures, vectors have the same sizes even if the total number of signals is less which does not affect the shapes of the outputs, only the last layer is different since it has three outputs instead of one, which increases its number of parameters a little and all the parameters are learnable.

# CHAPTER VI

## Evaluation Settings And Runtime Environment

In this chapter, the details of the training and evaluation processes will be discussed with the various metrics and scores of the 2-class and 3-class. The first section explains the runtime environment, the second section discusses the dataset, the third section presents different data distributions and labeling, the fourth section presents signal samples of different EEG cases, section five goes thoroughly into the preprocessing and modifications, the sixth section presents the architectures, in section seven models training setups are shown, the eighth section explains the evaluation process and training method and the last section shows the recorded metrics and scores.

### Runtime Environment

Almost all of the coding was done on the google colaboratory (colab), only the FFT and differentiation operations of the datasets were done by MATLAB. The free version of google colab operates with jupyter notebooks and python programming language which was the only used language in colab. The dominant libraries that were used are TensorFlow, Keras, sklearn, pandas and NumPy. TensorFlow and Keras are mostly used for building the models, fitting the data to the models for training and evaluating the models' accuracies while sklearn is used for splitting the data into training and testing splits and getting the used scores as sensitivity, precision, confusion matrix and F1-scores. the specificity score was got by manually building a code to calculate it since it does not exist in the sklearn. Google colab runtime was set to TPU runtime which gives an accelerator hardware resource of TPU V2 and model (10.50.201.250:8470). Since the resources are dynamic sometimes it provides different models of TPU but they generally have the same processing power, with 8 cores each 8GB for v2 TPUs. The RAM given is 13GB and the CPU is Intel(R) Xeon(R) CPU @ 2.20GHz or an equivalent model with relatively the same speed. These high resources and free environment encouraged us to do all the work on the colab. Note that, although google colab is a dynamic environment with many complicated operations behind the scene to guarantee stability for all users their VMs resets the runtimes if they were not active after 90 minutes and the quota is restricted for 12 hours of work within one day for the free user account, so knowing the exact resources in colab is virtually impossible but their administrators say the resources are almost the same for the same type of an account and runtime (Google, 2022).

### Dataset

The main dataset is the EEG dataset of the University of California Irvine (UCI) which is a restructured form of the infamous Bonn university EEG dataset that is unfortunately no longer available on the official website (Uni-Bonn, 2022)(Qiuyi, 2022). The UCI published the restructured version, done by a research team at Rochester Institute of technology, that has one file instead of five folders of 100 files each, 11,500 rows (signals) instead of 500 rows combined from five files, 178 segmented amplitudes of time series points instead of 4097 in the Bonn dataset to represent the data in one-second chunks, a label column was added instead of considering the file name as the label in the Bonn dataset and the research team shuffled the segmented rows. The dataset has EEG recordings from 500 people, each one has 23.5 seconds of recording as 4097-time series points converted by the research team related to UCI into $23 * 178$ points segments. The Bonn labels were filenames A, B, C, D and E which were converted into 1, 2, 3, 4 and 5. each label represents a class, A is equivalent to 5 which illustrates the eyes open category, B is equivalent to 4 which illustrates the eyes closed category and both represent the normal/healthy group. C is equivalent to 3 which illustrates inter-ictal seizure-free activity recorded from the healthy area category, D is equivalent to 4 which illustrates the inter-ictal seizure-free activity recorded from the seizure activity area category and both represent the inter-ictal/preictal group. E is equivalent to 1 which illustrates the seizure activity category or ictal group. Since label 1 categorizes recordings of seizure activity while other labels categorize non-seizure activity, this labeling was made the basis of the binary classification in the evaluated architectures. multiclass classification considered the three categories of B, D and E or 4, 2 and 1 labels representing normal, preictal and seizure classes. Together with the original dataset, some variations were done for model testing and comparisons, seeking if the variations or combinations of the original dataset with other forms of it will affect the model accuracy, scores and training and evaluation times.

**Data Visualization**

The UCI version of the Bonn dataset (UCI-Bonn) is a balanced set, it contains 2300 signals of each label. Figure 25 presents the overall distribution of the dataset.

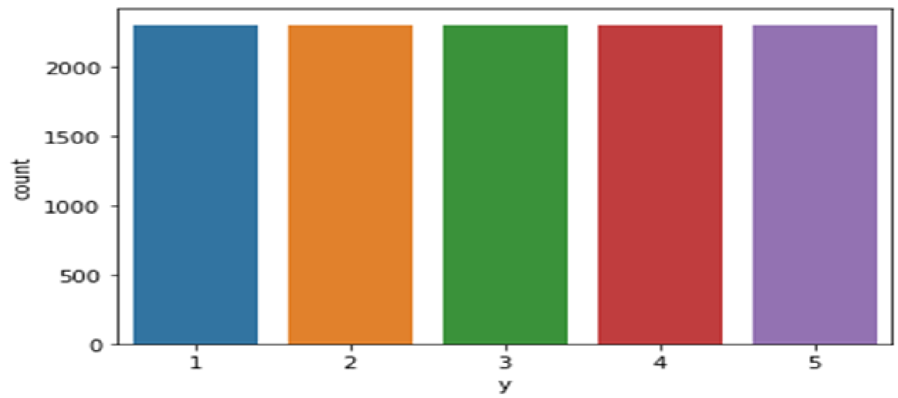


Figure 25
*Overall Distribution Of The Labels.*

For the binary classification problem of seizure vs non-seizure classes, the labels were modified to zero and one illustrating non-seizure and seizure activity, consequently. Labels 2, 3, 4 and 5 were placed as zero and label one is the same (seizure), with this modification, 2300 signals of seizure activity and 10200 signals of non-seizure activity. The next figure shows the modified binary distribution.

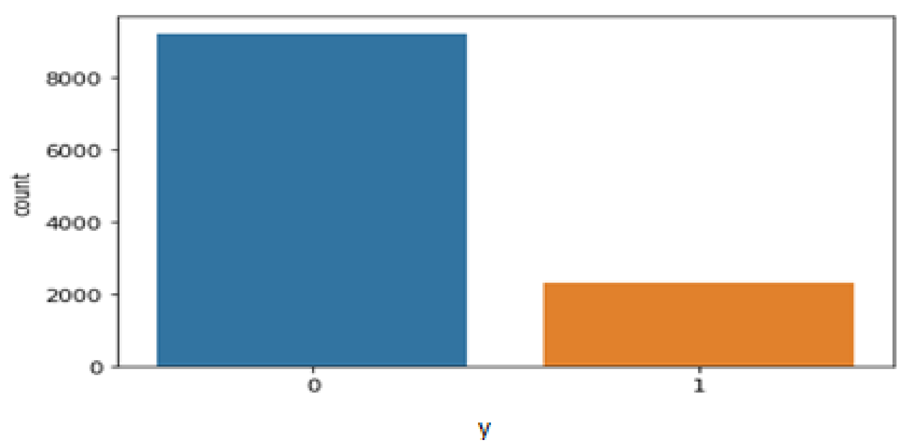


Figure 26
*Modified Labels For The 2-Class Classification.*

The multiclass classification problem was evaluated on three classes only by dropping the other two ones. Labels 1, 2 and 4 were kept representing seizure, normal and preictal categories respectively, then they were modified to zero, one and two for the training and evaluation. In figure 27, the 3-class labels balanced distribution is shown.

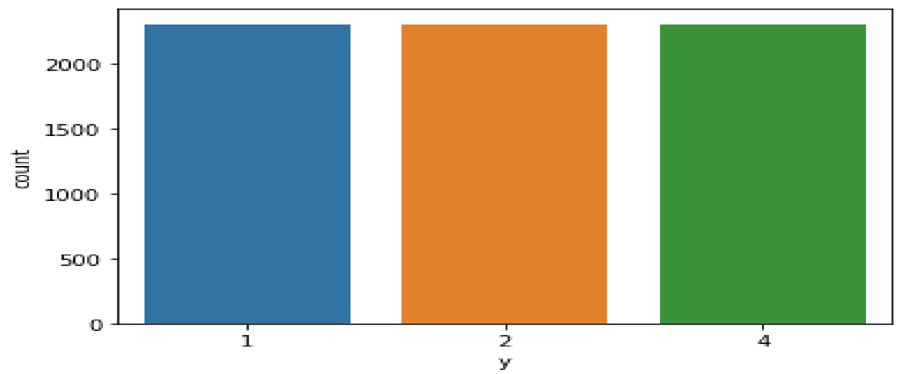


Figure 27
*Three Labels Of The 3-Class Classification.*

**Models Settings**

Settings include the activation functions, loss functions, optimizers, batch sizes, number of training epochs, splitting ratios and shuffling states. The binary models of DNN and 1D-CNN that were built for the evaluations other than (Abiyev et al., 2020) model had LeakyRelu activation within the network and sigmoid activation on the output layer, binary-crossentropy loss function, rmsprop optimizer, 128 batch size, 100 epochs, 50/50, 60/40, 70/30 and 80/20 splittings of train/test and random state (42) to make sure the random shuffling stays the same with each repetition. While (Abiyev et al., 2020) implemented 1D-CNN model had Relu activation within the network and sigmoid activation for the output layer, 100 batch size, 150 epochs and the rest of the settings are the same. For the multiclass settings, our DNN and 1D-CNN had softmax activation on the output layer, sparse-categorical-crossentropy loss function and the rest of the settings are the same as the previous equivalent binary models. In the implemented 1D-CNN of (Abiyev et al., 2020) multiclass case, the model had Relu activation as the binary equivalent one but with softmax output layer activation and sparse-categorical-crossentropy loss function as our DNN and 1D-CNN, the rest of the settings are the same as the binary equivalent model.

Note that the activation function LeakyRelu in python TensorFlow and Keras has 0.3 factor for the negative values instead of zero in the Relu activation function or 0.01 factor in MATLAB. Lastly, the dropout rate in all models is 0.5.

### Evaluations and Training

The evaluation process was mostly the same for all cases, with 128 batch sizes for our DNN and 1D-CNN and 100 batch sizes for the implemented 1D-CNN of (Abiyev et al., 2020), in the 2-class and 3-class classifications. The binary predictions were done on a 0.5 threshold while the 3-class predictions were got by the highest probability class as the accepted prediction. Each training and testing was repeated five times for the same case and all the results are the averages of that 5 runs.

### Metrics and Scores

The metrics and scores are values that represent the model behavior in terms of efficiency, classification and others. The recorded metrics and scores were accuracy, loss, sensitivity/recall, specificity, F1-score, precision and the area under curve (AUC). All metrics rely , generally, on four values which are TN, TP, FN and FP. TN and TP present the correctly classified classes of positive and negative while FP and FN present the misclassified classes. so, a good model will have higher TN and TP and lower FN and FP.

#### *Accuracy*

Accuracy is the percentage of the true predictions of the evaluated data which can be got by dividing the true predictions by the total number of predictions.

$$Accuracy = \frac{TP + TN}{TP + TN + FP + FN} \tag{9}$$

***Precision***

Precision is the ratio of true positive classifications to the total positive predictions. It is a measure of the model's ability to detect positive classes.

$$Precision = \frac{TP}{TP + FP} \tag{10}$$

***Sensitivity***

Sensitivity or recall is calculated by dividing the true positive predictions by all positive samples whether correctly predicted or not. so, this measure focuses on the ability to classify positive samples.

$$Sensitivity = \frac{TP}{TP + FN} \tag{11}$$

***F1-score***

F1-score is one of the F-measures which is represented as the harmonic mean of the recall and precision, it is useful to show the average rate of both the recall and precision. A high F1-score suggests high recall and precision while a moderate F1-score suggests that one of the measures is lower.

$$F1 - score = 2 * \frac{Recall * Precision}{Recall + Precision} \tag{12}$$

***Specificity***

Specificity is defined as the proportion of the true negative predictions to the total negatives. Ideally, it should be a high value indicating a good ability of negative class detection by the model.

$$Specificity = \frac{TN}{TN + FP} \tag{13}$$

***AUC***

Area under curve is usually used for binary classification problems. The curve of interest is the receiver operator characteristic (ROC) which is the probability curve of true positive rate (TPR) against the false positive rate (FPR). AUC measure points to the model's capability to distinguish between classes. Ideally, AUC equals one implying that all samples were classified accurately.

***Loss***

Loss is the metric reported by the loss function applied in the model which is the base of the optimizing process in the backward propagation. It suggests how well the model is performing given the data.

In the 2-class classification cases, the evaluation and training time was recorded, the evaluation loss and accuracy, sensitivity (recall), specificity, F1-score, precision and the area under curve (AUC). For the 3-class classification, evaluation and training time, evaluation loss and accuracy, sensitivity (recall), specificity, F1-score and precision for each class and the average of the 3 classes was recorded as well.

# CHAPTER VII

## Results, Comparisons and Discussions

This section discusses the evaluations and results that are carried out to assess the performance of the proposed 1D-CNN and DNN methods with various modified EEG signals. In this way, the performance of the modified EEG signals with the proposed 1D-CNN and DNN models can be compared. In addition, we tested the efficacy of the modified EEG signals using a recent 1D-CNN model that gives very promising results. Therefore, extensive evaluations are performed including, time evaluations, accuracy, sensitivity, specificity, precision, recall, F-measure and others. First section discusses various evaluations using two-class classifications. Second section discusses various evaluations using three-class classifications. The third section presents related methods as comparative results.

### Evaluation and Results for 2-Class Classification on UCI-Bonn Dataset

#### *Training And Evaluation Time*

This section discusses training and evaluation times of the proposed 1D-CNN (moderate) and DNN and compares this with the method of (Abiyev et al., 2020) named 1D-CNN (complex) which might be referred to as 1D-CNN complex or (Abiyev et al., 2020) model interchangeably in discussions. Note that the 1D-CNN complex model is a reproduction of the (Abiyev et al., 2020) model with our inputs. All of the methods are implemented on the same platform for fair a comparison.

Table 4.
*Comparing Training (T) and Evaluation (E) Time of the Methods (Results are average of 5 runs and in seconds).*

| EEG Signal | Splitting% Training/Test | DNN (Simple) T E | 1D-CNN (Moderate) T E | 1D-CNN (Complex) T E |
|---|---|---|---|---|

continue on the next page

Table 4. (continued).

| | | | | | | | |
|---|---|---|---|---|---|---|---|
| Original EEG Signal Only | 50/50 | 18.3 | 0.34 | 396.51 | 1.31 | 1501.49 | 1.52 |
| | 60/40 | 22.4 | 0.34 | 434.72 | 1.12 | 1608.22 | 1.35 |
| | 70/30 | 32.4 | 0.31 | 471.79 | 0.82 | 1743.79 | 1.06 |
| | 80/20 | 33.36 | 0.29 | 613.1 | 0.59 | 1992.83 | 0.87 |
| Standard Original EEG Signal | 50/50 | 21.98 | 0.36 | 525.45 | 1.8 | 1562.14 | 1.7 |
| | 60/40 | 28.54 | 0.33 | 457.63 | 1.26 | 1641.47 | 1.96 |
| | 70/30 | 29.86 | 0.31 | 540.66 | 0.73 | 1798.2 | 1.93 |
| | 80/20 | 36.32 | 0.3 | 600.2 | 0.65 | 1937.38 | 1.91 |
| Squared Signal Combined With Original EEG Signal | 50/50 | 22.46 | 0.36 | 694.97 | 2.22 | 2911.21 | 6.22 |
| | 60/40 | 26.47 | 0.34 | 857.35 | 1.82 | 2782.4 | 3.82 |
| | 70/30 | 28.60 | 0.30 | 920.36 | 1.31 | 3203.58 | 3.49 |
| | 80/20 | 35.32 | 0.28 | 1151.42 | 1.05 | 4099.61 | 7.4 |
| Differentiated Combined With Original EEG Signal | 50/50 | 26.09 | 0.36 | 679.39 | 2.24 | 2481.89 | 4.14 |
| | 60/40 | 32.67 | 0.37 | 852.93 | 2.06 | 3175.83 | 6.07 |
| | 70/30 | 33.09 | 0.41 | 857.27 | 0.93 | 3679.54 | 3.1 |
| | 80/20 | 33.31 | 0.29 | 1114.23 | 0.94 | 4106.35 | 2.43 |
| FFT Combined With Original EEG Signal | 50/50 | 24.94 | 0.35 | 708.35 | 2.08 | 2532.13 | 4.67 |
| | 60/40 | 25.64 | 0.34 | 851.42 | 1.81 | 2771.05 | 3.65 |
| | 70/30 | 29.47 | 0.37 | 974.1 | 1.22 | 3011.59 | 2.9 |
| | 80/20 | 34.3 | 0.28 | 1104.12 | 1.03 | 3759.8 | 2.46 |

From table 4., DNN overall training periods are increasing with the splitting ratio, since training sets are getting bigger, it is noticed that only original case has the lowest training time for all splitting cases. The differentiated combined with original case have, on average, the highest training times. evaluation times seem to change insignificantly among the cases.

In 1D-CNN moderate, training and evaluation times are significantly higher compared to the DNN. the overall period behavior of training times seems to be the same as DNN cases. However, FFT combined with original case seems to have the highest training times, on average. evaluation times are changing significantly between only original, standard original cases and other cases. Also, evaluation times are seemingly higher for 50/50 and 60/40 splits which are expected as the testing sets are larger.

In 1D-CNN complex model, the training times are 4 to 5 times longer than the proposed 1D-CNN cases and the overall training and evaluation time behavior is almost the same as in the proposed 1D-CNN moderate, but the differentiated case appears to have the longest training times for 60/40, 70/30 and 80/20 splittings.

***Evaluation Loss and Accuracy***

Table 5 shows loss and accuracy results are for 2-class classification using the UCI-Bonn dataset.

Table 5.

*Comparing Evaluation Loss (L) and Accuracy (ACC) of the Methods (Results are average of 5 runs).*

| EEG Signal | Splitting% Training/Test | DNN (Simple) L | DNN (Simple) ACC | 1D-CNN (Moderate) L | 1D-CNN (Moderate) ACC | 1D-CNN (Complex) L | 1D-CNN (Complex) ACC |
|---|---|---|---|---|---|---|---|
| Original EEG Signal Only | 50/50 | 0.2317 | 95.21 | 0.2662 | 97.08 | 0.1217 | 98.81 |
| | 60/40 | 0.2418 | 94.66 | 0.2078 | 97.36 | 0.0926 | 98.78 |
| | 70/30 | 0.2376 | 94.72 | 0.1818 | 97.42 | 0.1100 | 98.81 |
| | 80/20 | 0.2253 | 95.08 | 0.2829 | 97.48 | 0.0411 | 99.23 |
| Standard Original EEG Signal | 50/50 | 0.2051 | 96.68 | 0.4877 | 97.48 | 0.1956 | 98.79 |
| | 60/40 | 0.2019 | 96.66 | 0.3047 | 97.5 | 0.2545 | 98.73 |
| | 70/30 | 0.1924 | 96.61 | 0.2597 | 97.68 | 0.1326 | 98.93 |
| | 80/20 | 0.192 | 96.83 | 0.2439 | 97.87 | 0.0936 | 99.37 |

continue on the next page

Table 5. (continued).

| | | | | | | | |
|---|---|---|---|---|---|---|---|
| Squared Signal | 50/50 | 0.1899 | 96.54 | 0.4644 | 97.21 | 0.2675 | 97.82 |
| Combined | 60/40 | 0.1871 | 96.46 | 0.4069 | 97.3 | 0.1397 | 98.54 |
| With Original | 70/30 | 0.1809 | 96.40 | 0.3553 | 97.45 | 0.0983 | 98.67 |
| EEG Signal | 80/20 | 0.1769 | 96.81 | 0.4382 | 97.76 | 0.1838 | 98.82 |
| Differentiated | 50/50 | 0.2356 | 96.63 | 0.5234 | 96.81 | 0.1622 | 98.32 |
| Combined | 60/40 | 0.2259 | 96.51 | 0.4557 | 97.14 | 0.1496 | 98.41 |
| With Original | 70/30 | 0.2098 | 96.93 | 0.4131 | 97.27 | 0.0683 | 98.72 |
| EEG Signal | 80/20 | 0.2108 | 96.98 | 0.4723 | 97.29 | 0.0988 | 98.9 |
| FFT | 50/50 | 0.1295 | 97.84 | 0.2542 | 98.51 | 0.1239 | 98.72 |
| Combined | 60/40 | 0.128 | 97.86 | 0.2197 | 98.6 | 0.159 | 98.73 |
| With Original | 70/30 | 0.1179 | 98.06 | 0.2415 | 98.81 | 0.0911 | 98.96 |
| EEG Signal | 80/20 | 0.1155 | 98.23 | 0.1651 | 98.91 | 0.0599 | 99.13 |

In table 5., all cases, other than the only original 60/40 and 70/30 cases, have accuracy values higher than 95% which is a good indication. it is observed that FFT combined with original cases have the highest accuracies and lowest loss among all with an accuracy of 98.23% for the 80/20 splitting as the highest value. In principle, the global trend in the table is accuracy increase and loss decrease from only original to FFT combined with original cases and from 50/50 to 80/20 splittings. which is an indicator of combinations enhancement effects and standardization on the raw dataset of the only original.

The overall trends in the 1D-CNN moderate model look more complicated than the DNN ones. while accuracies are relatively higher than DNN accuracies, the loss is higher, in general. the FFT combined with original cases has the lowest loss and highest accuracy with 98.91% accuracy and 0.1651 loss for 80/20 splitting. Other combined cases and standard original cases have roughly 2 times more loss than others and the DNN values. The FFT combined with original and only original cases have slightly higher losses than DNN cases. Also, the differentiated combined with original case has the lowest accuracy and the highest loss.

1D-CNN complex model seem to have almost the exact behavior of the proposed 1D-CNN moderate, but, it has a significantly lower loss compared to the proposed DNN and 1D-CNN. the highest accuracy and lowest loss here is for the standard original case then the only original case and FFT combined with original, all three are above 99% accuracy and less than 0.06 loss. Notice that this model values are for 150 epochs of training, unlike the previous ones which had only 100 epochs.

### *Confusion Matrix for 2-Class Classification Results*

The confusion matrix for each case and architecture will be shown, then the binary classification model's scores of specificity, sensitivity, precision, F1 and AUC. note that the confusion matrix is in the shape of [TN, FP] as the first row and the second row is [FN, TP], respectively. the confusion matrix classes here are zero and one. zero represents the non-seizure which are labels two, three, four and five in the UCI version of the Bonn dataset and one represents the seizure which is label one in the UCI version of the Bonn dataset. Next in figure 28, the DNN confusion matrices are presented.

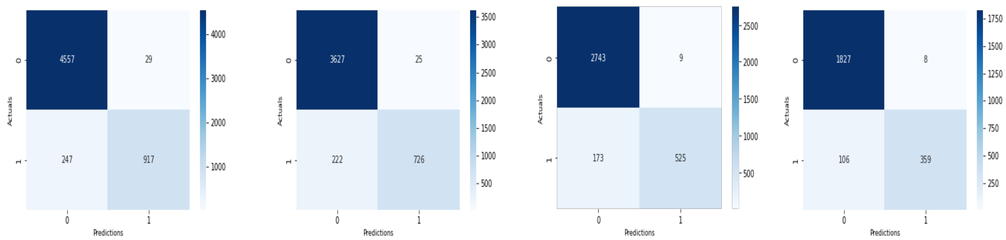


(a) DNN with Original EEG Signal (left 50/50, middle 60/40 then 70/30 and right 80/20)

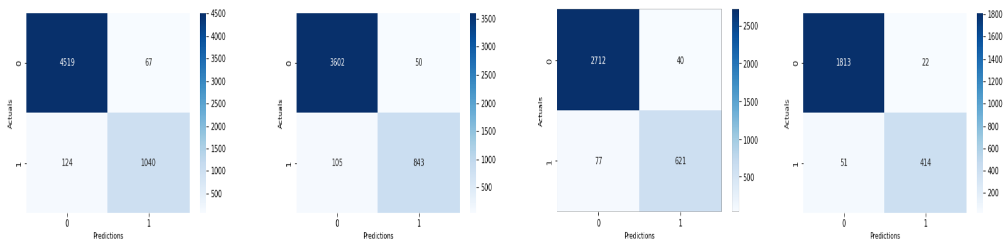


(b) DNN with Standard Original EEG Signal (left 50/50, middle 60/40 then 70/30 and right 80/20)

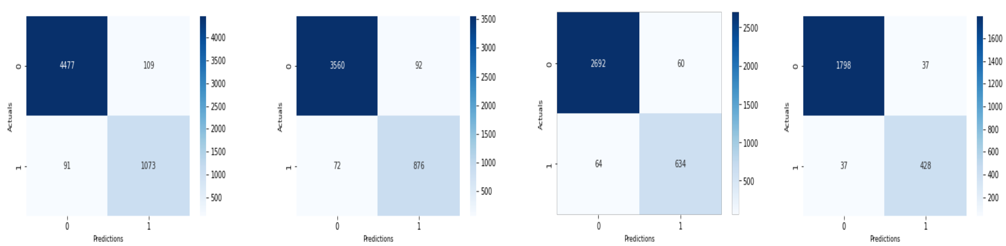


(c) DNN With Squared Signal Combined With Original EEG Signal (left 50/50, middle 60/40 then 70/30 and right 80/20)

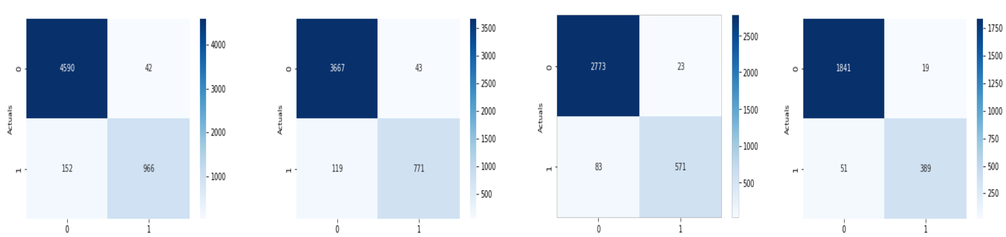


(d) DNN With Differentiated Combined With Original EEG Signal (left 50/50, middle 60/40 then 70/30 and right 80/20)

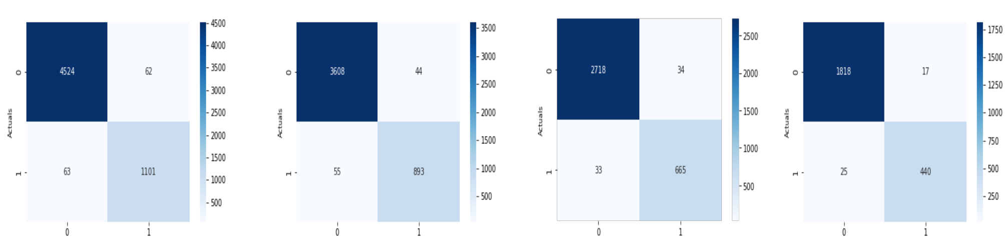


(e) DNN With FFT Combined With Original EEG Signal (left 50/50, middle 60/40 then 70/30 and right 80/20)

Figure 28
Confusion Matrix for 2-Class Classification on Bonn Dataset using the Proposed DNN with Modified EEG Signals

It can be seen that the TN and TP values are the highest which is the expected outcome of any good architecture in DL. it is seen that the numbers are decreasing with splitting changes which is reasonable as the testing sets decrease with splittings changes from 50/50 to 80/20. The differentiated combined with original case has the highest TN values which suggest it is the best in classifying negatives (non-seizure). FFT combined with original case has the highest TP values, implying it is the best in classifying positives (seizure). the only original cases have the lowest FP values indicating low misclassification of positives, but they also have the highest FN values indicating high misclassification of negatives.

Next, figure 29 will represent the confusion matrices of the 1D-CNN (moderate) model.

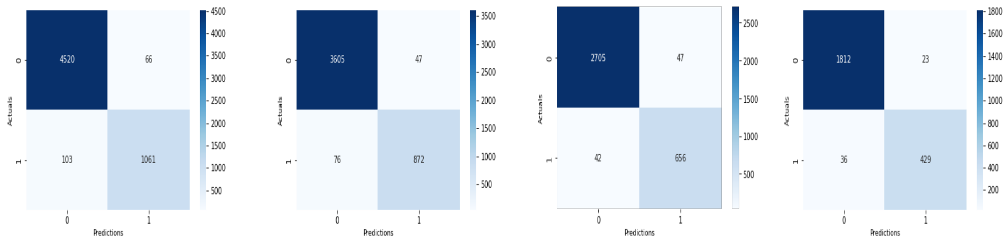


(a) 1D CNN (moderate) with Original EEG Signal (left 50/50, middle 60/40 and right 80/20

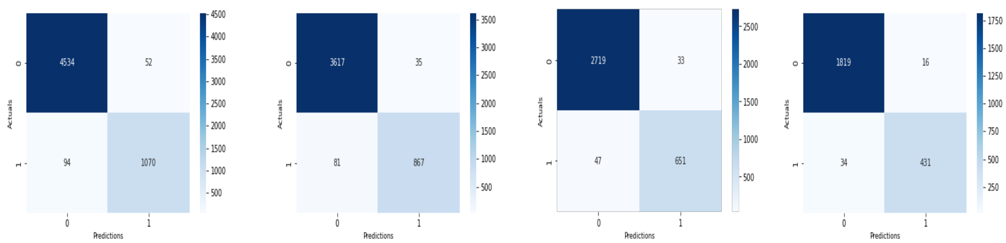


(b) 1D CNN (moderate) with Standard Original EEG Signal (left 50/50, middle 60/40 then 70/30 and right 80/20)

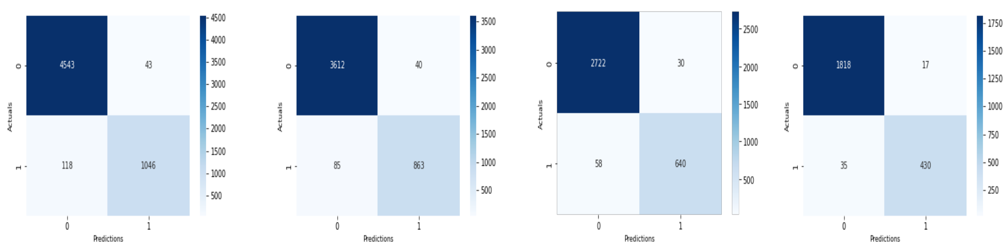


(c) 1D CNN (moderate) With Squared Signal Combined With Original EEG Signal (left 50/50, middle 60/40 then 70/30 and right 80/20)

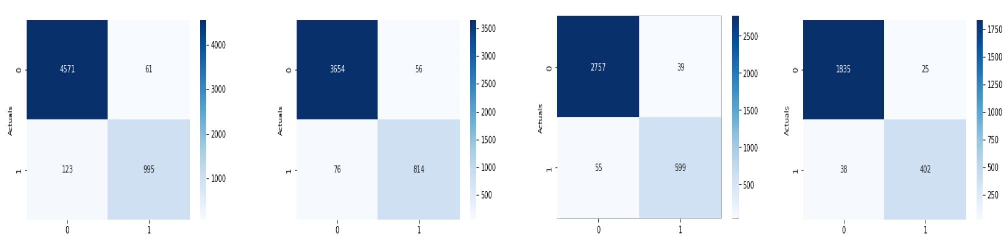


(d) 1D CNN (moderate) With Differentiated Combined With Original EEG Signal (left 50/50, middle 60/40 then 70/30 and right 80/20)

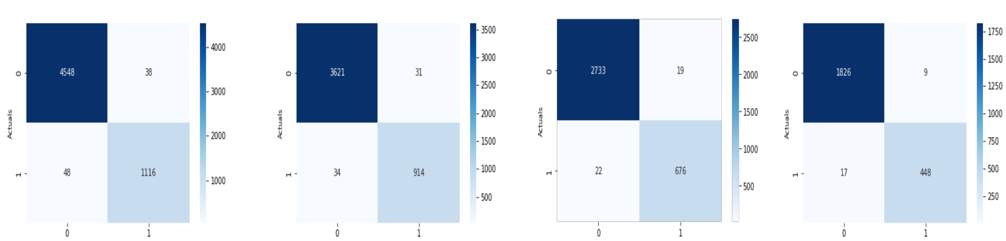


(e) 1D CNN (moderate) With FFT Combined With Original EEG Signal (left 50/50, middle 60/40 then 70/30 and right 80/20)

Figure 29
Confusion Matrix for 2-Class Classification on Bonn Dataset using the Proposed 1D-CNN with Modified EEG Signals

The behavior of the 1D-CNN moderate model seem to be almost the same as the DNN. However, the lowest FP and FN are for the FFT combined with original cases which makes them the best cases, in general. Also, there is no significant change in values compared with the DNN cases.

Figure 30 presents the confusion matrices for the implemented 1D-CNN (complex) of (Abiyev et al., 2020), evaluated for the binary classification scenario which was not tested by the original team.

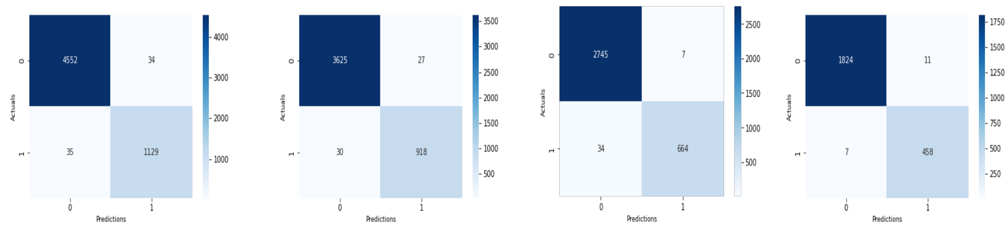


(a) 1D CNN (complex) with Original EEG Signal (left 50/50, middle 60/40 then 70/30 and right 80/20

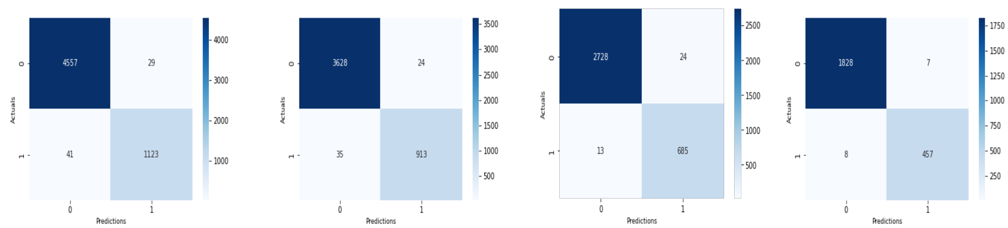


(b) 1D CNN (complex) with Standard Original EEG Signal (left 50/50, middle 60/40 then 70/30 and right 80/20)

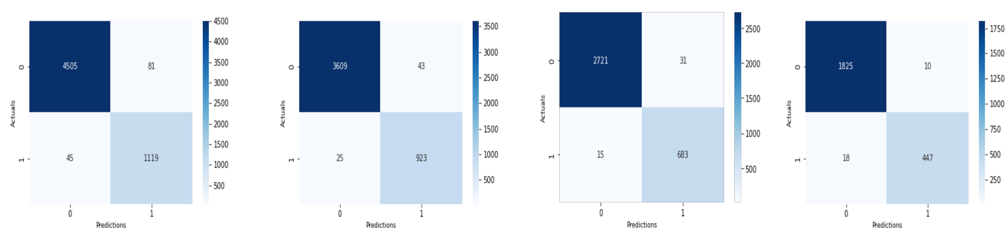


(c) 1D CNN (complex) With Squared Signal Combined With Original EEG Signal (left 50/50, middle 60/40 then 70/30 and right 80/20)

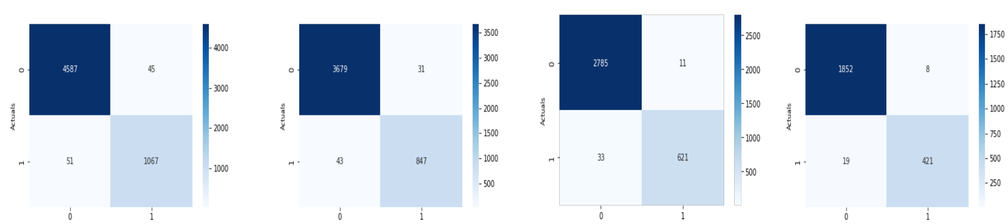


(d) 1D CNN (complex) With differentiated Combined With Original EEG Signal (left 50/50, middle 60/40 then 70/30 and right 80/20)

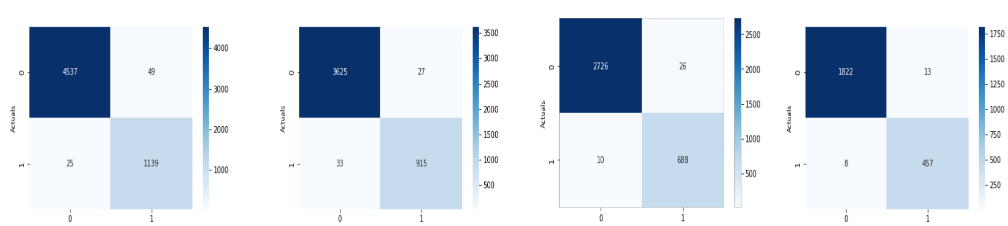


(e) 1D CNN (complex) With FFT Combined With Original EEG Signal (left 50/50, middle 60/40 then 70/30 and right 80/20)

Figure 30
Confusion Matrix for 2-Class Classification on Bonn Dataset using the 1D-CNN (complex) Model with Modified EEG Signals

For the previous figure, the model have similar behavior to the previous cases. standard original cases have the lowest FP here.

In the next section tables, the scores that will be shown are dependant on the TP, TN, FP and FN values so, the overall behavior of the scores is expected to be similar to the last three figures.

***Comparing Specificity, Sensitivity, Precision, F1-Score and AUC Scores of the Methods***

This section discusses the various scores recorded for the architectures. In table 6, the specificity, sensitivity and precision are shown.

Table 6.
*Comparing Specificity (SP), Sensitivity (SN) and Precision (P) of the Methods (Results are average of 5 runs).*

| EEG Signal | Splitting% Training/Test | DNN (Simple) SP SN P | 1D-CNN (Moderate) SP SN P | 1D-CNN (Complex) SP SN P |
|---|---|---|---|---|
| Original EEG Signal Only | 50/50 | 99.39 78.78 97.06 | 98.57 91.2 94.21 | 99.62 97.04 97.1 |
| | 60/40 | 99.34 76.62 96.79 | 98.73 92.07 94.99 | 99.27 96.9 97.21 |
| | 70/30 | 99.67 75.21 98.31 | 98.29 93.98 93.31 | 99.75 95.13 98.96 |
| | 80/20 | 99.57 77.33 97.88 | 98.79 92.3 95.12 | 99.42 98.49 97.76 |
| Standard Original EEG Signal | 50/50 | 98.54 89.35 93.96 | 98.88 91.96 95.49 | 99.37 96.51 97.48 |
| | 60/40 | 98.65 88.99 94.51 | 99.05 91.54 96.17 | 99.35 96.33 97.49 |
| | 70/30 | 98.55 88.97 93.95 | 98.80 93.27 95.18 | 99.13 98.14 96.61 |
| | 80/20 | 98.8 89.03 94.97 | 99.15 92.82 96.54 | 99.63 98.37 98.54 |
| Squared Signal Combined With Original EEG Signal | 50/50 | 97.64 92.22 90.86 | 99.07 89.86 96.1 | 98.24 96.15 93.92 |
| | 60/40 | 97.5 92.45 90.6 | 98.92 91.08 95.64 | 98.83 97.45 95.59 |
| | 70/30 | 97.82 90.83 91.35 | 98.91 91.69 95.52 | 98.87 97.85 95.66 |
| | 80/20 | 97.98 92.17 92.06 | 99.1 92.47 96.3 | 99.5 96.13 98.05 |

continue on the next page

Table 6. (continued).

| | | | | | | | | | | |
|---|---|---|---|---|---|---|---|---|---|---|
| Differentiated | 50/50 | 99.1 | 86.4 | 95.88 | 98.68 | 89.03 | 94.23 | 99.03 | 95.46 | 95.96 |
| Combined | 60/40 | 98.86 | 86.72 | 94.88 | 98.49 | 91.53 | 93.67 | 99.17 | 95.24 | 96.54 |
| With Original | 70/30 | 99.18 | 87.31 | 96.13 | 98.61 | 91.95 | 93.89 | 99.61 | 94.95 | 98.26 |
| EEG Signal | 80/20 | 98.98 | 88.55 | 95.38 | 98.68 | 91.41 | 94.29 | 99.61 | 95.86 | 98.34 |
| FFT | 50/50 | 98.65 | 94.66 | 94.7 | 99.18 | 95.88 | 96.73 | 98.94 | 97.85 | 95.91 |
| Combined | 60/40 | 98.81 | 94.2 | 95.35 | 99.15 | 96.48 | 96.73 | 99.28 | 96.6 | 97.24 |
| With Original | 70/30 | 98.76 | 95.27 | 95.14 | 99.31 | 96.85 | 97.27 | 99.06 | 98.57 | 96.36 |
| EEG Signal | 80/20 | 99.12 | 94.71 | 96.47 | 99.54 | 96.43 | 98.17 | 99.34 | 98.32 | 97.45 |

Next, table 7 show the F1-score and AUC of the 2-class models.

Table 7.
*Comparing F1-Score (F1) and AUC of the Methods (Results are average of 5 runs).*

| EEG Signal | Splitting% Training/Test | DNN (Simple) | | 1D-CNN (Moderate) | | 1D-CNN (Complex) | |
|---|---|---|---|---|---|---|---|
| | | F1 | AUC | F1 | AUC | F1 | AUC |
| Original EEG Signal Only | 50/50 | 86.93 | 99.04 | 92.67 | 98.93 | 97.07 | 99.72 |
| | 60/40 | 85.49 | 98.96 | 93.49 | 99.24 | 97.04 | 99.78 |
| | 70/30 | 85.23 | 99.16 | 93.65 | 99.28 | 97.01 | 99.63 |
| | 80/20 | 86.85 | 99.2 | 93.66 | 99.08 | 98.12 | 99.93 |
| Standard Original EEG Signal | 50/50 | 91.59 | 99.05 | 93.66 | 99.14 | 97 | 99.27 |
| | 60/40 | 91.66 | 99.08 | 93.79 | 99.27 | 96.9 | 99.38 |
| | 70/30 | 91.39 | 99.37 | 94.21 | 99.33 | 97.37 | 99.76 |
| | 80/20 | 91.88 | 99.3 | 94.63 | 99.34 | 98.45 | 99.86 |

continue on the next page

Table 7. (continued).

| | | | | | | | |
|---|---|---|---|---|---|---|---|
| Squared Signal | 50/50 | 91.52 | 99.08 | 92.86 | 99.01 | 94.8 | 99.1 |
| Combined | 60/40 | 91.5 | 99.07 | 93.29 | 99.16 | 96.5 | 99.55 |
| With Original | 70/30 | 91.10 | 99.08 | 93.57 | 98.92 | 96.74 | 99.72 |
| EEG Signal | 80/20 | 92.11 | 99.12 | 94.34 | 98.82 | 97.02 | 99.67 |
| Differentiated | 50/50 | 90.85 | 99.08 | 91.55 | 98.09 | 95.7 | 99.56 |
| Combined | 60/40 | 90.57 | 99.16 | 92.53 | 98.6 | 95.86 | 99.65 |
| With Original | 70/30 | 91.50 | 99.42 | 92.72 | 99.02 | 96.58 | 99.81 |
| EEG Signal | 80/20 | 91.81 | 99.3 | 92.8 | 98.62 | 97.07 | 99.82 |
| FFT | 50/50 | 94.67 | 99.72 | 96.3 | 99.64 | 96.87 | 99.63 |
| Combined | 60/40 | 94.77 | 99.7 | 96.6 | 99.69 | 96.91 | 99.56 |
| With Original | 70/30 | 95.20 | 99.80 | 97.06 | 99.53 | 97.45 | 99.85 |
| EEG Signal | 80/20 | 95.57 | 99.82 | 97.29 | 99.82 | 97.87 | 99.89 |

From tables 6 and 7, DNN case of FFT combined with original have the best scores on 80/20 among all, considering all of the cases together. The combination and standardization of the original case seem to enhance the values, in general.

For the proposed 1D-CNN moderate, the overall observation is similar to the DNN cases with slightly higher values and there are virtually no scores less than 80% which indicates it is a better model.

In 1D-CNN complex model, approximately all scores are higher than 95% implying significant improvements on the DNN and the proposed 1D-CNN models. The standard original case appears to have higher scores, in general, unlike the last two models where the FFT combination was the best.

As an overall observation on the last three models, for simple models like the proposed DNN and 1D-CNN moderate model, combinations enhance the scores, but for more complicated models like the implemented 1D-CNN complex, the scores are decreased to some degree, in general. The best case is the non-combined standardization of the EEG signal which implies that changing the model architecture is more effective as was noticed among the last three models.

## Evaluation and Results for 3-Class Classification on Bonn Dataset

This section discusses various evaluations of the 3-class cases of the proposed 1D-CNN and DNN, and compares this with the reproduced method of (Abiyev et al., 2020) named as 1D-CNN complex. All of the methods are implemented on the same platform for a fair comparison.

### *Training and Evaluation Time*

This section will talk about the training and evaluation time of the evaluated 1D-CNN, DNN and the implemented 1D-CNN model of (Abiyev et al., 2020) in table 8.

Table 8.
*Comparing Training (T) and Evaluation (E) Time of the Methods (Results are average of 5 runs and in seconds).*

| EEG Signal | Splitting% Training/Test | DNN (Simple) T E | 1D-CNN (Moderate) T E | 1D-CNN (Complex) T E |
|---|---|---|---|---|
| Original EEG Signal Only | 50/50 | 15.03 0.33 | 244.42 0.75 | 1041.51 1.39 |
| | 60/40 | 18.09 0.32 | 275.29 0.75 | 989.41 1.22 |
| | 70/30 | 19.46 0.29 | 302.49 0.74 | 1034.64 0.97 |
| | 80/20 | 21.27 0.28 | 353.01 0.45 | 1337.75 1.79 |
| Standard Original EEG Signal | 50/50 | 18.56 0.32 | 253.27 0.75 | 1036.62 1.71 |
| | 60/40 | 25.13 0.34 | 261.12 0.74 | 1010 1.64 |
| | 70/30 | 27.77 0.29 | 294.15 0.66 | 1034.93 1.3 |
| | 80/20 | 33.86 0.35 | 354.66 0.47 | 1412.48 1.34 |

continue on the next page

Table 8. (continued).

| | | | | | | | |
|---|---|---|---|---|---|---|---|
| Squared Signal | 50/50 | 15.5 | 0.32 | 422.44 | 1.34 | 1513.61 | 1.75 |
| Combined | 60/40 | 17.65 | 0.31 | 512.45 | 1.12 | 2035.95 | 2.72 |
| With Original | 70/30 | 21.70 | 0.28 | 589.07 | 0.84 | 1904.1 | 1.06 |
| EEG Signal | 80/20 | 24.93 | 0.29 | 671.67 | 0.82 | 2358.74 | 1.17 |
| | | | | | | | |
| Differentiated | 50/50 | 19.28 | 0.33 | 428.33 | 1.41 | 1566.52 | 1.54 |
| Combined | 60/40 | 23.75 | 0.31 | 501.5 | 1.03 | 2031.99 | 1.23 |
| With Original | 70/30 | 21.57 | 0.30 | 594.01 | 0.96 | 2240.59 | 1.08 |
| EEG Signal | 80/20 | 29.31 | 0.3 | 674.66 | 0.79 | 2395.18 | 1.64 |
| | | | | | | | |
| FFT | 50/50 | 16.61 | 0.35 | 443 | 1.38 | 1540.31 | 1.44 |
| Combined | 60/40 | 19.13 | 0.29 | 512.44 | 1.13 | 2023.51 | 1.13 |
| With Original | 70/30 | 19.91 | 0.28 | 593.09 | 0.95 | 2078.12 | 1.15 |
| EEG Signal | 80/20 | 21.58 | 0.3 | 673.75 | 0.8 | 2374.94 | 1.01 |

In table 8, the DNN training and evaluation periods are close to the 2-class DNN with the exact behavior.

For the prposed 1D-CNN moderate, the last observation on DNN is valid, but the periods are mainly shorter than the binary equivalent model, which might be odd since the multiclass classification is expected to be harder and more complex computation-wise. However, different loss functions and optimizers were used for the 3-class classification which plays a dominant role in periods and since they are different than the binary models, the differences are justifiable, observation-based and hard to predict.

There seems to be a strange deviation at 60/40 splittings for the only original and standard original cases in 1D-CNN complex model as they are less than the 50/50 splitting for the same cases, this might refer to some changes in the runtime environment (temporary resource shortage) which affects processing speeds or time miscalculation (by code) because this deviation is inconsistent with the rest of the results. Also, the periods are less than the binary equivalent model with a behavior trend similar to the previous ones.

***Evaluation Loss and Accuracy***

Table 9 shows loss and accuracy results are for 3-class classification using the UCI-Bonn dataset.

Table 9.
*Comparing Evaluation Loss (L) and Accuracy (ACC) of the Methods (Results are average of 5 runs).*

| EEG Signal | Splitting% Training/Test | DNN (Simple) L | DNN (Simple) ACC | 1D-CNN (Moderate) L | 1D-CNN (Moderate) ACC | 1D-CNN (Complex) L | 1D-CNN (Complex) ACC |
|---|---|---|---|---|---|---|---|
| Original EEG Signal Only | 50/50 | 0.76 | 87.51 | 0.5464 | 92.42 | 0.2058 | 96.58 |
| | 60/40 | 0.665 | 87.89 | 0.4877 | 93.34 | 0.1857 | 95.74 |
| | 70/30 | 0.6605 | 85.31 | 0.3868 | 94.11 | 0.2821 | 96.04 |
| | 80/20 | 0.6245 | 86.9 | 0.4559 | 94.06 | 0.169 | 96.32 |
| Standard Original EEG Signal | 50/50 | 0.7175 | 69.57 | 0.5312 | 93.77 | 0.2338 | 96.54 |
| | 60/40 | 0.6938 | 70.09 | 0.5169 | 93.9 | 0.1906 | 96.4 |
| | 70/30 | 0.7121 | 68.99 | 0.4544 | 94.64 | 0.1906 | 96.81 |
| | 80/20 | 0.7028 | 69.87 | 0.4916 | 94.39 | 0.2278 | 96.65 |
| Squared Signal Combined With Original EEG Signal | 50/50 | 0.7321 | 67.84 | 0.6938 | 93.6 | 0.2126 | 96.48 |
| | 60/40 | 0.7235 | 67.54 | 0.6107 | 94.03 | 0.234 | 96.46 |
| | 70/30 | 0.7036 | 69.57 | 0.9528 | 93.62 | 0.2623 | 96.18 |
| | 80/20 | 0.7416 | 65.78 | 0.9429 | 93.23 | 0.3535 | 96.28 |
| Differentiated Combined With Original EEG Signal | 50/50 | 0.7775 | 67.73 | 0.9421 | 90.52 | 0.3159 | 93.76 |
| | 60/40 | 0.7539 | 68.62 | 0.8984 | 90.9 | 0.4077 | 92.38 |
| | 70/30 | 0.7629 | 66.96 | 0.7775 | 91.88 | 0.3247 | 93.82 |
| | 80/20 | 0.7576 | 67.43 | 0.8085 | 91.99 | 0.3006 | 94.7 |

continue on the next page

Table 9. (continued).

| | | | | | | | |
|---|---|---|---|---|---|---|---|
| FFT | 50/50 | 0.3223 | 95.34 | 0.2959 | 97.06 | 0.1587 | 97.01 |
| Combined | 60/40 | 0.2797 | 96.33 | 0.2278 | 97.67 | 0.1455 | 97.51 |
| With Original | 70/30 | 0.2634 | 95.99 | 0.2497 | 97.68 | 0.1531 | 96.86 |
| EEG Signal | 80/20 | 0.3289 | 93.8 | 0.2432 | 97.83 | 0.2821 | 96.06 |

At the first glance on table 9, in the DNN model a recognizable drop of accuracies and prevail of loss is noticed compared with the binary equivalent model or other binary ones, Although The overall trend is similar to the binary DNN. The best case is still the FFT combined with the original which has 93.8% accuracy here after it was 98.23% in the 2-class equivalent but the worst one is the squared combined with original case which is a first since this case was moderate in all of the previous evaluations.

For the proposed 1D-CNN moderate, the global trend is kept the same as the binary equivalent model with the loss being less than the 3-class DNN. There is an improvement leap in the values compared to the 3-class DNN model. The highest loss is in the squared combined with original case, although it does not have the lowest accuracy.

1D-CNN complex model, shows an excellent improvement on the last two models, especially regarding the loss. Accuracies of its cases appear close to each other values which is a new observation in 3-class classifications, but a consistent one for binary models. In (Abiyev et al., 2020) paper which has the same architecture for multiclass classification as our reproduction, the testing accuracy and loss for a standardized original input were 96.67% and 0.013878. Comparing the results with them, the standard original case has almost identical accuracy on 80/20 splitting but a much higher loss which might be related to the different vector input, or the researchers' 90/10 splitting and 10-fold-cross-validation. the next most close value is the only original case then the squared combined with original case. The differentiated combined with original case seems to negatively affect the values. But, if we consider the 50/50, 60/40 and 70/30 cases, the FFT combined with original has the highest accuracy. In principle, the combinations do not have a significant effect on this architecture while they can be good for other architectures especially the FFT combined with original case that dominantly showed enhancements in the proposed models and a vital improvement role in 50/50, 60/40 and 70/30 splittings in (Abiyev et al., 2020) reproduced model.

### *Confusion Matrix for 3-Class Classification Results*

The confusion matrices will be shown for multiclass classification models as figures, then the specificity, sensitivity, precision and f1 scores as tables. The 3-class confusion matrix is a 3*3 shaped one, its diagonal represents the true values (predictions with the ground truth). class zero represents the seizure, class one represents the preictal and class two represents the normal case which will be referred to as class one, two and three, respectively, in the scores tables. Remember that the original labels in the UCI version of the Bonn dataset are label one for seizure, label two for preictal and label four for normal cases. Figure 31 will represent the DNN 3-class confusion matrices. It can be observed that the FFT combined with the original case has the least confusion among all which is an indicator of excellence. the only original cases also seem to have lower confusion than others, but it is not the best case. Also, since the confusion matrices depend on the predictions (test splits) it is noticed that from 50/50 splits to 80/20 splits, in general, the values decrease in all cases which are expected. Figure 32 represent the confusion matrices for the proposed 1D-CNN moderate model. As an overall observation, the 1D-CNN cases have lower confusion than the DNN cases which suggests that more complex architectures play a significant role in confusion matrices. Also, as the DNN cases, the FFT combined with the original cases have the lowest confusion which confirms that the combinations also play a sufficient role in confusion enhancement. Next, the figure 33, will represent the confusion matrices of the 1D-CNN (complex) suggested by (Abiyev et al., 2020). The observation of figure 33 strengthens the last observation. However, the overall trends suggest slightly less confusion from the last 1D-CNN moderate case. Generally, the FFT combined with the original still has the lowest confusion among all but the deviation from other cases is less than other models.

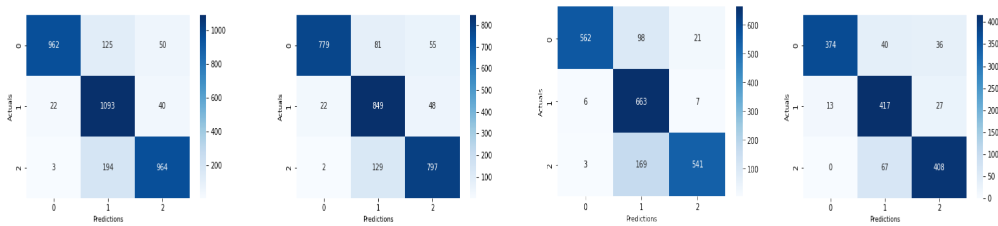


(a) DNN with Original EEG Signal (left 50/50, middle 60/40 then 70/30 and right 80/20

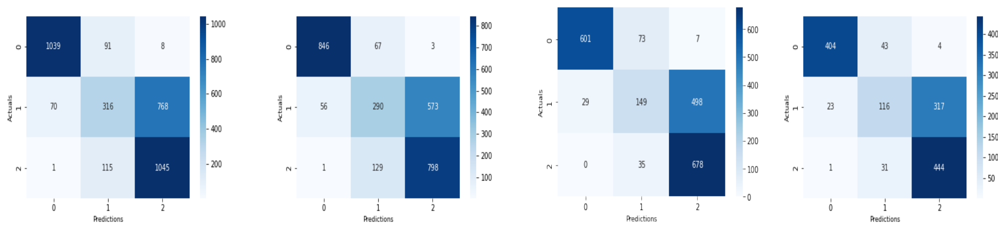


(b) DNN with Standard Original EEG Signal (left 50/50, middle 60/40 then 70/30 and right 80/20)

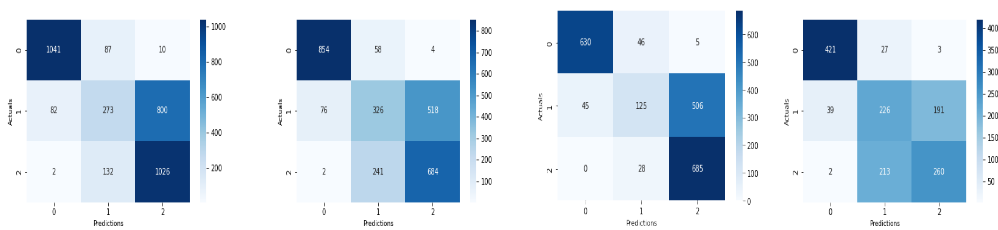


(c) DNN With Squared Signal Combined With Original EEG Signal (left 50/50, middle 60/40 then 70/30 and right 80/20)

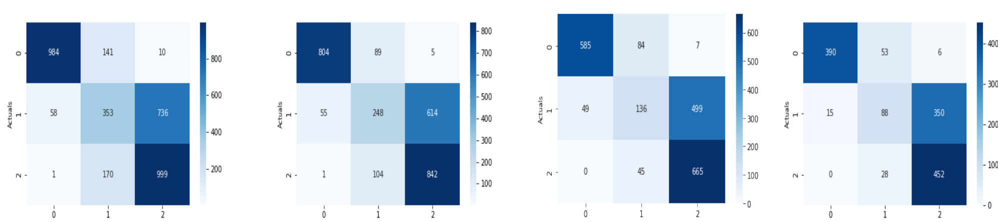


(d) DNN With Differentiated Combined With Original EEG Signal (left 50/50, middle 60/40 then 70/30 and right 80/20)

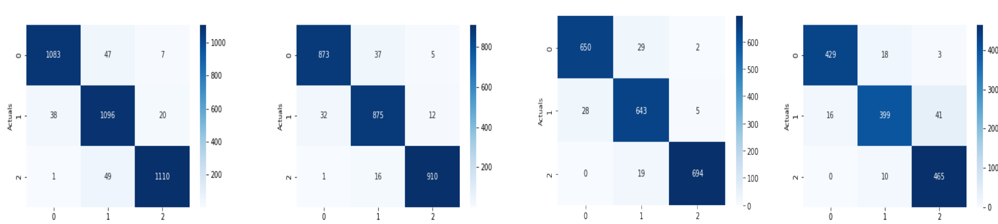


(e) DNN With FFT Combined With Original EEG Signal (left 50/50, middle 60/40 then 70/30 and right 80/20)

Figure 31
Confusion Matrix for 3-Class Classification on Bonn Dataset using the Proposed DNN with Modified EEG Signals

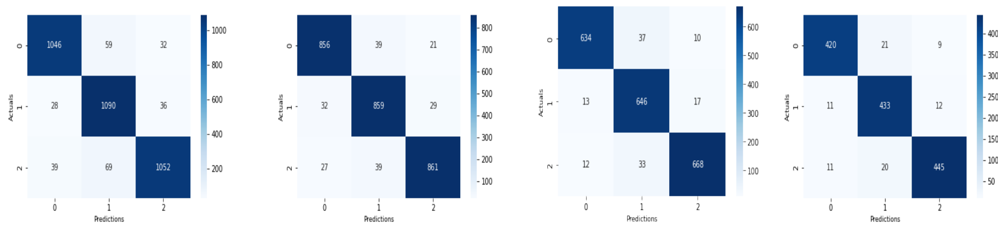

(a) 1D CNN (moderate) with Original EEG Signal (left 50/50, middle 60/40 then 70/30 and right 80/20

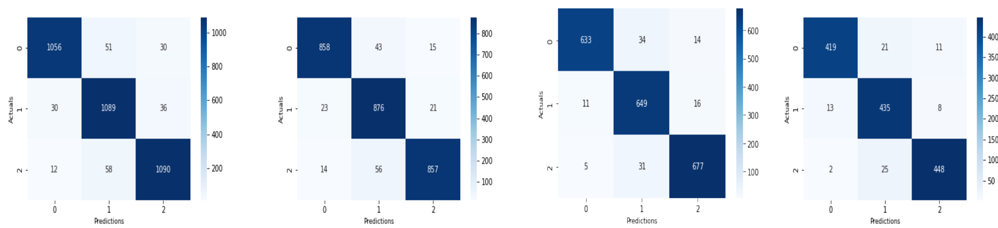

(b) 1D CNN (moderate) with Standard Original EEG Signal (left 50/50, middle 60/40 then 70/30 and right 80/20)

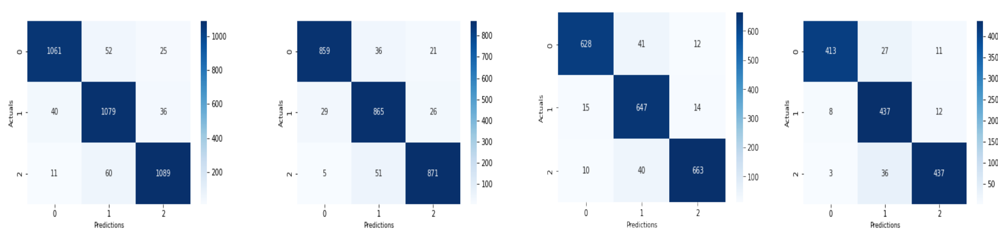

(c) 1D CNN (moderate) With Squared Signal Combined With Original EEG Signal (left 50/50, middle 60/40 then 70/30 and right 80/20)

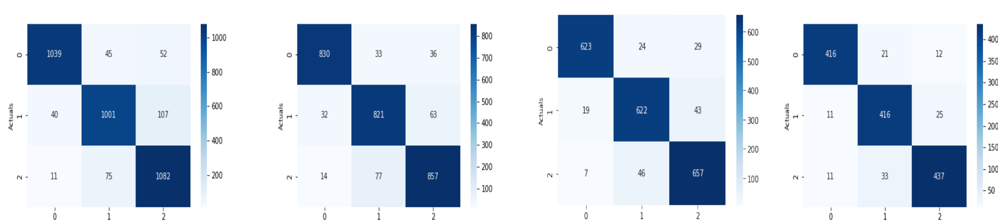

(d) 1D CNN (moderate) With Differentiated Combined With Original EEG Signal (left 50/50, middle 60/40 then 70/30 and right 80/20)

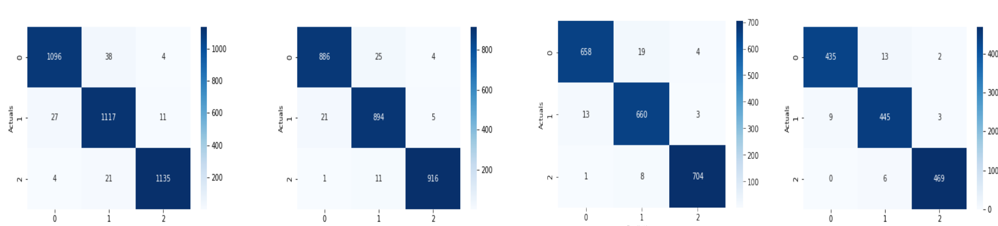

(e) 1D CNN (moderate) With FFT Combined With Original EEG Signal (left 50/50, middle 60/40 then 70/30 and right 80/20)

Figure 32
Confusion Matrix for 3-Class Classification on Bonn Dataset using the Proposed 1D-CNN (moderate) with Modified EEG Signals

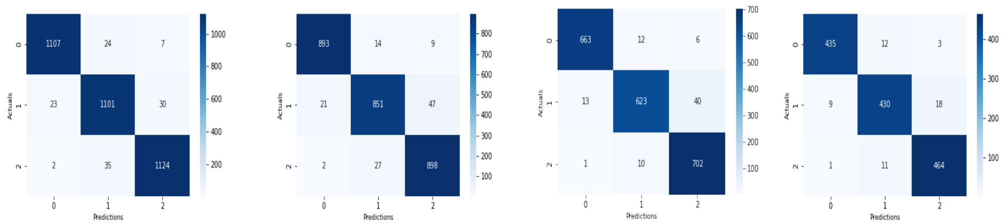

(a) 1D CNN (complex) with Original EEG Signal (left 50/50, middle 60/40 then 70/30 and right 80/20

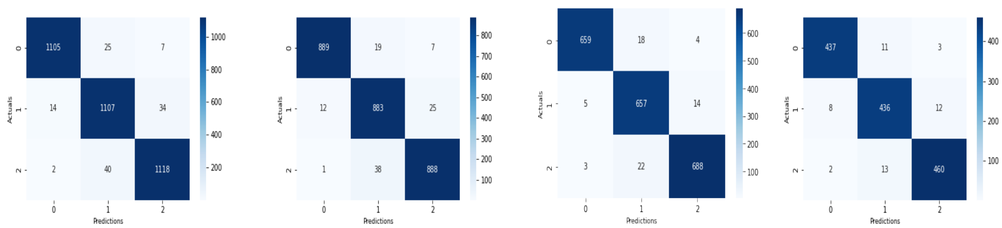

(b) 1D CNN (complex) with Standard Original EEG Signal (left 50/50, middle 60/40 then 70/30 and right 80/20)

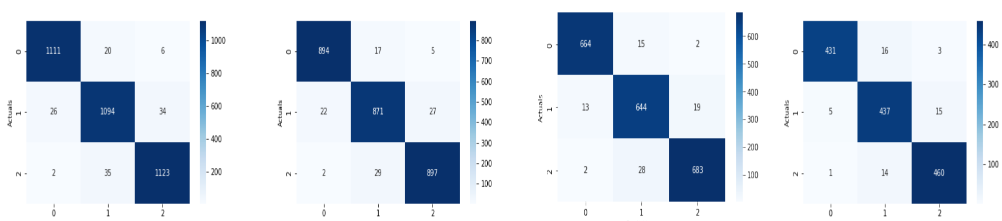

(c) 1D CNN (complex) With Squared Signal Combined With Original EEG Signal (left 50/50, middle 60/40 then 70/30 and right 80/20)

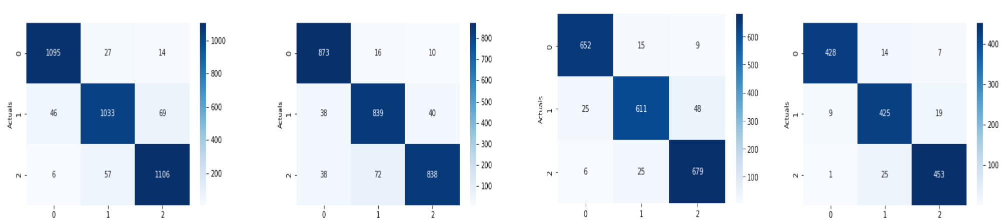

(d) 1D CNN (complex) With Differentiated Combined With Original EEG Signal (left 50/50, middle 60/40 then 70/30 and right 80/20)

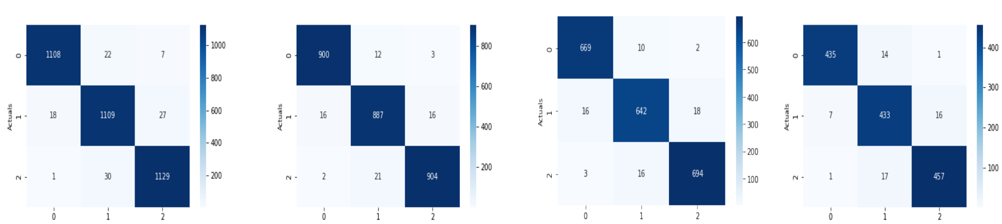

(e) 1D CNN (complex) With FFT Combined With Original EEG Signal (left 50/50, middle 60/40 then 70/30 and right 80/20)

Figure 33

Confusion Matrix for 3-Class Classification on Bonn Dataset using the 1D-CNN (complex) Model With Modified EEG Signals

***Comparing Specificity, Sensitivity, Precision and F1-Score Scores of the Methods***

In table 10, the 3-class classification result of the evaluated methods will be presented. The scores for each class will be presented as class 1, 2 and 3 representing seizure, preictal and normal classes respectively then the average of the three class on each splitting ratio will be presented.

Table 10.
*Comparing Specificity (SP), Sensitivity (SN)and Precision (P) of the Methods (Results are average of 5 runs).*

| EEG Signal | Class | Splitting % | DNN (Simple) | | | | 1D-CNN (Moderate) | | | | 1D-CNN (Complex) | | | |
|---|---|---|---|---|---|---|---|---|---|---|---|---|---|---|
| | | | SP | SN | P | F1 | SP | SN | P | F1 | SP | SN | P | F1 |
| Original EEG Signal Only | Class 1 | 50/50 | 98.97 | 84.66 | 97.6 | 90.65 | 97.14 | 92.07 | 94.09 | 93.05 | 98.95 | 97.4 | 97.85 | 97.62 |
| | | 60/40 | 98.72 | 85.22 | 97.11 | 90.73 | 96.83 | 93.62 | 93.66 | 93.62 | 98.76 | 97.62 | 97.52 | 97.57 |
| | | 70/30 | 99.35 | 82.53 | 98.42 | 89.78 | 98.2 | 93.1 | 96.21 | 94.63 | 98.99 | 97.36 | 97.93 | 97.64 |
| | | 80/20 | 98.62 | 83.29 | 96.77 | 89.44 | 97.72 | 93.47 | 95.22 | 94.33 | 99.08 | 96.84 | 98.08 | 97.45 |
| | Class 2 | 50/50 | 86.16 | 94.71 | 77.53 | 85.24 | 94.43 | 94.51 | 89.54 | 91.94 | 97.48 | 95.44 | 95.01 | 95.22 |
| | | 60/40 | 88.67 | 92.47 | 80.56 | 85.96 | 95.82 | 93.51 | 91.84 | 92.64 | 97.84 | 92.67 | 95.62 | 94.02 |
| | | 70/30 | 80.85 | 98.08 | 71.29 | 82.57 | 94.98 | 95.56 | 90.22 | 92.82 | 98.42 | 92.16 | 96.59 | 94.32 |
| | | 80/20 | 88.46 | 91.45 | 80.14 | 85.19 | 95.69 | 95 | 91.64 | 93.27 | 97.66 | 94.3 | 95.22 | 94.74 |
| | Class 3 | 50/50 | 96.1 | 83.12 | 91.64 | 87.11 | 97.07 | 90.7 | 94.08 | 92.29 | 98.44 | 96.91 | 96.91 | 96.91 |
| | | 60/40 | 94.44 | 85.98 | 88.87 | 87.27 | 97.36 | 92.89 | 94.71 | 93.77 | 97 | 96.93 | 94.39 | 95.59 |
| | | 70/30 | 97.94 | 75.88 | 95.08 | 84.4 | 98.01 | 93.69 | 96.12 | 94.89 | 96.61 | 98.46 | 93.85 | 96.1 |
| | | 80/20 | 93.22 | 85.95 | 87.4 | 86.44 | 97.68 | 93.71 | 95.52 | 94.58 | 97.73 | 97.76 | 95.81 | 96.76 |
| | Average | 50/50 | 93.74 | 87.5 | 88.92 | 87.67 | 96.21 | 92.43 | 92.57 | 92.43 | 98.29 | 96.58 | 96.59 | 96.58 |
| | | 60/40 | 93.94 | 87.89 | 88.85 | 87.99 | 96.67 | 93.34 | 93.4 | 93.34 | 97.87 | 95.74 | 95.84 | 95.73 |
| | | 70/30 | 92.71 | 85.5 | 88.26 | 85.58 | 97.06 | 94.12 | 94.18 | 94.11 | 98.01 | 95.99 | 96.12 | 96.02 |
| | | 80/20 | 93.43 | 86.9 | 88.1 | 87.02 | 97.03 | 94.06 | 94.13 | 94.06 | 98.16 | 96.3 | 96.37 | 96.32 |

continue on the next page

Table 10. (continued).

| | | | | | |
|---|---|---|---|---|---|
| Standard Original EEG Signal | Class 1 | 50/50 | 96.96 91.38 93.67 92.51 | 98.2 92.91 96.24 94.52 | 99.33 97.24 98.62 97.92 |
| | | 60/40 | 96.99 92.46 93.85 93.13 | 98.05 93.81 96 94.89 | 99.33 97.25 98.63 97.93 |
| | | 70/30 | 97.91 88.25 95.4 91.69 | 98.85 92.95 97.53 95.19 | 99.42 96.77 98.8 97.77 |
| | | 80/20 | 97.51 89.82 94.59 92.13 | 98.47 93.16 96.72 94.9 | 99.03 97.11 97.98 97.54 |
| | Class 2 | 50/50 | 91.07 27.44 60.77 37.52 | 95.27 94.37 90.95 92.62 | 97.2 95.94 94.53 95.22 |
| | | 60/40 | 89.44 31.64 60.28 40.92 | 94.69 95.36 90 92.59 | 96.99 96.08 94.16 95.07 |
| | | 70/30 | 92.25 22.04 57.98 31.94 | 95.34 96.01 90.9 93.38 | 97.13 97.19 94.26 95.7 |
| | | 80/20 | 92.12 25.53 60.3 35.34 | 95.17 95.57 90.75 93.09 | 97.51 95.79 95 95.39 |
| | Class 3 | 50/50 | 66.18 90.11 57.46 70.1 | 97.17 94.01 94.43 94.2 | 98.27 96.45 96.59 96.51 |
| | | 60/40 | 68.62 86.13 58.21 69.29 | 98.11 92.53 96.15 94.27 | 98.28 95.87 96.64 96.22 |
| | | 70/30 | 62.79 95.09 57.31 71.52 | 97.79 94.95 95.76 95.35 | 98.67 96.49 97.45 96.97 |
| | | 80/20 | 64.7 93.59 58.29 71.72 | 97.95 94.43 96.02 95.21 | 98.43 97.05 97.02 97.03 |
| | Average | 50/50 | 84.74 69.64 70.63 66.71 | 96.88 93.76 93.87 93.78 | 98.27 96.54 96.58 96.55 |
| | | 60/40 | 85.02 70.08 70.78 67.78 | 96.95 93.9 94.05 93.92 | 98.2 96.4 96.48 96.41 |
| | | 70/30 | 84.32 68.46 70.23 65.05 | 97.33 94.64 94.73 94.64 | 98.41 96.82 96.84 96.81 |
| | | 80/20 | 84.78 69.65 71.06 66.4 | 97.2 94.39 94.5 94.4 | 98.32 96.65 96.67 96.65 |

continue on the next page

Table 10. (continued).

| | | | | | | | | | | | | | | |
|---|---|---|---|---|---|---|---|---|---|---|---|---|---|---|
| Squared Signal Combined With Original EEG Signal | Class 1 | 50/50 | 96.44 | 91.57 | 92.68 | 92.11 | 97.84 | 93.33 | 95.51 | 94.4 | 98.81 | 97.73 | 97.58 | 97.65 |
| | | 60/40 | 95.86 | 93.38 | 91.87 | 92.58 | 98.2 | 93.9 | 96.29 | 95.08 | 98.78 | 97.75 | 97.57 | 97.64 |
| | | 70/30 | 96.76 | 92.51 | 93.33 | 92.92 | 98.2 | 92.22 | 96.17 | 94.15 | 98.92 | 97.5 | 97.79 | 97.65 |
| | | 80/20 | 95.68 | 93.6 | 91.38 | 92.43 | 98.95 | 91.78 | 97.69 | 94.63 | 99.4 | 95.96 | 98.75 | 97.3 |
| | Class 2 | 50/50 | 90.49 | 23.69 | 55.68 | 33.07 | 95.17 | 93.54 | 90.74 | 92.1 | 97.62 | 94.87 | 95.26 | 95.06 |
| | | 60/40 | 83.8 | 35.47 | 54.17 | 40.72 | 95.33 | 94.17 | 90.97 | 92.54 | 97.58 | 94.82 | 95.15 | 94.97 |
| | | 70/30 | 94.69 | 18.49 | 62.81 | 28.57 | 94.19 | 95.71 | 88.87 | 92.17 | 96.92 | 95.27 | 93.74 | 94.5 |
| | | 80/20 | 74.2 | 49.69 | 50.62 | 45.27 | 93.29 | 95.83 | 97.94 | 91.6 | 96.88 | 95.83 | 93.97 | 94.83 |
| | Class 3 | 50/50 | 64.71 | 88.52 | 55.94 | 68.52 | 97.38 | 93.93 | 94.79 | 94.34 | 98.29 | 96.86 | 96.63 | 96.74 |
| | | 60/40 | 71.58 | 73.84 | 56.69 | 62.23 | 97.51 | 94.02 | 95.04 | 94.52 | 98.33 | 96.8 | 96.7 | 96.75 |
| | | 70/30 | 62.34 | 96.07 | 57.27 | 71.77 | 98.08 | 92.99 | 96.23 | 94.58 | 98.45 | 95.79 | 97.02 | 96.4 |
| | | 80/20 | 78.63 | 54.85 | 57.75 | 49.99 | 97.62 | 92.11 | 95.32 | 93.56 | 98.12 | 97 | 96.46 | 96.72 |
| | Average | 50/50 | 83.88 | 67.93 | 68.1 | 64.57 | 96.8 | 93.6 | 93.68 | 93.61 | 98.24 | 96.49 | 96.49 | 96.48 |
| | | 60/40 | 83.75 | 67.56 | 67.58 | 65.18 | 97.01 | 94.03 | 94.1 | 94.05 | 98.23 | 96.46 | 96.47 | 96.45 |
| | | 70/30 | 84.6 | 69.02 | 71.14 | 64.42 | 96.82 | 93.64 | 93.76 | 93.63 | 98.1 | 96.19 | 96.18 | 96.18 |
| | | 80/20 | 82.84 | 66.05 | 66.58 | 62.56 | 96.62 | 93.24 | 93.65 | 93.26 | 98.13 | 96.26 | 96.39 | 96.28 |

continue on the next page

Table 10. (continued).

| | | | | | | | | | | | | | | |
|---|---|---|---|---|---|---|---|---|---|---|---|---|---|---|
| Differentiated Combined With Original EEG Signal | Class 1 | 50/50 | 97.49 | 86.75 | 94.43 | 90.41 | 97.81 | 91.59 | 95.38 | 93.44 | 97.81 | 96.51 | 95.6 | 96.04 |
| | | 60/40 | 97 | 89.58 | 93.52 | 91.5 | 97.59 | 92.47 | 94.92 | 93.66 | 95.97 | 97.26 | 92.86 | 94.8 |
| | | 70/30 | 96.48 | 86.54 | 92.27 | 89.31 | 98.13 | 92.16 | 95.99 | 94.04 | 97.78 | 96.45 | 95.46 | 95.95 |
| | | 80/20 | 98.45 | 87.04 | 96.45 | 91.49 | 97.72 | 92.74 | 95.22 | 93.92 | 98.97 | 95.5 | 97.84 | 96.64 |
| | Class 2 | 50/50 | 86.51 | 30.85 | 53.2 | 38.9 | 94.82 | 87.29 | 89.47 | 88.3 | 96.4 | 90.1 | 92.73 | 91.28 |
| | | 60/40 | 89.59 | 27.07 | 56.34 | 36.53 | 94.11 | 89.72 | 88.36 | 89.01 | 95.3 | 91.62 | 90.84 | 91.17 |
| | | 70/30 | 90.69 | 19.88 | 51.32 | 28.66 | 94.95 | 90.94 | 89.88 | 90.41 | 97.11 | 89.33 | 93.86 | 91.54 |
| | | 80/20 | 91.34 | 19.51 | 51.88 | 28.25 | 94.25 | 92.21 | 88.77 | 90.4 | 95.88 | 94.03 | 91.92 | 92.87 |
| | Class 3 | 50/50 | 67.37 | 85.46 | 57.31 | 68.55 | 93.1 | 92.64 | 87.35 | 89.89 | 96.42 | 94.67 | 93.22 | 93.9 |
| | | 60/40 | 65.92 | 88.96 | 57.66 | 69.96 | 94.61 | 90.55 | 89.8 | 90.16 | 97.32 | 88.5 | 94.79 | 90.91 |
| | | 70/30 | 62.79 | 93.66 | 56.79 | 70.71 | 94.71 | 92.54 | 90.12 | 91.31 | 95.81 | 95.63 | 92.26 | 93.91 |
| | | 80/20 | 60.64 | 94.28 | 56.05 | 70.28 | 96 | 91.06 | 92.41 | 91.72 | 97.18 | 94.57 | 94.76 | 94.63 |
| | Average | 50/50 | 83.79 | 67.69 | 68.31 | 65.95 | 95.24 | 90.51 | 90.73 | 90.54 | 96.88 | 93.76 | 93.85 | 93.74 |
| | | 60/40 | 84.17 | 68.54 | 69.17 | 66 | 95.44 | 90.91 | 91.03 | 90.94 | 96.2 | 92.46 | 92.83 | 92.29 |
| | | 70/30 | 83.32 | 66.69 | 66.79 | 62.89 | 95.93 | 91.88 | 92 | 91.92 | 96.9 | 93.8 | 93.86 | 93.8 |
| | | 80/20 | 83.48 | 66.94 | 68.13 | 63.34 | 95.99 | 92 | 92.13 | 92.01 | 97.34 | 94.7 | 94.84 | 94.71 |

continue on the next page

Table 10. (continued).

| | | | | | |
|---|---|---|---|---|---|
| FFT Combined With Original EEG Signal | Class 1 | 50/50 | 98.33 95.29 96.57 95.92 | 98.71 96.39 97.36 96.87 | 99.19 97.47 98.34 97.9 |
| | | 60/40 | 98.27 95.43 96.49 95.94 | 98.85 96.85 97.67 97.26 | 99.05 98.45 98.09 98.26 |
| | | 70/30 | 97.98 95.45 95.87 95.66 | 98.99 96.62 97.92 97.27 | 98.63 98.24 97.24 97.74 |
| | | 80/20 | 98.37 95.51 96.6 96.04 | 99.1 96.84 98.11 97.47 | 99.14 96.76 98.23 97.45 |
| | Class 2 | 50/50 | 95.82 95.04 92.2 93.52 | 97.48 96.85 95.1 95.96 | 97.76 96.17 95.58 95.87 |
| | | 60/40 | 97.13 95.28 94.32 94.79 | 98.1 97.3 96.24 96.77 | 98.24 96.56 96.49 96.52 |
| | | 70/30 | 96.56 95.12 93.05 94.07 | 98.06 97.63 96.07 96.85 | 98.13 94.97 96.11 95.54 |
| | | 80/20 | 97.06 87.68 93.68 89.92 | 98.07 97.68 96.16 96.91 | 96.73 95.13 94.01 94.32 |
| | Class 3 | 50/50 | 98.87 95.7 97.78 96.62 | 99.39 97.91 98.78 98.34 | 98.56 97.39 97.16 97.28 |
| | | 60/40 | 99.09 98.25 98.21 98.23 | 99.55 98.83 99.12 98.97 | 98.99 97.54 97.99 97.76 |
| | | 70/30 | 99.48 97.34 99 98.16 | 99.48 98.74 99.02 98.88 | 98.53 97.34 97.2 97.27 |
| | | 80/20 | 95.23 98.06 92.84 95.03 | 99.58 98.9 99.2 99.05 | 98.21 96.29 96.8 96.43 |
| | Average | 50/50 | 97.67 95.34 95.52 95.35 | 98.53 97.05 97.08 97.06 | 98.5 97.01 97.03 97.02 |
| | | 60/40 | 98.16 96.32 96.34 96.32 | 98.83 97.66 97.68 97.67 | 98.76 97.52 97.52 97.51 |
| | | 70/30 | 98.01 95.97 95.97 95.96 | 98.84 97.66 97.67 97.67 | 98.43 96.85 96.85 96.85 |
| | | 80/20 | 96.89 93.75 94.37 93.66 | 98.92 97.81 97.82 97.81 | 98.03 96.06 96.35 96.07 |

It can be observed that the per class results are severely fluctuating, so, the discussions will focus on the averaged values. Table 10, shows that DNN 3-class classification has a harsh effect on the scores compared with the binary equivalent case in tables 6 and 7. Although the combinations do not seem to suggest any enhancement, the FFT combined with the original cases present a significant superiority for per class and averaged behavior. The only competitor is the only original cases and both of the mentioned cases are much better than others. This observation may hint at a hidden relation or features that were kept and enhanced from the only original cases to the FFT combined with the original.

A noticeable stride in scores is observed in the proposed 1D-CNN moderate model. Showing that more complicated models can enhance the behavior which is a consistent observation in all our evaluations. The other important thing to see is that the FFT combined with the original is still the best case with relatively higher scores than the DNN equivalent and any other value of the same model although the other combinations are doing slightly less than the only original and standard original cases which leads us to another consistent observation, that the FFT combination usually improves any model.

In the reproduced 1D-CNN complex model suggested by (Abiyev et al., 2020), the original team did only one case which is the standard original case as was explained before in the table 9 discussion. The original team recorded the results of the average test specificity and sensitivity of the standard original case as 98.33% and 96.67%, respectively. Comparing their results with our 80/20 standard original case which is the closest case to theirs, we got 98.32% and 96.65% for specificity and sensitivity, respectively. our results are quite close, suggesting an accurate reproduction. Also, the standard original case averages are seen as the best values, although the combinations are mainly good competitors especially considering their enhancement effects on the DNN and the proposed 1D-CNN moderate cases. In addition, the best scores from the proposed 1D-CNN moderate model are a little better than the best scores in this model since the FFT combined with the original 80/20 case averages gave 98.92%, 97.81%, 97.82%, and 97.81% for the same arrangement of the scores in the table, respectively compared with the best case here, the standard original 80/20 averages 98.32%, 96.65%, 96.67% and 96.65% for the same arrangement of the scores in the table, respectively. the last observation empowers the consistent claim and observations of the positive effect of the FFT combination on the original signal, in all 3-class models which can point to some hidden features in the discrete frequency domain revealed by the FFT.

The overall observations are that the more deep and complex architectures give improved scores and the combinations can give good improvements and approximations of complex architectures on simpler ones, especially.

### Comparison of the Proposed Work with Other Related Methods

In this section, some comparisons from research teams that applied the same or close setting to our evaluations will be presented. The next table show 3-class and binary classification results that used the same dataset we used (Bonn dataset). Note that some of the research teams did not report all the metrics and scores that we recorded, also all of them who evaluated multiclass cases used the averaged metrics and scores for the three classes which are equivalent to the average results in our 3-class tables. Figure 34 shows summarized evaluations of many cases and table 12 puts focus on the 2-class classification only.

Table 11.
*Comparative Results, Accuracy (ACC), Sensitivity (SN) and Specificity (SP)*

| Author | Model | Train/Test And Validation% | ACC% | SN% | SP% |
|---|---|---|---|---|---|
| Abiyev et al. (2020) | Deep CNN | 90/10 and 30 from the training for validation | 98.67 | 97.67 | 98.83 |
| Akyol (2020) | SEA-DNN | 90/10 and 10 from the training for validation | 97.17 | 93.11 | 98.18 |
| Hassan et al. (2020) | CEEMDAN | No splits | 98.67 | 98.67 | 98.72 |
| Thara et al. (2019) | DNN | 80/20 | 97.21 | 98.59 | 91.47 |
| Ullah et al. (2018) | P-1D-CNN | 90/10 | 99.6 | - | - |
| Vipani et al. (2017) | HT and LVQ | 20/80 | 89.31 | - | - |
| Gupta and Pachori (2019) | FBSE, WMRPE and Regression | - | 98.6 | - | - |
| Al-Sharhan and Bimba (2019) | MPC-GA | 80/20 | 98.01 | 94.99 | 98.65 |
| Acharya, Oh, Hagiwara, Tan, and Adeli (2018) | Deep CNN | 90/10 and 30 from the training for validation | 88.7 | 95 | 90 |
| M. Sharma et al. (2017) | OWFB | 90/10 | 99.2 | 98 | 99.75 |

continue on the next page

Table 11. (continued).

| | | | | | |
|---|---|---|---|---|---|
| Bhattacharyya et al. (2017) | TQWT-SVM | - | 98.6 | - | - |
| Bhattacharyya and Pachori (2017) | Random forest | - | 99.4 | 97.9 | 99.5 |
| Martis et al. (2012) | C4.5 decision tree | - | 95.33 | 98 | 97 |
| Acharya et al. (2012) | WPD-Fuzzy Sugeno | 90/10 | 96.7 | 95 | 99 |
| Acharya, Sree, Chattopadhyay, et al. (2011) | SVM | 67/33 | 95.6 | 98.9 | 97.8 |
| Guo et al. (2011) | GP-KNN | 40/60 | 93.5 | - | - |
| Acharya, Sree, and Suri (2011) | DWT(WPD)-SVM | 67/33 | 96.3 | 100 | 97.9 |
| Faust et al. (2010) | SVM | 70/30 | 93.3 | 98.3 | 96.7 |
| Chua et al. (2011) | HOS-GMM | 70/30 | 93.11 | 89.67 | 94.83 |
| Ghosh-Dastidar et al. (2008) | PCA-enhanced cosine RBFNN | - | 99.3 | - | - |
| Ghosh-Dastidar et al. (2007) | LMBPNN | 20/80 | 96.7 | - | - |
| Ghosh-Dastidar and Adeli (2007) | SNN | 80/20 | 92.5 | - | - |
| Proposed | 3-Class DNN (simple) (FFT combination) | 80/20 | 93.8 | 93.75 | 96.89 |
| Proposed | 3-Class 1D-CNN (moderate) (FFT combination) | 80/20 | 97.83 | 97.81 | 98.92 |
| Proposed | 3-Class 1D-CNN (complex) (FFT combination) | 60/40 | 97.51 | 92.46 | 96.2 |

continue on the next page

Table 11. (continued).

Next in figure 34, a summary based on the Bonn dataset will present many cases. The binary classification that was done in this thesis is equivalent to the ABCD-E case. Other 2-class classifications are also close as all of them regarded the E label which represents the seizure class in the Bonn dataset. The presented 3-class case of AB-CD-E is not the same as the one used in the thesis, which is equivalent to B-D-E, however, it is still a close and valid comparison. It can be observed that the results are above 95%, which is the same range that our FFT combination results fall into, in general.

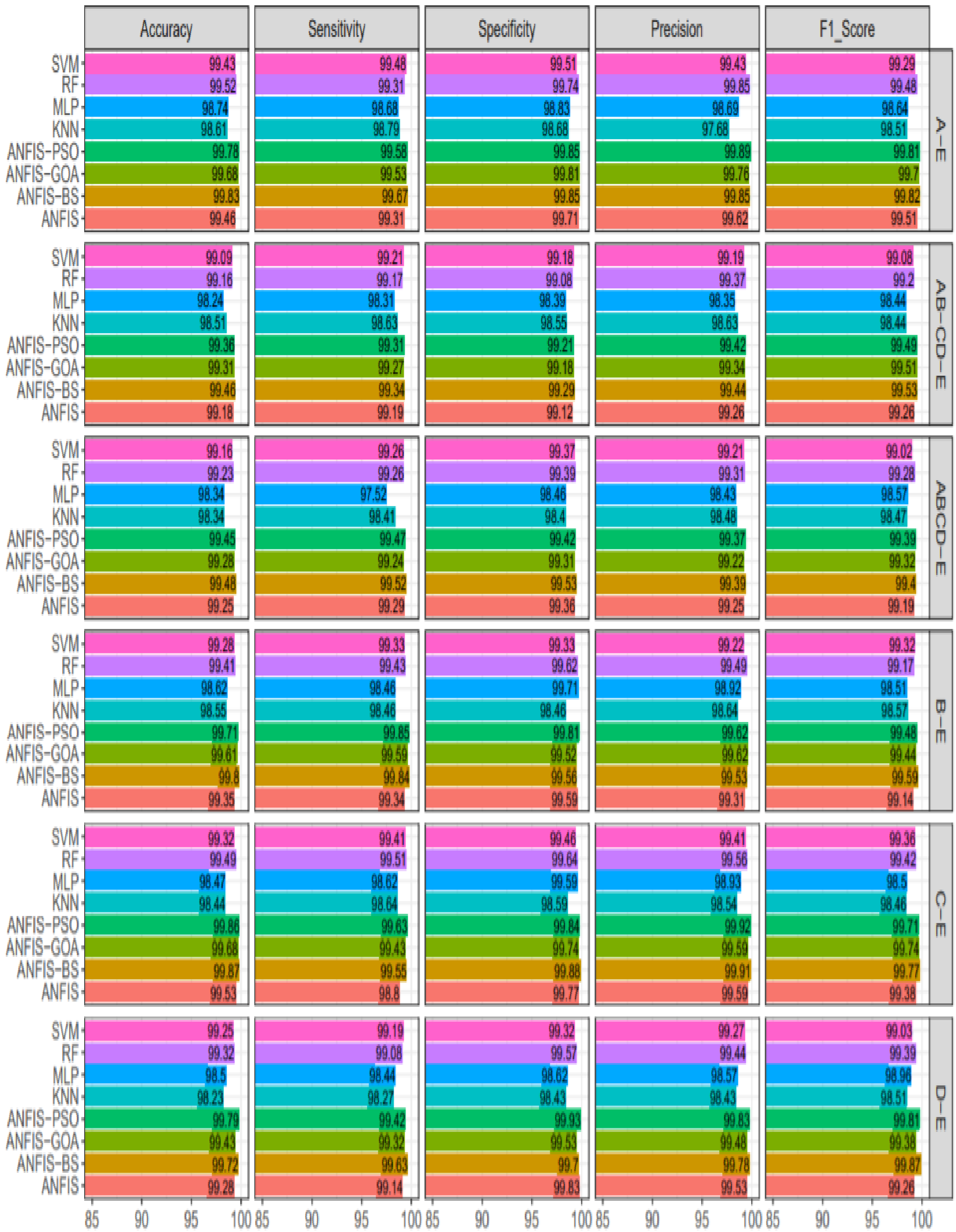


Figure 34
*(Shoeibi et al., 2022, Fig. 9)*

The next table will further focus on binary classification comparisons.

Table 12.
*Additional 2-Class Only Comparative Results, Accuracy (ACC), Sensitivity (SN), Specificity (SP), F1-score (F1) and Precision (P)*

| Author | Model | Train/Test And validation% | ACC% | SN% | SP% | F1% | P % |
|---|---|---|---|---|---|---|---|
| Nagabushanam et al. (2020) | NN | No splits | 61.43 | 61.65 | - | 62.18 | 62.72 |
| Nagabushanam et al. (2020) | LSTM | No splits | 71.38 | 73.38 | - | 72.51 | 71.66 |
| Nagabushanam et al. (2020) | INN | No splits | 78.92 | 93.70 | - | 82.05 | 72.98 |
| S.-H. Lee et al. (2014) | WT, PSR, ED | 62.5/37.5 | 98.17 | 96.33 | 100 | - | - |
| Polat and Güneş (2007) | FFT and Decision Tree | 90/10 | 98.72 | 99.40 | 99.31 | - | - |
| Wang et al. (2019) | GSO-SVM | - | 98.4 | - | - | - | - |
| Türk and Özerdem (2019) | CNN with Scalogram (A-E) | 72/10 and 18 validation | 99.50 | 99.00 | 100 | 99.50 | - |
| Türk and Özerdem (2019) | CNN with Scalogram (B-E) | 72/10 and 18 validation | 99.50 | 100 | 100 | 99.50 | - |
| Türk and Özerdem (2019) | CNN with Scalogram (C-E) | 72/10 and 18 validation | 98.50 | 98.01 | 98.98 | 98.50 | - |
| Türk and Özerdem (2019) | CNN with Scalogram (D-E) | 72/10 and 18 validation | 98.01 | 98.98 | 98.50 | - | |
| Proposed | 2-Class DNN (simple) (FFT combination) | 80/20 | 98.23 | 94.71 | 99.12 | 95.57 | 96.47 |
| Proposed | 2-Class 1D-CNN (moderate) (FFT combination) | 80/20 | 98.91 | 96.43 | 99.54 | 97.29 | 98.17 |

continue on the next page

Table 12. (continued).

| | | | | | | | |
|---|---|---|---|---|---|---|---|
| Proposed | 2-Class 1D-CNN (complex) (FFT combination) | 80/20 | 99.13 | 98.32 | 99.34 | 97.87 | 97.45 |

As it was noticed from the previous tables, our contribution is a good competitor with any work in binary or 3-class classification cases and it is superior sometimes considering the simplicity of the evaluated architectures and the low training times.

# CHAPTER VIII

## Conclusions And Future Work

This chapter highlights the conclusions that were observed in the discussions of the previous chapter, then some suggestions for the future work are discussed.

### Conclusions

In this thesis, we successfully evaluated three different architectures of deep learning, namely, DNN, 1D-CNN, and (Abiyev et al., 2020) 1D-CNN. The evaluation was conducted based on forming various input data to these architectures. Our contribution is about using preprocessed and combined EEG signals as an input. The combined EEG signals after the following pre-processing stages: the squaring of the original EEG, the discrete differentiation, and FFT. Also, we evaluated the raw EEG signal and the standardized version of it. Four different splitting ratios were tested, the 50/50, 60/40, 70/30 and 80/20, and each test was repeated five times.

Our Our work was also compared to many other state-of-art papers other than the comparisons among the thesis evaluations themselves as comparing the only original and modified inputs against each other and against (Abiyev et al., 2020) model. We have seen consistent observations in favor of our proposed method. Our proposed method achieved the highest performance in DNN, 1DCNN, and (Abiyev et al., 2020) models for 2-class classification and they showed a vast stride of performance in the 3-class classifications with the DNN. Also, with the proposed 1D-CNN which were superior to the (Abiyev et al., 2020) 1D-CNN 3-class results, in general, and the FFT combination was superior in the 50/50, 60/40 and 70/30 cases to all others of the same model. Our proposed FFT combination was the best among all, generally, which might be an indication of some hidden features in the discrete frequency domain that were revealed and combined with time-series samples.

Another consistent observation is that the proposed modified inputs can have better enhancement effects on simple models and can increase their performance drastically close to deeper and more complex architectures with much lower training times which is a huge advantage for practical availability of simple deep learning models.

Some of our highest achieving results are 99.13%, 98.32%, 99.34%, 97.87% and 97.45% for accuracy, sensitivity, specificity, f1-score and precision respectively with (Abiyev et al., 2020) reproduced 1D-CNN in 2-class classification with FFT combination and 97.83% accuracy 97.81% sensitivity and 98.92% specificity with the proposed 1D-CNN moderate model in 3-class classification with FFT combination.

The promise of our proposal is those input modifications, which can be crucial as the architecture types, that can simulate the behavior of deeper and more complex models with virtually the same performance.

**Future Work**

The proposed work is based on preprocessed and combined EEG signals input to deep learning models. In our study, we combined two set inputs such as original EEG data combined with the FFT of the data. In future, combination of three sets of data can be considered.

Also, more operations can be tested on the datasets as combinations other than the FFT, discrete differentiation and squaring. Wavelet transform is a recommended operation.

Another suggestion is evaluating the proposed method on other datasets, the CHB-MIT dataset is recommended for 2-class cases, and with other classes of brain activity such as the available non-tested ones in the Bonn dataset. In addition, the proposed input EEG signals can be evaluated with other architectures in the state-of-art.

Trying other preprocessing and scalars of the EEG data also should be taken into consideration since our method relayed on standardization.

Finally, interpolation operations can be applied to our input signals for size adjustment.

**REFERENCES**

Abdelhameed, A., & Bayoumi, M. (2021). A deep learning approach for automatic seizure detection in children with epilepsy. *Frontiers in Computational Neuroscience*, *15*, 29.

Abdelhameed, A. M., Daoud, H. G., & Bayoumi, M. (2018). Epileptic seizure detection using deep convolutional autoencoder. *2018 IEEE International Workshop on Signal Processing Systems (SiPS)*, 223–228.

Abiyev, R., Arslan, M., Bush Idoko, J., Sekeroglu, B., & Ilhan, A. (2020). Identification of epileptic eeg signals using convolutional neural networks. *Applied Sciences*, *10*(12), 4089.

Acharya, U. R., Oh, S. L., Hagiwara, Y., Tan, J. H., & Adeli, H. (2018). Deep convolutional neural network for the automated detection and diagnosis of seizure using eeg signals. *Computers in biology and medicine*, *100*, 270–278.

Acharya, U. R., Oh, S. L., Hagiwara, Y., Tan, J. H., Adeli, H., & Subha, D. P. (2018). Automated eeg-based screening of depression using deep convolutional neural network. *Computer methods and programs in biomedicine*, *161*, 103–113.

Acharya, U. R., Sree, S. V., Alvin, A. P. C., & Suri, J. S. (2012). Use of principal component analysis for automatic classification of epileptic eeg activities in wavelet framework. *Expert Systems with Applications*, *39*(10), 9072–9078.

Acharya, U. R., Sree, S. V., Chattopadhyay, S., Yu, W., & Ang, P. C. A. (2011). Application of recurrence quantification analysis for the automated identification of epileptic eeg signals. *International journal of neural systems*, *21*(03), 199–211.

Acharya, U. R., Sree, S. V., & Suri, J. S. (2011). Automatic detection of epileptic eeg signals using higher order cumulant features. *International journal of neural systems*, *21*(05), 403–414.

Akyol, K. (2020). Stacking ensemble based deep neural networks modeling for effective epileptic seizure detection. *Expert Systems with Applications*, *148*, 113239.

Al-Sharhan, S., & Bimba, A. (2019). Adaptive multi-parent crossover ga for feature optimization in epileptic seizure identification. *Applied Soft Computing*, *75*, 575–587.

Ball, T., Kern, M., Mutschler, I., Aertsen, A., & Schulze-Bonhage, A. (2009). Signal quality of simultaneously recorded invasive and non-invasive eeg. *Neuroimage*, *46*(3), 708–716.

Bhattacharyya, A., & Pachori, R. B. (2017). A multivariate approach for patient-specific eeg seizure detection using empirical wavelet transform. *IEEE Transactions on Biomedical Engineering*, *64*(9), 2003–2015.

Bhattacharyya, A., Pachori, R. B., Upadhyay, A., & Acharya, U. R. (2017). Tunable-q wavelet transform based multiscale entropy measure for automated classification of epileptic eeg signals. *Applied Sciences*, *7*(4), 385.

Biasiucci, A., Franceschiello, B., & Murray, M. M. (2019). Electroencephalography. *Current Biology*, *29*(3), R80–R85.

Boonyakitanont, P., Lek-Uthai, A., Chomtho, K., & Songsiri, J. (2020). A review of feature extraction and performance evaluation in epileptic seizure detection using eeg. *Biomedical Signal Processing and Control*, *57*, 101702.

Chen, B., Deng, W., & Du, J. (2017). Noisy softmax: Improving the generalization ability of dcnn via postponing the early softmax saturation. *Proceedings of the IEEE Conference on Computer Vision and Pattern Recognition*, 5372–5381.

Chua, K. C., Chandran, V., Acharya, U. R., & Lim, C. M. (2011). Application of higher order spectra to identify epileptic eeg. *Journal of medical systems*, *35*(6), 1563–1571.

Das, K., Daschakladar, D., Roy, P. P., Chatterjee, A., & Saha, S. P. (2020). Epileptic seizure prediction by the detection of seizure waveform from the pre-ictal phase of eeg signal. *Biomedical Signal Processing and Control*, *57*, 101720.

Emotiv. (2021). *Eeg guide*. Retrieved February 1, 2022, from https://www.emotiv.com/eeg-guide/

Faust, O., Acharya, U. R., Min, L. C., & Sputh, B. H. (2010). Automatic identification of epileptic and background eeg signals using frequency domain parameters. *International journal of neural systems*, *20*(02), 159–176.

Ghassemi, N., Shoeibi, A., Rouhani, M., & Hosseini-Nejad, H. (2019). Epileptic seizures detection in eeg signals using tqwt and ensemble learning. *2019 9th International Conference on Computer and Knowledge Engineering (ICCKE)*, 403–408.

Ghosh-Dastidar, S., & Adeli, H. (2007). Improved spiking neural networks for eeg classification and epilepsy and seizure detection. *Integrated Computer-Aided Engineering*, *14*(3), 187–212.

Ghosh-Dastidar, S., Adeli, H., & Dadmehr, N. (2007). Mixed-band wavelet-chaos-neural network methodology for epilepsy and epileptic seizure detection. *IEEE transactions on biomedical engineering*, *54*(9), 1545–1551.

Ghosh-Dastidar, S., Adeli, H., & Dadmehr, N. (2008). Principal component analysis-enhanced cosine radial basis function neural network for robust epilepsy and seizure detection. *IEEE Transactions on Biomedical Engineering*, *55*(2), 512–518. https://doi.org/10.1109/TBME.2007.905490

Google. (2022). *Google colab*. Retrieved January 5, 2022, from https://research.google.com/colaboratory/faq.html

Gotman, J., Ives, J., & Gloor, P. (1979). Automatic recognition of inter-ictal epileptic activity in prolonged eeg recordings. *Electroencephalography and clinical neurophysiology*, *46*(5), 510–520.

Guo, L., Rivero, D., Dorado, J., Munteanu, C. R., & Pazos, A. (2011). Automatic feature extraction using genetic programming: An application to epileptic eeg classification. *Expert Systems with Applications*, *38*(8), 10425–10436.

Gupta, V., & Pachori, R. B. (2019). Epileptic seizure identification using entropy of fbse based eeg rhythms. *Biomedical Signal Processing and Control*, *53*, 101569.

Hassan, A. R., Subasi, A., & Zhang, Y. (2020). Epilepsy seizure detection using complete ensemble empirical mode decomposition with adaptive noise. *Knowledge-Based Systems*, *191*, 105333.

Hossain, M. S., Amin, S. U., Alsulaiman, M., & Muhammad, G. (2019). Applying deep learning for epilepsy seizure detection and brain mapping visualization. *ACM Transactions on Multimedia Computing, Communications, and Applications (TOMM)*, *15*(1s), 1–17.

Jebelli, H., Hwang, S., & Lee, S. (2018). Eeg signal-processing framework to obtain high-quality brain waves from an off-the-shelf wearable eeg device. *Journal of Computing in Civil Engineering*, *32*(1), 04017070.

Karadurmuş, E., Taşkın, N., Göz, E., & Yüceer, M. (2019). Prediction of bromate removal in drinking water using artificial neural networks. *Ozone: Science & Engineering*, *41*(2), 118–127.

Lee, S.-H., Lim, J. S., Kim, J.-K., Yang, J., & Lee, Y. (2014). Classification of normal and epileptic seizure eeg signals using wavelet transform, phase-space reconstruction, and euclidean distance. *Computer methods and programs in biomedicine*, *116*(1), 10–25.

Lee, T.-H. (2008). Loss functions in time series forecasting. *International encyclopedia of the social sciences*, 495–502.

Martis, R. J., Acharya, U. R., Tan, J. H., Petznick, A., Yanti, R., Chua, C. K., Ng, E. K., & Tong, L. (2012). Application of empirical mode decomposition (emd) for automated detection of epilepsy using eeg signals. *International journal of neural systems*, *22*(06), 1250027.

McGill, P. V. L. (2021). *Eeg*. Retrieved January 31, 2022, from https://www.medicine.mcgill.ca/physio/vlab/biomed_signals/eeg_n.htm

Mozaffari, M. H., & Tay, L.-L. (2020). A review of 1d convolutional neural networks toward unknown substance identification in portable raman spectrometer. *arXiv preprint arXiv:2006.10575*.

Mujeeb, S., Alghamdi, T. A., Ullah, S., Fatima, A., Javaid, N., & Saba, T. (2019). Exploiting deep learning for wind power forecasting based on big data analytics. *Applied Sciences*, *9*(20), 4417.

Nagabushanam, P., Thomas George, S., & Radha, S. (2020). Eeg signal classification using lstm and improved neural network algorithms. *Soft Computing*, *24*(13), 9981–10003.

Nandy, A., Alahe, M. A., Uddin, S. N., Alam, S., Nahid, A.-A., & Awal, M. A. (2019). Feature extraction and classification of eeg signals for seizure detection. *2019 In-*

*ternational Conference on Robotics, Electrical and Signal Processing Techniques (ICREST)*, 480–485.

Nayak, C., & Anilkumar, A. (2021). *Eeg normal waveforms*. Retrieved January 12, 2022, from https://www.ncbi.nlm.nih.gov/books/NBK539805/

Peltarion. (2022). *Global average pooling 1d*. Retrieved January 12, 2022, from https://peltarion.com/knowledge-center/documentation/modeling-view/build-an-ai-model/blocks/global-average-pooling-1d

Polat, K., & Güneş, S. (2007). Classification of epileptiform eeg using a hybrid system based on decision tree classifier and fast fourier transform. *Applied Mathematics and Computation*, *187*(2), 1017–1026.

Postalcıoğlu, S. (2020). Performance analysis of different optimizers for deep learning-based image recognition. *International Journal of Pattern Recognition and Artificial Intelligence*, *34*(02), 2051003.

Qiuyi, W. (2022). *Epileptic seizure recognition data set. uci machine learning repository (2017)*. Retrieved January 5, 2022, from https://www.ukbonn.de/epileptologie/

Ragab, M. G., Abdulkadir, S. J., Aziz, N., Al-Tashi, Q., Alyousifi, Y., Alhussian, H., & Alqushaibi, A. (2020). A novel one-dimensional cnn with exponential adaptive gradients for air pollution index prediction. *Sustainability*, *12*(23), 10090.

Roman-Gonzalez, A. (2010). Communication technologies based on brain activity. *2010 World Congress in Computer Science, Computer Engineering and Applied Computing-WORLDCOMP 2010*, 91–96.

Sharma, M., Pachori, R. B., & Acharya, U. R. (2017). A new approach to characterize epileptic seizures using analytic time-frequency flexible wavelet transform and fractal dimension. *Pattern Recognition Letters*, *94*, 172–179.

Sharma, O. (2019). A new activation function for deep neural network. *2019 international conference on machine learning, big data, cloud and parallel computing (COMIT-Con)*, 84–86.

Shoeibi, A., Ghassemi, N., Alizadehsani, R., Rouhani, M., Hosseini-Nejad, H., Khosravi, A., Panahiazar, M., & Nahavandi, S. (2021). A comprehensive comparison of handcrafted features and convolutional autoencoders for epileptic seizures detection in eeg signals. *Expert Systems with Applications*, *163*, 113788.

Shoeibi, A., Ghassemi, N., Khodatars, M., Moridian, P., Alizadehsani, R., Zare, A., Khosravi, A., Subasi, A., Acharya, U. R., & Gorriz, J. M. (2022). Detection of epileptic seizures on eeg signals using anfis classifier, autoencoders and fuzzy entropies. *Biomedical Signal Processing and Control*, *73*, 103417.

Shoeibi, A., Khodatars, M., Ghassemi, N., Jafari, M., Moridian, P., Alizadehsani, R., Panahiazar, M., Khozeimeh, F., Zare, A., Hosseini-Nejad, H., et al. (2021). Epileptic seizures detection using deep learning techniques: A review. *International Journal of Environmental Research and Public Health*, *18*(11), 5780.

Stamoulis, C., Gruber, L. J., Schomer, D. L., & Chang, B. S. (2012). High-frequency neuronal network modulations encoded in scalp eeg precede the onset of focal seizures. *Epilepsy & Behavior*, *23*(4), 471–480.

Subasi, A., Kevric, J., & Canbaz, M. A. (2019). Epileptic seizure detection using hybrid machine learning methods. *Neural Computing and Applications*, *31*(1), 317–325.

Swami, P., Gandhi, T. K., Panigrahi, B. K., Tripathi, M., & Anand, S. (2016). A novel robust diagnostic model to detect seizures in electroencephalography. *Expert Systems with Applications*, *56*, 116–130.

Talathi, S. S. (2017). Deep recurrent neural networks for seizure detection and early seizure detection systems. *arXiv preprint arXiv:1706.03283*.

Thara, D., PremaSudha, B., & Xiong, F. (2019). Auto-detection of epileptic seizure events using deep neural network with different feature scaling techniques. *Pattern Recognition Letters*, *128*, 544–550.

Türk, Ö., & Özerdem, M. S. (2019). Epilepsy detection by using scalogram based convolutional neural network from eeg signals. *Brain sciences*, *9*(5), 115.

Ullah, I., Hussain, M., Aboalsamh, H., et al. (2018). An automated system for epilepsy detection using eeg brain signals based on deep learning approach. *Expert Systems with Applications*, *107*, 61–71.

Uni-Bonn. (2022). *Epileptologie*. Retrieved January 5, 2022, from https://www.ukbonn.de/epileptologie/

vidyasheela. (2022). *Leakyrelu*. Retrieved January 12, 2022, from https://vidyasheela.com/post/leaky-relu-activation-function-with-python-code

Vipani, R., Hore, S., Basu, S., Basak, S., & Dutta, S. (2017). Identification of epileptic seizures using hilbert transform and learning vector quantization based classifier. *2017 IEEE Calcutta Conference (CALCON)*, 90–94.

Waldert, S. (2016). Invasive vs. non-invasive neuronal signals for brain-machine interfaces: Will one prevail? *Frontiers in Neuroscience*, *10*. https://doi.org/10.3389/fnins.2016.00295

Wang, X., Gong, G., & Li, N. (2019). Automated recognition of epileptic eeg states using a combination of symlet wavelet processing, gradient boosting machine, and grid search optimizer. *Sensors*, *19*(2), 219.

WHO. (2022). *Epilepsy*. Retrieved January 12, 2022, from https://www.who.int/en/news-room/fact-sheets/detail/epilepsy

Zhou, M., Tian, C., Cao, R., Wang, B., Niu, Y., Hu, T., Guo, H., & Xiang, J. (2018). Epileptic seizure detection based on eeg signals and cnn. *Frontiers in neuroinformatics*, *12*, 95.

# APPENDECIES

## Appendix A

## Python Code

```
sample_size = x_train.shape[0]
time_steps = x_train.shape[1]
input_dimension = 1
sample_sizet = x_test.shape[0]
time_stepst = x_test.shape[1]
x_train_reshaped = x_train.reshape(sample_size,time_steps,input_dimension)
x_test_reshaped = x_test.reshape(sample_sizet,time_stepst,input_dimension)
# implementing Proposed DNN model for 2-class
from keras.models import Sequential
from keras import layers
model = Sequential()
model.add(layers.Dense(64, activation="LeakyReLU", input_shape =( x_train.shape[2],))
model.add(layers.Dropout(0.5))
model.add(layers.Dense(64, activation="LeakyReLU"))
model.add(layers.Dense(64, activation="LeakyReLU"))
model.add(layers.Dense(64, activation="LeakyReLU"))
model.add(layers.Dense(64, activation="LeakyReLU"))
model.add(layers.Dense(64, activation="LeakyReLU"))
model.add(layers.Dense(1, activation="sigmoid"))
model.summary()

# implementing Proposed 1D-CNN model for 2-class
```

```
from tensorflow import keras
from tensorflow.keras import datasets, layers, models, Sequential
import time
model =keras.Sequential(name="model_conv1D")
model.add(keras.layers.Input(shape=( x_train_reshaped.shape[1],x_train_reshaped.shape[2])))
model.add(keras.layers.Conv1D(filters=64, kernel_size=7, activation='LeakyReLU', name="C
onv1D_1"))
model.add(keras.layers.Dropout(0.5))
model.add(keras.layers.Conv1D(filters=32, kernel_size=3, activation='LeakyReLU', name="C
onv1D_2"))
model.add(keras.layers.Conv1D(filters=16, kernel_size=2, activation='LeakyReLU', name="C
onv1D_3"))
model.add(keras.layers.Flatten())
model.add(keras.layers.Dense(64, activation='LeakyReLU', name="Dense_1"))
model.add(keras.layers.Dense(64, activation='LeakyReLU', name="Dense_2"))
model.add(keras.layers.Dense(x_train_reshaped.shape[2], activation="sigmoid", name="Dens
e_3"))
model.compile(optimizer="rmsprop", loss="binary_crossentropy", metrics=["acc"])
model.summary()
start_time = time.time()
history = model.fit(x_train_reshaped, y_train, verbose=1, epochs=100, batch_size=128
                    )
train_time = (time.time() - start_time)
print("--- %s seconds ---" % train_time)
#implementing State-of-art 1D-CNN for 2-class
from tensorflow import keras
from tensorflow.keras import datasets, layers, models, Sequential
import time
```

```
model =keras.Sequential(name="model_conv1D")

model.add(keras.layers.Input(shape=( x_train_reshaped.shape[1],x_train_reshaped.shape[2])))

model.add(keras.layers.Conv1D(filters=32, kernel_size=7, activation='ReLU', name="Conv1
D_1"))

model.add(keras.layers.Conv1D(filters=32, kernel_size=3, activation='ReLU', name="Conv1
D_2"))

model.add(keras.layers.MaxPooling1D(pool_size=2, name="MaxPooling1D_1"))

model.add(keras.layers.Conv1D(filters=64, kernel_size=2, activation='ReLU', name="Conv1
D_3"))

model.add(keras.layers.Conv1D(filters=64, kernel_size=2, activation='ReLU', name="Conv1
D_4"))

model.add(keras.layers.MaxPooling1D(pool_size=2, name="MaxPooling1D_2"))

model.add(keras.layers.Conv1D(filters=128, kernel_size=2, activation='ReLU', name="Conv1
D_5"))

model.add(keras.layers.Conv1D(filters=128, kernel_size=2, activation='ReLU', name="Conv1
D_6"))

model.add(keras.layers.MaxPooling1D(pool_size=2, name="MaxPooling1D_3"))

model.add(keras.layers.Conv1D(filters=256, kernel_size=2, activation='ReLU', name="Conv1
D_7"))

model.add(keras.layers.Conv1D(filters=256, kernel_size=2, activation='ReLU', name="Conv1
D_8"))

model.add(keras.layers.GlobalAveragePooling1D())

model.add(keras.layers.Dropout(0.5))

model.add(keras.layers.Dense(32, activation='ReLU', name="Dense_1"))

model.add(keras.layers.Dense(64, activation='ReLU', name="Dense_2"))

model.add(keras.layers.Dense(1, activation="sigmoid", name="Dense_3"))

model.compile(optimizer="rmsprop", loss="binary_crossentropy", metrics=["acc"])

model.summary()

start_time = time.time()
```

```
history = model.fit(x_train_reshaped, y_train, verbose=1, epochs=150, batch_size=100
                    )
train_time = (time.time() - start_time)
print("--- %s seconds ---" % train_time)
```

# APPENDIX B

## ETHICAL APROVAL DOCUMENT

Date: _18__/_1__/_2022___

To the **Graduate School of Applied Sciences**

The research project titled "Pre-Processed And Combined EEG Data For Epileptic Seizure Classification Using Deep Learning" has been evaluated. Since the researcher(s) will not collect primary data from humans, animals, plants or earth, this project does not need to go through the ethics committee.

**Title: Assoc Prof Dr**

**Name Surname: Melike Şah Direkoğlu**

**Signature:** 

**Role in the Research Project:** Supervisor

# APPENDIX C

## Similarity Report

| Chapters | Percentages |
|---|---|
| Abstract.doc/docx | 0% |
| Chapter 1.doc/docx | 0% |
| Chapter 2.doc/docx | 8% |
| Chapter 3.doc/docx | 0% |
| Chapter 4.doc/docx | 3% |
| Chapter 5.doc/docx | 0% |
| Chapter 6.doc/docx | 5% |
| Chapter 7.doc/docx | 1% |
| Conclusions.doc/docx | 0% |
| *All.doc/docx | 3% |

*All.doc/docx document must include all your thesis chapters (except cover page, table of contents, acknowledge, declaration, references, appendix, list of figures, list of tables, and abbreviations list).

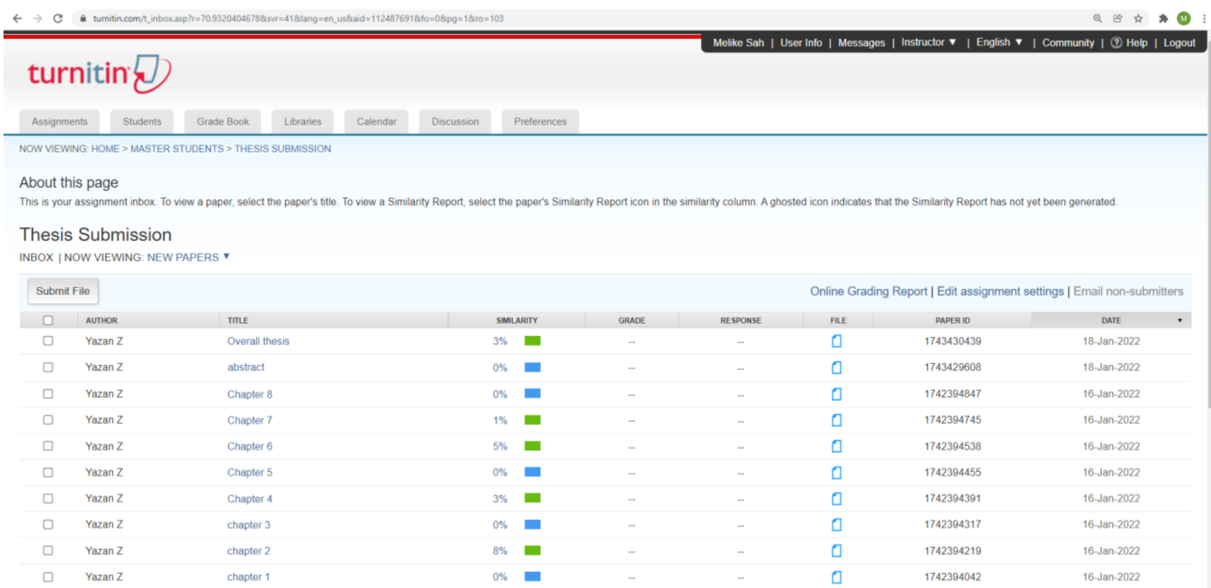
turnitin.com/t_inbox.asp?r=70.9320404678&svr=41&lang=en_us&aid=112487691&fo=0&pg=1&ro=103

Melike Sah | User Info | Messages | Instructor ▼ | English ▼ | Community | Help | Logout

turnitin

Assignments | Students | Grade Book | Libraries | Calendar | Discussion | Preferences

NOW VIEWING: HOME > MASTER STUDENTS > THESIS SUBMISSION

About this page

This is your assignment inbox. To view a paper, select the paper's title. To view a Similarity Report, select the paper's Similarity Report icon in the similarity column. A ghosted icon indicates that the Similarity Report has not yet been generated.

Thesis Submission

INBOX | NOW VIEWING: NEW PAPERS ▼

Submit File

Online Grading Report | Edit assignment settings | Email non-submitters

| AUTHOR | TITLE | SIMILARITY | GRADE | RESPONSE | FILE | PAPER ID | DATE |
|---|---|---|---|---|---|---|---|
| Yazan Z | Overall thesis | 3% | -- | -- | | 1743430439 | 18-Jan-2022 |
| Yazan Z | abstract | 0% | -- | -- | | 1743429608 | 18-Jan-2022 |
| Yazan Z | Chapter 8 | 0% | -- | -- | | 1742394847 | 16-Jan-2022 |
| Yazan Z | Chapter 7 | 1% | -- | -- | | 1742394745 | 16-Jan-2022 |
| Yazan Z | Chapter 6 | 5% | -- | -- | | 1742394538 | 16-Jan-2022 |
| Yazan Z | Chapter 5 | 0% | -- | -- | | 1742394455 | 16-Jan-2022 |
| Yazan Z | Chapter 4 | 3% | -- | -- | | 1742394391 | 16-Jan-2022 |
| Yazan Z | chapter 3 | 0% | -- | -- | | 1742394317 | 16-Jan-2022 |
| Yazan Z | chapter 2 | 8% | -- | -- | | 1742394219 | 16-Jan-2022 |
| Yazan Z | chapter 1 | 0% | -- | -- | | 1742394042 | 16-Jan-2022 |

Regards,

Assoc. Prof Dr Melike Sah Direkoglu.